Constructive Global Analysis of Hybrid Systems

by

Jorge Manuel Mendes Silva Gonçalves

Submitted to the Department of Electrical Engineering and Computer Science
in partial fulfillment of the requirements for the degree of

Doctor of Philosophy

at the

MASSACHUSETTS INSTITUTE OF TECHNOLOGY

September 2000

Author .....
Department of Electrical Engineering and Computer Science
August 29, 2000

Certified by .....
Munther A. Dahleh
Professor
Thesis Supervisor

Certified by .....
Alexandre Megretski
Associate Professor
Thesis Supervisor

Accepted by .....
Arthur C. Smith
Chairman, Department Committee on Graduate Students

Constructive Global Analysis of Hybrid Systems

by

Jorge Manuel Mendes Silva Gonçalves

Submitted to the Department of Electrical Engineering and Computer Science
on August 29, 2000, in partial fulfillment of the
requirements for the degree of
Doctor of Philosophy

Abstract

Many systems of interest are dynamic systems whose behavior is determined by the interaction of continuous and discrete dynamics. These systems typically contain variables or signals that take values from a continuous set and also variables that take values from a discrete, typically finite set. These continuous or discrete-valued variables or signals depend on independent variables such as time, which may also be continuous or discrete. Such systems are known as *Hybrid Systems*. Although widely used, not much is known about analysis of hybrid systems. This thesis attempts to take a step forward in understanding and developing tools to systematically analyze certain classes of hybrid systems. In particular, it focuses on a class of hybrid systems known as *Piecewise Linear Systems* (PLS). These are characterized by a finite number of affine linear dynamical models together with a set of rules for switching among these models. Even for simple classes of PLS, very little theoretical results are known. More precisely, one typically cannot assess a priori the guaranteed stability, robustness, and performance properties of PLS designs. Rather, any such properties are inferred from extensive computer simulations. In other words, complete and systematic analysis and design methodologies have yet to emerge.

In this thesis, we develop an entirely new constructive global analysis methodology for PLS. This methodology consists in inferring global properties of PLS solely by studying their behavior at switching surfaces associated with PLS. The main idea is to analyze impact maps, i.e., maps from one switching surface to the next switching surface. These maps are proven globally stable by constructing quadratic Lyapunov functions on switching surfaces. Impact maps are known to be "unfriendly" maps in the sense that they are highly nonlinear, multivalued, and not continuous. We found, however, that an impact map induced by an LTI flow between two switching surfaces can be represented as a linear transformation analytically parametrized by a scalar function of the state. Moreover, level sets of this function are convex subsets of linear manifolds. This representation of impact maps allows the search for quadratic Lyapunov functions on switching surfaces to be done by simply solving a set of LMIs. Global asymptotic stability of limit cycles and equilibrium points of PLS can this way be efficiently checked. The classes of PLS analyzed in this thesis are LTI systems in feedback with an hysteresis, an on/off controller, or a saturation. Although this analysis methodology yields only sufficient criteria of stability, it has shown to be very successful in globally analyzing a large number of examples with a locally stable

limit cycle or equilibrium point. In fact, it is still an open problem whether there exists an example with a globally stable limit cycle or equilibrium point that could not be successfully analyzed with this new methodology. Examples analyzed include systems of relative degree larger than one and of high dimension, for which no other analysis methodology could be applied. We have shown that this methodology can be efficiently applied to not only globally analyze stability of limit cycles and equilibrium points, but also robustness, and performance of PLS. Using similar ideas, performance of on/off systems in the sense that bounded inputs generate bounded outputs, can also be checked. Among those on/off and saturation systems analyzed are systems with unstable nonlinearity sectors for which classical methods like Popov criterion, Zames-Falb criterion, IQCs, fail to analyze. This success in globally analyzing stability, robustness, and performance of certain classes of PLS has shown the power of this new methodology, and suggests its potential towards the analysis of larger and more complex PLS.

Thesis Supervisor: Munther A. Dahleh
Title: Professor

Thesis Supervisor: Alexandre Megretski
Title: Associate Professor

To my Parents

Dedicado aos meus Pais

Acknowledgments

Wow!... Is my thesis really finished? I cannot believe this is over. Somehow, it seems not that long ago since the day I first arrived to MIT. I guess when you enjoy what you do, time really flies. Looking back at the last few years, I cannot even start to put in words how my stay at MIT has changed my life. What I can say for sure is that I am not the same person that came here. I have improved in every aspect of my life, from professional to personal. Obviously, such changes do not happen by yourself. People around you influence you and change you in ways that you typically do not realize until many years later. Over the last years at MIT, I had the pleasure of meeting and interacting with many great people. I am just grateful that, consciously or not, I have learned so much from all of them, sometimes even the hard way.

I would like to thank my advisors Munther Dahleh and Alexandre Megretski. What else can I say about them? Just that they are the best advisors in the world, and I was lucky enough to find them. I would like to thank the members of my Thesis Committee Sanjoy Mitter and Eric Feron, and also George Verghese, Michael Athans, and John Tsitsiklis for their support.

Obviously, not only professors influenced my learning experience at MIT. I have been fortunate to benefit from helpful discussions with many graduate students and post-doctoral fellows at the Laboratory for Information and Decision Systems (LIDS). The numerous discussions about nearly anything with my officemates Sean Warnick, Fadi Karameh, and Marcos Escobar helped me keep my mind and soul in balance. I would also like to thank other colleagues at LIDS which I had the luck to have around to discuss and exchange research ideas: Nicola Elia, Isaac Kao, Georgios Kotsalis, Ulf Jönsson, Nuno Martins, Reza Olfati-Saber, and Fernando Paganini. Other students that I would like to acknowledge are: Ola Ayaso, Soosan Beheshti, Constantinos Boussios, Michael Branicky, Julio Castrillón, Kuang Han Chen, Emilio Frazzoli, John Harper, Jianjuen Hu, Venkatesh Saligrama, Sri Sarma. Still in LIDS, I want to thank the great support and help I had from Fifa Monserrate, Doris Inslee, Ellen McMillan, Kathleen O'Sullivan, Kathy Sullivan, Monica Bell, and Marilyn Pierce.

As I mentioned, my stay at MIT changed me in many ways. Academically is just one of these ways. Outside the lab, many people have influenced me for the best. I want to thank Jacinto and Maria Figueiredo for making feel like I was at home. I especially thank everyone on my floor, Conner 3, for all these great years as a GRT on the best floor on campus. You guys are the best. In my dorm, I also want to thank Halston and Kathy Taylor, and Rosa and Manuel.

While a competitor ballroom dancer, I had the pleasure of making many friends that helped me keep my mind off MIT, even if just for a little while. Among them are Yumiko Osawa, David Johnson, Zoe Antoniou, Aamir Rashi, Wendy Luo, and, of course, Stephanie Kong.

I would like to thank Nuno Vasconcelos and Manuela Pereira for their constant support. Other friends that I was lucky to meet here are José Monteiro, Luís Silveira, Nuno Martins, Luisa Marcelino, Miguel and Inês Castro, Miguel and Helga Arsénio.

Back home, I want to thank Jorge Reis Lima. If it was not for him, I would have never been here. I am happy that his incentives to apply and come to MIT were

strong enough. I also want to thank Fernando Lobo Pereira for his constant support and unconditional help.

My friends back home Vitor Seabra, José Paulo Sá, Luís Costa, Valter Henriques, Sérgio Alexandre, João Carlos, Eixo and many other members of the *Tuna*, João Carlos Pimenta, Sérgio Reis Cunha, Pedro Correia, Manuel Correia, Mário Valente, Sílvia Lopes, and Inês Oliveira helped me greatly in making me believe I did the right thing in coming here in the first place, and have always made me feel at home when I go back on vacations.

Of all the people I have met while at MIT, there was one special person that had the most influence in making me a better person. Paula Waicman has showed me the world through different eyes, and for that I am truly thankful. We have shared incredible moments of happiness and joy that made my journey through MIT unforgettable. Undoubtfully, part of what I am today I owe it to her.

Of course, my family members have always given me tremendous and unconditional support. I could have not done it without their support. In particular, I want to thank my Godmother São, my sister Cristina, Mário Rui, and my adorable little nephews Rui Pedro and Rita Filipa, whom I miss greatly. And to the best parents in the world, from the bottom of my heart: Thank You. This thesis is dedicated to both of you.

Last, but not least, I want to acknowledge and thank the support of my research. This research was supported in part by the Portuguese "Fundação para a Ciência e Tecnologia" under the program "PRAXIS XXI", by the NSF under grants ECS-9410531, ECS-9796099, ECS-9796033, and ECS-9612558 and by the AFOSR under grants F49620-96-1-0123, F49620-00-1-0096, AFOSR F49620-95-0219 and F49620-99-1-0320.

Jorge M. M. S. Gonçalves
August 29, 2000

Contents

List of Figures

List of Tables

Chapter 1

Introduction

The purpose of this first chapter is to give some background and discuss previous work and related literature as well as to introduce the problem we propose to solve. This chapter is divided into six parts. The first three introduce three major concepts in this work: feedback systems, nonlinear systems, and hybrid systems, respectively. They also express the need for analysis tools for these classes of systems. The following two parts introduce a class of hybrid systems known as piecewise linear systems and describes the kind of problems we propose to solve in the thesis. Finally, part six of this section is dedicated to give an outline of how this thesis is organized.

1.1 Analysis of Feedback Systems

The main purpose of most *feedback* loops created by nature is to reduce the effect of uncertainty on vital systems functions. For example, consider a man walking down a corridor with no sensors, i.e., no vision, no ear, etc. Even if the man starts walking perfectly aligned with the corridor, he will sooner or later bump into a wall if this corridor is long enough. This is because the controller in our brain is not perfect. If it were, the man would make it all the way to the end of the corridor (independent of its length) without hitting any wall. Now, if he opens his eyes, the controller in his brain receives information about his position relatively to the walls and sends command instructions to the muscles. Thus, by using feedback he counteracted against uncertainty and, as a result, he is able to walk down the corridor without hitting the walls.

With the same principle, engineers design feedback loops to reduce the effect of uncertainty. Indeed, feedback as a design paradigm for dynamic systems has the potential to counteract uncertainty. Through feedback, one can obtain the desired behavior with only partial and imprecise knowledge of the plant. For standard references on examples and general theory for feedback systems see, for instance, [48, 38, 19, 36].

But, design is not an easy task. Often the engineer finds himself/herself in situations where no design tools exist. In those circumstances, ad hoc heuristics and trial-and-error are common techniques used to build feedback loops. In general, no guarantees can be given that the system will perform as desired or will be robust to

uncertainties. In fact, there are no guarantees that it will even be stable. In some cases, such as the design of a *on-off* controller for a typical heating system, one can just test and adjust the feedback loop until it performs satisfactorily. This adjustment may simply be choosing T_{min} and T_{max}, where T_{min} is the temperature that makes the controller turn *on* the heating system if $T < T_{min}$ (T is the temperature in the room), and T_{max} is the temperature that makes the controller turn *off* the system if $T > T_{max}$. If T_{min} and T_{max} are too close, the controller switches many times which may lead to its premature failure. If they are too much apart, it may lead to overheating or causing the room to be too cold. A solution is to choose the difference between T_{max} and T_{min} relatively large and then make it smaller until the system behaves satisfactory. In many cases, like this one, failure of the designed controller is not expensive. If it does not work, we just make the appropriate modifications and try it again. But, in other cases failure is just too expensive. For example, if an engineer designs a controller for an autopilot of a commercial airplane, then he/she has to guarantee somehow the system will work –be *stable*– once the autopilot is switched on during a flight, even in the presence of severe weather. Failure is not an option here. Therefore, it is essential to know beforehand whether a certain feedback system is reliable (stable) or not.

Experiment

There are several ways to check if a feedback system is stable. The oldest and most basic method is *experiment*. Basically, if you want to see if something works, just turn it on and see what happens. In many situations this is a reasonable thing to do. Like tuning an air conditioner controller: after building it, just test it through experiments. But, there are several problems with this widely used approach. First, the engineer cannot (or should not) just send an airplane up to test if a certain controller works. The pilot's life and the cost of the airplane are crucial factors that make experiment the last resort. Second, even if the feedback system is tested in a large number of different situations and initial conditions, these will always be a finite number of experiments. The fact that a certain experiment worked in a certain setting does not mean it will work even when those settings change slightly.

Simulation

Another way of checking stability of a feedback system is using *simulation*. In this case, a model of the physical system is needed. With the help of computers, several scenarios can be recreated. On one hand, simulation losses over experiment since the simulation models can never capture the complete dynamics of the physical system. On the other hand, simulation gains over experiment since it can be much cheaper and safer. But, as in experiment, we still have the problem that only a finite number of scenarios can be simulated and there is no guarantee that other scenarios (even very similar to the ones simulated) will be stable. Nevertheless, in spite of all this, simulation is fairly used when the dynamics of the feedback system are too complicated and no analysis tools are available [53]. And even if analysis tools exist, as a first test, simulation can help understand inherent properties of the physical process we have in our hands and also give an idea about the stability of the feedback system. A big advantage of simulation is when a scenario is found to make the system unsta-

ble. When this happens, it can immediately be concluded that the feedback system is not stable.

Analysis

A different approach is *analysis*. As in the case of simulation, analysis requires a model of the physical plant. Mathematical analysis tools do not exist for every feedback system. In fact, even very simple nonlinear dynamic equations can exhibit complex behaviors and be extremely hard (if not impossible) to analyze. However, for certain classes of systems, there exist many mathematical analysis tools that can be used (see for example [48, 19, 15, 67]). For some of these systems, it is often possible to determine if they are stable for any initial condition or at least for some sets of initial conditions. In some cases, it is also possible to tell if the system is unstable. However, analysis can reveal a lot more about feedback systems. Sometimes, it can characterize, for example, sets of initial conditions that result in stable trajectories and sets of initial conditions that result in unstable ones. Or it can determine which trajectories will converge faster to the desired objective. The biggest advantage of analysis versus experiment and simulation is that in many cases stability can be guaranteed for an infinite number of initial conditions. In addition, sometimes this is true even in the presence of perturbations and uncertainty.

Robustness Analysis

In general, what analysis can show about a certain feedback system depends on what class of systems it fits in and what kind of analysis tools are available for that class of systems. Unfortunately, only a few classes of systems have useful analysis tools. This is the main reason why, due to the complexity of most plants, one is forced to construct oversimplified and approximate models for the purpose of analysis and design of a feedback control systems. This leads us to *robustness* theory. Broadly speaking, robustness is a property, which guarantees that essential functions of the designed system are maintained under adverse conditions in which the model no longer accurately reflects reality. In modeling for robust control design, an exactly known nominal plant is accompanied by a description of the plant uncertainty, that is, a characterization of how the "true" plant might differ from the nominal one.

Although the basic robust synthesis and analysis problem has been studied for many years, only in last few decades has received the proper attention. In 1932, with his now classical stability criterion, Nyquist [47] presented a simple frequency domain criterion to determine the stability of feedback systems in terms of its loop gain. The Nyquist theory dictated how large the loop gain could possibly be if the closed-loop stability was to be achieved. In [9], with the goal of analyzing networks and designing feedback amplifiers for electronic circuits, Bode developed a theory of robust system design. In 1966, Zames [69] presented for the first time the so-called *small gain theorem*. Later, in the book by Desoer and Vidyasagar [17], quite an extensive treatment and applications of this theorem in various forms are presented. A collection of important results from the eighties ranging from robust stability theory and performance design (with different approaches discussed) to applications can be found in [18]. Some recent results in robust control theory of linear systems under various uncertainty assumptions and perturbations may be found in [15, 70, 44].

1.2 Nonlinear Systems

It is often possible to linearize a system, i.e., to obtain a linear representation of its behavior. That representation may approximate the true dynamics well in a small region. For example, the true equations of the pendulum are never linear but, for very small deviations (a few degrees) they may be satisfactorily replaced by linear equations. In other words, for small deviations, the pendulum may be replaced by a harmonic oscillator. This ceases to hold, however, for large deviations and, in dealing with these, one must consider the nonlinear equation itself and not merely a linear substitute.

Basically, most physical systems are nonlinear from the outset. The linearizations commonly practiced are approximating devices that are good enough or quite satisfactory for most purposes. There are, however, certain cases in which linear treatments may not be applicable at all. Frequently, many phenomena occur in nonlinear systems that cannot, in principle, occur in linear systems. In these cases, the engineer is forced to make use of the nonlinear dynamics in order to do design or analysis. The problem is that there does not exist a general theory capable of robustly synthesize and analyze nonlinear systems. There are, however, several tools that can be applied to certain classes of nonlinear systems. The following is a list of some of these tools in no particular order:

- Linearization [36]. Linearization of nonlinear systems is a common practice as approximating devices since for this class of systems there are many available analysis and design tools [15, 70]. This is a good technique if the system is evolving "close" to the equilibrium point from which the system was linearized. Here, "close" depends on the nonlinearities of the system.

- Feedback Linearization [32, 67]. The idea here is to invert the plant dynamics in order to get a simple and treatable mathematical model.

- Adaptive Control [37, 61]. The basic idea in adaptive control is to estimate uncertain plant parameters (or, equivalently, corresponding controller parameters) on-line based on the measured system signals, and then to use those estimated parameters in the control input computation. This technique gives good results when a good mathematical model of the physical system, with some uncertain parameters, is available and those uncertain parameters are constant or slowly varying. For instance, robot manipulators may carry large objects with unknown inertial conditions. This technique is very often used together with feedback linearization [61, 57].

- Sliding Mode Control [65]. Sliding mode usually results in discontinuous dynamic systems. Here, the design problem is usually reducible to the selection of surfaces in the state space where all the trajectories tend to. Once in an invariant surface, the state space trajectories belong to manifolds of lower dimension than that of the whole space. As a consequence, these trajectories should be easier to control. Such performance, however, is obtained at the price of extremely high control activity.

- Lyapunov Control Techniques [20, 36, 57]. Although this approach is general enough to cover all nonlinear systems, there is no assurance that an appropriate Lyapunov function can be constructed for a given system.

- Gain Scheduling [56, 36]. This is an intuitive approach based on performing several linearization-based control designs at many operating conditions and then interpolating the local designs to yield an overall nonlinear controller. This engine control technique is especially prevalent in flight control systems. Although it is known to be used successfully in many applications, theoretically there are still many fundamental open questions to be answered. There are, however, some theoretical results in this area like analysis and design of slow varying systems [56] and Lyapunov-based procedures [40, 39].

Both [36, 57] give complete introductions to all these and more methodologies. The problem with all of them is that none alone is sufficient for satisfactory feedback design or analysis of general nonlinear systems. Each of them works well only for specific classes of systems. This is because nonlinear systems exhibit a very large diversity of behaviors. This suggests that, with a single design approach, most of the results would end up being unnecessarily conservative.

As mentioned before, the methodologies presented above work well for certain classes of systems. There are, however, many other classes of nonlinear systems that we do not know how to analyze, or they cannot be efficiently analyzed with available methodologies. Simulation and experiment are frequently the only tools available to check stability, robustness, and performance of such systems. In this thesis, we develop constructive global analysis tools for some of those classes of nonlinear systems.

1.3 Hybrid Systems

Most of the nonlinear systems of interest in this thesis are dynamic systems whose behavior is determined by the interaction of continuous and discrete dynamics. These systems typically contain variables or signals that take values from a continuous set (e.g., the set of real numbers) and also variables that take values from a discrete, typically finite set (e.g., the set of symbols $\{a, b, c\}$). These continuous or discrete-valued variables or signals depend on independent variables such as time, which may also be continuous or discrete. Such systems are known as *hybrid systems*.

Reducing complexity was, and still is, an important reason for using hybrid models to represent the dynamic behavior of physical systems. In fact, many physical systems can be naturally represented as hybrid systems with very simple, but adequate for the tasks at hand, models of the complex physical phenomena. For example, a very well-known instance of a hybrid system is a sampled data system (see figure 1-1). Here, a continuous-time linear time-invariant plant described by differential equations (which involve continuous-valued variables that depend on continuous time) is controlled by a discrete-time linear time-invariant plant described by linear difference equations (which involve continuous-valued variables that depend on discrete time). A typical

application is a digital control system where a computer (evolving in discrete-time) controls a physical system (evolving in continuous-time).

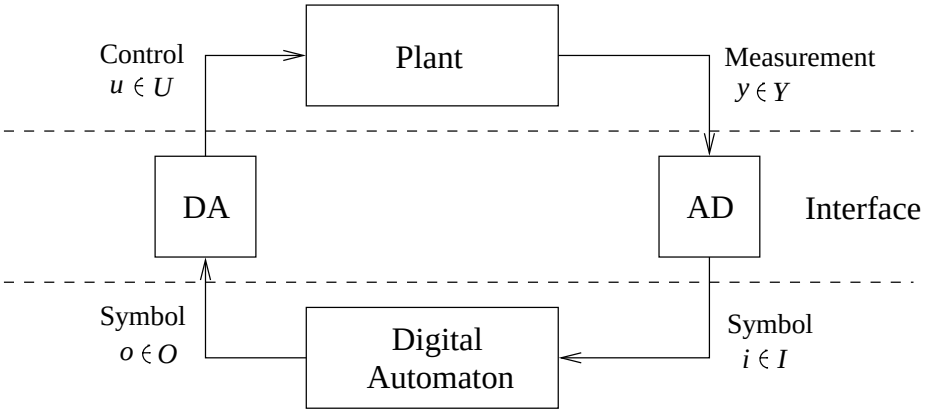

Figure 1-1: Sampled data system

Another familiar example of hybrid systems (of particular interest to us in this thesis) are *switching systems*. Here, the dynamic behavior of interest can be adequately described by a finite number of dynamical models that are typically sets of differential or difference equations, together with a set of rules for switching among these models. A simple application of switching systems is the heating and cooling system of a house. The furnace (providing the heat) and the air conditioner (providing the cool), along with the heat flow characteristics of the house, form a continuous-time system which is to be controlled. The thermostat is a simple asynchronous discrete-event driven system which basically handles the symbols {hot, normal, cold}. The temperature of the room is translated into these representations in the thermostat and the thermostat's response is translated back to electrical currents, which control the furnace and the air conditioner.

For a broad review of hybrid phenomenon we refer to [12]. There, several models available in the literature are surveyed along with more examples and discussions on design and analysis issues.

1.4 Piecewise Linear Systems

As described above, switching systems are characterized by a finite number of dynamical models together with a set of rules for switching among these models. A class of switching systems we will be particularly interested in this thesis is *piecewise linear systems* (PLS). PLS are characterized by having both the logic in the controller and the nonlinearities in the system model (such as saturations, hysteresis, etc.) appearing as piecewise linear functions, with the system dynamics described by standard integration elements as with linear systems. Therefore, this model description causes a partitioning of the state space into cells. These cells have distinctive properties in that the dynamics within each cell are described by linear dynamic equations. The

boundaries of each cell are in effect switches between different linear systems. Those switches arise from the breakpoints in the piecewise linear functions of the model. As we will see in chapter 3, depending if the switching rule associated with the PLS has memory or not, the cells may or may not intersect each other.

The reason why we are interested in studying this class of systems is to capture discontinuity actions in the dynamics from either the controller or system nonlinearities. On one hand, a wide variety of physical systems are naturally modeled this way due to real-time changes in the plant dynamics. On the other hand, an engineer can introduce intentional nonlinearities to improve system performance, to effect economy in component selection, or to simplify the dynamic equations of the system by working with sets of simpler equations (e.g., linear) and switch among these simpler models (in order to avoid dealing directly with a set of nonlinear equations). In the next two sections we will talk about these two types of occurrences along with some illustrative examples.

1.4.1 Modeling with Switches

There are numerous examples where a system changes its dynamic equations. For instance, this can happen due to hitting certain boundaries (like a ball hitting a wall) or due to certain control actions (like the space shuttle separating itself from the rockets during a launch). A model for such systems can be seen in figure 1-2. Here we have several models and a switch. The purpose of the switch is to decide at every instant of time which model better represents the physical system. This decision is based on all available information, which may include present and/or past values of the states.

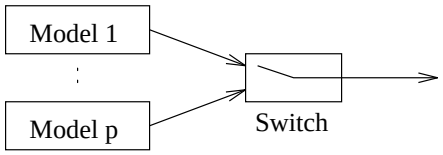

Figure 1-2: Switching between different models

Next we have some examples where this model can be naturally used.

- *Friction.* Another simple example is the modeling of static friction [49]. If an engineer chooses, for example, the Coulomb model (see figure 1-3) to describe friction on a certain physical system, then the dynamics of the system switches (the friction force changes sign) every time the velocity changes sign. The Coulomb friction model is an ideal relay that will be discussed in more detail in chapter 5.

- *Hysteresis.* Many physical applications can be modeled as an LTI system in feedback with an hysteresis (see figure 1-4). Such systems are similar to the ideal relay, like in the example of static friction, but with the difference that

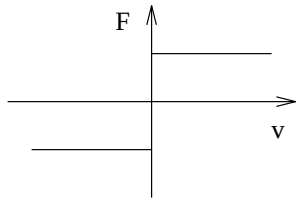

Figure 1-3: Coulomb friction

the switches from "high" to "low" and from "low" to "high" do not occur at the same values of y. In other words, the hysteresis differs from the ideal relay in that it introduces memory into the nonlinearity. For instance, the single information that $y(t) = 0$ is not enough to decide on the value of $u(t)$. This is determined not only by present values of y but also by past values of y. If $y(t) = 0$ and if $u(t - 0) =$ high then $u(t) =$ high; otherwise, $u(t) =$ low. Since the switching rule has memory, the two cells, resulting from the two state space partitions, intersect each other in a region containing the origin. More details on hysteresis can be found in chapter 5.

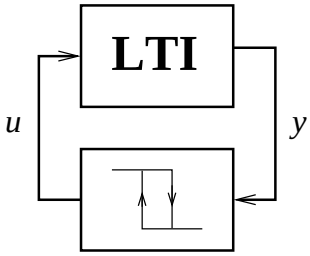

Figure 1-4: Hysteresis

- *Saturation.* Every actuator in physical systems eventually saturates if the input command exceeds certain levels. A very common model of a saturated actuator can be seen in figure 1-5. Here, y is the input to the actuator and u is the approximate input to the plant. Saturation systems will be studied in detail in chapter 7.

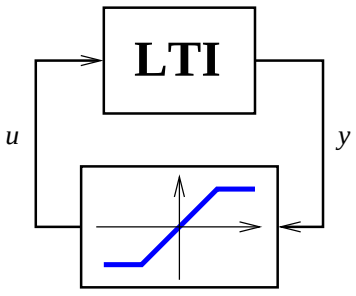

Figure 1-5: Saturation

- *Collisions.* A system where its dynamics change as it hits certain boundaries is a simple ball in a room under gravity. A usual way of modeling such a system is to set instantaneously the velocity from v to $-\rho v$, where $\rho \in [0, 1]$ is the coefficient of restitution, when the ball hits the floor.

- *Spring with damage protection.* Consider a spring connected with a mass. In order to protect the spring from over extension and avoid its damage, a "stop" device is placed at a desired position (see figure 1-6).

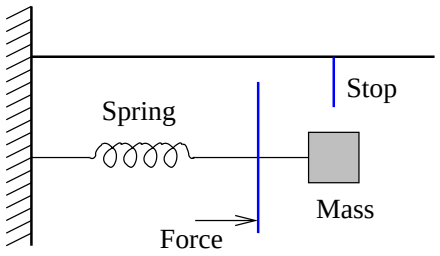

Figure 1-6: Mass-spring with damage protection

Once the spring reaches the maximum allowed extension, the dynamics of the system change. We have then a different model depending if the spring protection is touching the "stop" or not.

1.4.2 Control with Switches

It is well known that plant models are inherently inaccurate, and controllers regulating processes described by such models must be able to ensure satisfactory closed-loop performance in the presence of exogenous process disturbances which cannot be measured. Modern linear control theories (e.g., pole-placement/observer theory, linear quadratic theory, H_∞ theory, and the like) are now very highly developed. Those theories can be used to design controllers with such capabilities for processes admitting linear models, providing the models uncertainties are time-invariant and "sufficiently small". However, for "large" model uncertainties derived from real-time changes in the plant dynamics, common sense suggests (and simple examples prove it) that no single, fixed-parameter linear controller can possibly regulate in a satisfactory way. This is the reason why control switching strategies like the ones in figures 1-7 and 1-8 must be used to control such systems.

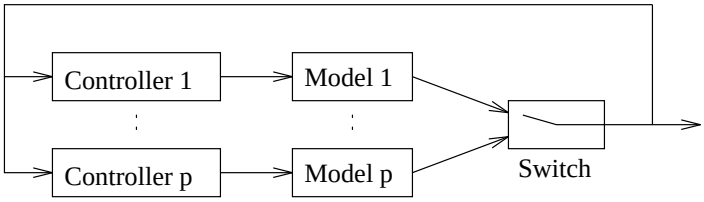

Figure 1-7: Switching between different pairs of models/controllers

Figure 1-7 shows a rather common approach in modeling and controlling physical phenomena. In this case, we have sets of simpler equations and we switch among these simpler models in order to avoid dealing directly with a set of nonlinear equations. A controller is then designed individually for each model and a switch decides at every instant of time which one to use.

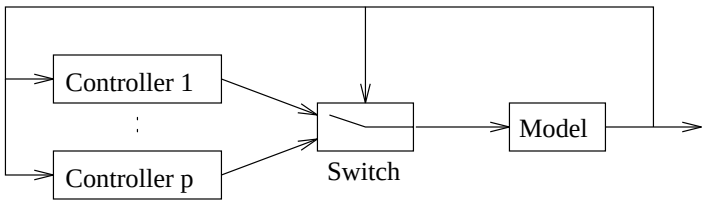

Figure 1-8: Switching between different controllers

In some cases (see figure 1-8), one model together with several controllers may be enough (when compared with figure 1-7). Once again, a switch decides which controller to use at any given time.

Next we present some examples of control with switches.

- *Inverted pendulum.* In [4], an inverted pendulum is modeled and controlled differently in two distinct regions of the state space. The first objective is to bring the pendulum close to the upright position. Once there, a linearize model and controller can be used to keep the pendulum in the upright position.

- *Anti-lock brake system (ABS) for a car.* The aim of the ABS is to improve the effectiveness of a vehicle to brake by maintaining the tire braking torque at or near its maximum value. The key factor is the tire adhesion to the road as braking torque is applied. A typical torque curve can be seen in figure 1-9.

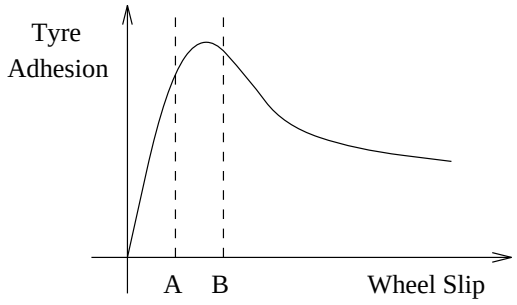

Figure 1-9: Typical tire adhesion curve for brake control

The tire adhesion is at its highest value between wheel slip A and B in figure 1-9. If wheel slip increases beyond B the wheel 'locks', tire adhesion decreases, and more importantly the driver looses the ability to steer the vehicle, i.e. the system is considered unstable. The aim of the ABS controller is to keep wheel

slip between A and B in the figure. A control strategy is proposed in [52]. There, a rule-based controller of ten rules was constructed resulting in something like 50 cells dividing the state-space.

- *Hopping robots.* More complex examples are hopping robots [53] or the dribbling of a basketball. In the case of the hopping robot, the boundary is the floor. As for the dribbling of a basketball, besides the floor, we have the hand of the player as another boundary (and also as the control). As they hit the floor (and the hand in the case of the basketball), their dynamics change. These phenomena can be captured by PLS making the mathematical representation of their complicated dynamics simple.

  Let's take the hopping robot, for instance. Consider a one legged robot (monopod) that hops (see figure 1-10). As described in [53], the hopping cycle is divided into three segments. Imagine we start when monopod touches the ground (figure 1-10.a). The spring will then begin to compress until this is fully compressed (figure 1-10.b). In this segment, gravity together with the leg spring, damping, and the controller determines the monopod's motion. These forces remain active during the second segment, except for the controller that switches sign in order to decompress the spring. This continues until the spring is completely decompressed (figure 1-10.c), indicating the end of the second segment. The third and last segment of the cycle starts when the monopod leaves the floor. Here, gravity alone determines the monopod's motion. Eventually, it reaches its highest altitude (figure 1-10.d) and, finally, comes back to the ground (figure 1-10.a) where the cycle starts all over again.

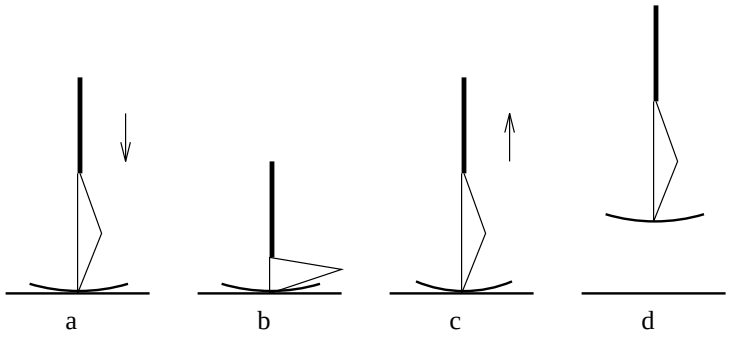

Figure 1-10: Different stages of a hopping monopod

In general, a hopping robot is to follow a certain prescribed nominal trajectory. Since such nominal trajectory returns to its initial condition every cycle, we call these *closed trajectories* (see figure 1-11). The idea is to make sure the robot returns to this closed trajectory if, for some reason, it starts away from it, in a way that it does not fall over.

- *Automatic tuning of PID regulators* and *delta-sigma modulators.* An important application is the automatic tuning of PID regulators which is implemented

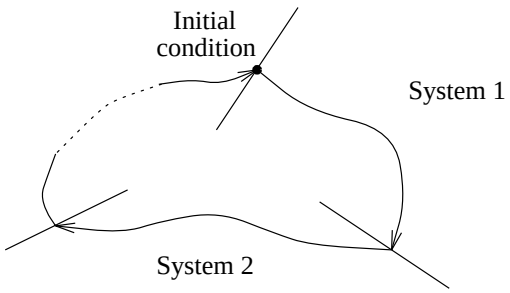

Figure 1-11: Closed trajectory switching among different systems

in many industrial controllers [6]. The basic idea behind this technique is to induce an oscillator (closed trajectory) by introducing an hysteresis in feedback with a stable open loop plant (see figure 1-4). Under certain assumptions, it is possible to determine several points on the Nyquist curve of the plant by measuring the frequency of the oscillation induced by the relay feedback. With this information, it is possible to calculate suitable parameters for simple controllers of the PID type.

Another application is the delta-sigma modulator as an alternative to conventional A/D converters [2]. Here, a relay is again used to produce a bit stream output whose pulse density depends on the applied input signal amplitude.

1.5 Analysis of Piecewise Linear Systems

As seen before, sometimes it is natural and easy to model systems as a hybrid systems. However, the same cannot be said about analyzing or designing controllers for these systems. In practice, the designer of hybrid systems is usually confronted with relations for which no general mathematical solutions exist. The problem is compounded by the peculiar behavior of hybrid systems: superposition no longer applies, the response of an hybrid system often depends on its initial state, and the nature of the system transient usually changes at different nominal operating points in the state space. For all these reasons, there does not exist a unified and generalized method of hybrid system analysis. In fact, the large diversity of hybrid systems suggests that, with a single design approach, most of the results would end up being unnecessarily conservative. To deal with diverse hybrid systems we need to break this large class of systems into several smaller classes. Each of these classes of hybrid systems should consist of systems that have certain properties in common. For instance, static systems could be one class; or linear systems; or more complex ones like piecewise linear systems (PLS). Then, a comparable diversity of design and analysis tolls and procedures should be developed for each one of them. The goal of this thesis is to give a step forward in understanding and developing tools for a class of hybrid systems known as PLS.

1.5.1 Previous Results

Although widely used and intuitively simple, PLS are computationally hard and very few theoretical results are available to analyze most PLS. More precisely, one typically cannot assess *a priori* the guaranteed stability, robustness, and performance properties of PLS designs. Rather, any such properties are inferred from extensive computer simulations. But, despite the lack of good theoretical analysis tools, PLS are used as an analysis and design methodology which is known to work in many engineering applications (like hopping robots, ABS, inverted pendulum, missile autopilots [13], robotic manipulators [14], autopilot of aircrafts [63]). However, in the absence of such analysis tools, these designs come with no guarantees. In other words, complete and systematic analysis and design methodologies have yet to emerge.

There are, however, some results for special classes of PLS. For instance, analysis in the phase plane of second-order systems has been studied for a while now. Early classical references discussing oscillations in mostly second-order systems using phase-plane analysis can be found in [1, 10, 29, 31, 60]. Other more recent references are [28, 36, 45, 46, 57]. Phase portrait analysis is a powerful graphical technique that presents global dynamic behavior for linear, piecewise linear, and even many nonlinear model descriptions. However, it is essentially restricted to models with two states only (or perhaps three states with todays computational graphic tools).

In [28], sketches of analysis and numerical simulations of a few model problems showed that "simple" differential equations of dimension three or greater can possess solutions of stunning complexity. Since such systems play an important role in the modeling, analysis, and design of nonlinear processes, an understanding of typical structures of their solutions is essential.

In the analysis of equilibrium points of PLS, recent results on the stability of equilibrium points for certain classes of PLS can be found in [34, 51, 30]. There, a search for piecewise quadratic Lyapunov functions is performed using convex optimization. Partitioning of the state-space is the key in this approach. For most PLS, construction of piecewise quadratic Lyapunov functions is only possible after a more refined partition of the state space, in addition to the already existent natural state space partition of the system. As a consequence, the analysis method is efficient only when the number of partitions required to prove stability is small. In chapter 4 we show that even for a simple second order system, the method can become computationally intractable. Also, the method does not scale well with the dimension of the system. For high-order systems, it is extremely hard to obtain a refinement of partitions in the state-space to efficiently analyze PLS. Another disadvantage of finding Lyapunov functions in the state space is that they are not capable of analyzing limit cycles.

Over many years, there has been extensive research on certain classes of PLS. Relay feedback systems (RFS) (a simple PLS that will be the topic of chapter 5) is one of these classes. Many results exist in the literature to analyze RFS. Research for this class of PLS was motivated by relays in electromechanical systems and simple models of dry friction (see the friction example in section 1.4.1). [8] and [64] are references that survey a number of analysis methods and results. Rigorous results for analysis

of *local*[1] stability of relay feedback systems can be found, for example, in [3, 33, 66]. In [23], reasonably large regions of stability around locally stable limit cycles were characterized. However, even for this simple class of PLS, very little is known about its *global* behavior. [60, 28] presents global analysis results for second order systems and [41] presents global stability results that can be applied to systems of order higher than two, including infinite-dimensional and uncertain systems. Unfortunately, many important relay feedback systems are not covered by this result.

Another class of PLS that has received great attention from researchers is saturation systems (see figure 1-5). The study of such systems is motivated by the possibility of actuator saturation or constraints on the actuators, reflected in bounds on available power supply or rate limits. These cannot be naturally dealt with within the context of standard (algebraic) linear control theory, but are ubiquitous in control applications. The fact that linear feedback laws when saturated can lead to instability has motived a large amount of research. The well known result which states that a controllable linear system is globally state feedback stabilizable, holds as long as the control does not saturate. In many applications, more often than not, the control is restricted to take values within certain bounds which may be met under closed-loop operation. Because feedback is cut, control saturation induces a nonlinear behavior on the closed-loop system. The problem of stabilizing linear systems with bounded controls has been studied extensively. See, for example, [59, 55, 62] and references therein.

Analysis of saturation systems (SAT) does not have such an extensive list of publications as synthesis. Some SAT can be analyzed by just using the circle or Popov criterion. Both of these criterion, however, are expected to be very conservative for systems of order greater than three. The Zames-Falb criterion [68] reduces the conservatism of both the circle and Popov criterion by taking in consideration the slope restrictions of the saturation. This method, however, is difficult to implement. Integral quadratic constraints (IQC) [35, 16, 44, 42] gives conditions in the form of LMIs that, when satisfied, guarantee stability of SAT. However, all of these analysis tools fail to analyze SAT with unstable nonlinearity sectors.

Example 1.1 Consider the SAT on the left of figure 1-12. If the saturation in the system is replaced by a linear constant gain of 1/2, the system becomes unstable (see the right side of figure 1-12). This means the system has an unstable nonlinearity sector. All the analysis tools described above fail to analyze systems with unstable nonlinearity sectors, like this one.

As we will see in chapter 7, the origin of this system is globally asymptotically stable. ■

Other PLS, like on/off systems (see figure 1-13), can also be analyzed with the tools described above, basically with the same advantages and disadvantages as SAT. On/off systems (OFS) system are characterized by an LTI system in feedback with

[1] The terms *local* and *global* stability will be rigorously defined in chapter 2.

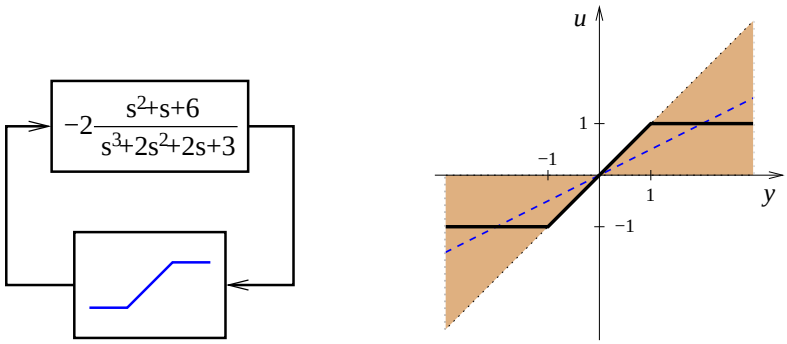

Figure 1-12: 3^{rd}-order system with unstable nonlinearity sector

an on/off controller defined as

$$u(t) = \max\{0, y(t) - d\}$$

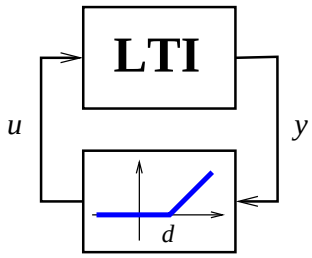

Figure 1-13: On/Off System

OFS can be found in many engineering applications. In electronic circuits, diodes can be approximated by on/off controllers. Transient behavior of logical circuits that involve latches/flip-flops performing very fast on/off switching can be modeled using on/off circuits and saturations. In general, on/off circuits have many applications in electronics and circuit design. Another area of application of OFS is aircraft control. For instance, in [12], a *max* controller is designed to achieve good tracking of the pilot's input without violating safety margins.

1.5.2 Contributions

The fact that PLS must be studied as a whole is one of the reasons that makes this class of systems so hard to analyze. This is due to their hybrid nature. It is not enough, for instance, to study their subsystems separately. Even if each individual subsystem is stable, there is no guarantee that the PLS is also stable (see example 3.4). In practice, due to the unavailability of rigorous mathematical tools, exhaustive simulation and/or experiment are, in most situations, the only alternatives to analyze most PLS.

In this thesis, we introduce an entirely new methodology to globally analyze PLS.

The idea consists in finding quadratic Lyapunov functions on switching surfaces that can be used to prove that *impact maps*, i.e., maps from one switching surface to the next switching surface, are contracting in some sense. The search for surface quadratic Lyapunov functions is done by solving sets of linear matrix inequalities (LMIs) using efficient computational algorithms. Contractions of impact maps can then be used to conclude about global stability, robustness, and performance of PLS.

The novelty of this work comes from expressing impact maps induced by an LTI flow between two hyperplanes as linear transformations analytically parametrized by a scalar function of the state. Furthermore, level sets of this function are convex subsets of linear manifolds with dimension lower than that of the switching surfaces. This allows us to reduce the problem of finding quadratic surface Lyapunov functions to solving a set of LMIs, which can be efficiently done using available computational tools.

The main difference between this and previous work [30, 34, 50], is that we look for quadratic Lyapunov functions on switching surfaces instead of quadratic Lyapunov functions in the state space. An immediate advantage is that this allows us to analyze not only equilibrium points but also limit cycles. Another advantage is that, for a given class of PLS, the complexity of analysis does not increase with the dimension of the system. On the other hand, the analysis methodology in [30, 34, 50] requires, in general, a further partition of the state space (besides the natural one imposed by the PLS). In our case, we only need the natural partitions imposed by the PLS. In chapter 4, we have an example of a second order system for which the number of partitions required in [30, 34, 50] is so high that it is computationally intractable. Quadratic surface Lyapunov functions, however, are easily found.

In the first part of this thesis, we will study global stability analysis of limit cycles and equilibrium points of PLS. We start with limit cycles. The study and understanding of limit cycles are of great interest in many applications. Hopping robots are examples of such applications. Here, it is important to show a certain design control strategy of a hopping robot is globally stable in its domain of operation. This ensures that as long as the robot starts within its domain it will not fall and, moreover, it will converge asymptotically to its nominal trajectory. However, no results are available to prove such properties. Although many walking robots are known to walk, their stability and robustness have only been shown through exhaustive simulations and experiments. This is true, even for simple walking robots, like monopods. This, together with the fact that walking robots is a very active area of research, motivates the development of such analysis tools.

In general, there is little known about global stability of periodic solutions. In this thesis, we will first give existence and local stability results of periodic solutions of PLS, and then focus on global stability analysis. We start by analyzing a simple class of PLS known as relay feedback systems (RFS). One of the motivations to consider RFS first is that for symmetric unimodal limit cycles[2], only a single impact map needs to be analyzed. Thus, this is a perfect class of systems to introduce global analysis using quadratic surface Lyapunov functions. The idea is to find a quadratic

[2]A limit cycle is *unimodal* if it only switches twice per cycle.

surface Lyapunov function for the associated impact map of a RFS. The search for such function is efficiently done by solving a set of LMIs. Global asymptotic stability of symmetric unimodal limit cycles of RFS can this way be efficiently checked. This new analysis methodology gave us great confidence in analyzing more complex classes of PLS since a large number of examples analyzed (with a unique locally stable symmetric unimodal limit cycle) was proven globally stable. In fact, existence of an example with a globally stable symmetric unimodal limit cycle that could not be successfully analyzed with this new methodology is still an open problem. Examples analyzed include minimum-phase systems, systems of relative degree larger than one, and of high dimension, for which no other analysis methodology could be applied.

Next, we analyze equilibrium points of PLS. We chose to first analyze on/off systems (OFS), for their simplicity when compared with other classes of PLS. In the state space, an OFS has a unique switching surface. The main goals of analyzing OFS are (1) to show that this new methodology can be used to not only globally analyze limit cycles but also to globally analyze equilibrium points, and also (2) to learn how to simultaneously analyze more than one impact map. Remember that in RFS there was only one impact map to analyze. In the case of OFS, there are two impact maps that need to be simultaneously analyzed. We will show that global asymptotically stability of equilibrium points of OFS can be checked, even when these do not belong to the switching surface. Moreover, a large number of examples was successfully proven globally stable, including those OFS with unstable nonlinearity sectors. As in RFS, existence of an example with a globally stable equilibrium point that could not be successfully analyzed with this new methodology is still an open problem.

The question of whether PLS with multiple switching surfaces can or cannot be analyzed using quadratic surface Lyapunov functions is answered when we analyze saturation systems (SAT). Here, the state space is divided in three regions by two switching surfaces. As before, the goal is to show the origin is globally asymptotically stable. The added difficulty from OFS is on how to deal with more than one switching surface. As we will see, in the case of SAT this reduces to the analysis of an extra impact map. Once again, the results were extremely positive in the sense that a large number of examples was successfully proven globally stable, including example 1.1 where the system had an unstable nonlinearity sector. Again, existence of an example with a globally stable equilibrium point that could not be successfully analyzed with this new methodology is still an open problem.

The second part of the thesis is dedicated to robustness and performance of PLS using impact maps and quadratic surface Lyapunov functions. In particular, we apply these ideas to study OFS. There, we show that performance properties of many OFS can be checked, including those OFS with unstable nonlinearity sectors.

The success in globally analyzing stability, robustness, and performance of certain classes of PLS has shown the power of this new methodology, and suggests its potential towards the analysis of larger and more complex PLS. Although much research is still ahead of us, the goal is to use impact maps and quadratic surface Lyapunov functions to systematically and efficiently analyze large classes of PLS.

1.6 Thesis Organization

This thesis is organized as follows. The next chapter presents mathematical tools that will be used throughout the rest of the thesis. Among others, the S-procedure and linear matrix inequalities will be introduced there. This chapter will also establish standard notation and include a brief introduction to dynamic systems. Chapter 3 is dedicated to introduce a class of hybrid systems known as piecewise linear systems.

The main results of this thesis can be found in chapter 4. There, we show that an impact map induced by an LTI flow can be represented as a linear transformation analytically parametrized by a scalar function of the state. Such representation allows us to efficiently construct quadratic Lyapunov functions on switching surfaces that can be used to globally analyze PLS in terms of stability, performance, and robustness.

The following three chapters show how the results from chapter 4 can be used to globally analyze certain classes of PLS. Each of these classes was carefully chosen to (1) separately deal with different issues and behaviors of PLS and (2) illustrate with examples the efficiency of the developed tools. By increasing complexity, we first analyze relay feedback systems (chapter 5), then on/off systems (chapter 6), and finally saturation systems (chapter 7). The success in globally analyzing a large number of examples of these classes of PLS demonstrates the potential of these new ideas in globally analyzing other, more complex classes of PLS.

In chapter 8, we show that the idea of global analysis of PLS using impact maps and quadratic surface Lyapunov functions can also be applied to study robustness and performance of PLS. For that, we use on/off systems to develop the main results. We show that many times, not only an OFS is globally asymptotically stable, but also finite-gain $\mathcal{L}_2$ stable, i.e., "well-behaved" inputs generate "well-behaved" outputs.

Finally, conclusions and future remarks are presented in chapter 9. Some of the topics reported in this thesis are published in various journal and conference papers [25, 26, 24, 21, 22].

Chapter 2

Mathematical Preliminaries

The purpose of this chapter is to introduce several mathematical concepts and tools that will be used throughout the thesis. Mathematical tools like linear matrix inequalities and the S-procedure are the engines behind many results presented later. For this reason, these topics are briefly introduced for completeness. We also include a short introduction to dynamic systems, including equilibrium points and limit cycles.

2.1 Standard Concepts

Let the field of *real* numbers be denoted by $\mathbb{R}$, the set of $n \times 1$ *vectors* with elements in $\mathbb{R}$ by $\mathbb{R}^n$, and the set of all $n \times m$ *matrices* with elements in $\mathbb{R}$ by $\mathbb{R}^{n\times m}$. Let I denote the *identity* matrix and superscript $(\cdot)'$ denote *transpose*. A matrix $D \in \mathbb{R}^{n\times n}$ is called *symmetric* if $D = D'$ and *positive definite* (*positive semidefinite*) if $x'Dx > 0$ ($x'Dx \geq 0$) for all nonzero $x \in \mathbb{R}^n$. "$D > 0$ on S" stands for $x'Dx > 0$ for all nonzero $x \in S \subset \mathbb{R}^n$. A matrix A is *Hurwitz* if the real part of each eigenvalue of A is negative.

The *p-norm* of a vector $x = (\, x_1 \quad x_2 \quad \cdots \quad x_n \,)' \in \mathbb{R}^n$ is given by

$$\|x\|_p = \left(\sum_{i=1}^{n} |x_i|^p \right)^{\frac{1}{p}}$$

In this thesis, we reserve the notation $\|\cdot\| = \|\cdot\|_2$ for the *2-norm*. This means $\|x\|^2 = x'x$. For some $D > 0$, define the *weighted Euclidean norm* of x as $\|x\|_D^2 = \|D^{1/2}x\|^2 = x'Dx$. Let $\mathcal{L}_p$ denote the space of all real-valued functions $u(\cdot)$ on $[0, \infty)$ such that

$$\|u(t)\|_{\mathcal{L}_p} = \left(\int_0^\infty |u(t)|^p dt \right)^{\frac{1}{p}} < \infty$$

For $p = \infty$,

$$\|u(t)\|_{\mathcal{L}_\infty} = \sup_{t\geq 0} |u(t)|$$

A set $X \subset \mathbb{R}^n$ is *convex* if $\lambda x + (1-\lambda)y \in X$ whenever $x, y \in X$ and $0 < \lambda < 1$, and is a *cone* if $x \in X$ implies $\lambda x \in X$ for any $\lambda \geq 0$.

A function $f : \mathbb{R} \to \mathbb{R}$ is *piecewise constant* if there exists a sequence of points $\{t_k\}$ with $t_{k+1} > t_k$ and $t_k \to +\infty$ as $k \to +\infty$, $t_k \to -\infty$ as $k \to -\infty$, such that the function is constant in $[t_k, t_{k+1})$. Let $f(t-0)$ stand for the $\lim_{\epsilon>0,\epsilon\to 0} f(t-\epsilon)$ and $f(t+0)$ for the $\lim_{\epsilon>0,\epsilon\to 0} f(t+\epsilon)$.

The following definitions are taken from [54] and will be used throughout the thesis.

Definition 2.1 All points and sets mentioned below are understood to be elements and subsets of $\mathbb{R}^n$.

(*a*) A *neighborhood* of a point p is a set $N_\epsilon(p)$ consisting of all points q such that $\|p-q\| < \epsilon$. The number ϵ is called the *radius* of $N_\epsilon(p)$.

(*b*) A point p is a *limit point* of the set X if every neighborhood of p contains a point $q \neq p$ such that $q \in X$.

(*c*) If $p \in X$ and p is not a limit point of X then p is called an *isolated point* of X.

(*d*) X is *closed* if every limit point of X is a point of X.

(*e*) The *closure* of X is the set $\bar{X} = X \cup \{p|\ p \text{ is a limit point of } X\}$.

(*f*) A point p is an *interior point* of X if there is a neighborhood N of p such that $N \subset X$.

(*g*) X is *open* if every point of X is an interior point of X.

(*h*) X is *bounded* if there is a real number M and a point $q \in \mathbb{R}^n$ such that $\|p-q\| < M$ for all $p \in X$.

2.2 Linear Matrix Inequalities

A *linear matrix inequality* (LMI) has the form

$$F(x) = F_0 + \sum_{i=1}^{n} x_i F_i > 0 \tag{2.1}$$

where $x \in \mathbb{R}^n$ is the variable and the symmetric matrices $F_i \in \mathbb{R}^{n\times n}$, $i = 0, 1, ..., n$ are given. The LMI (2.1) is a convex constraint on x, i.e., the set $\{x|\ F(x) > 0\}$ is convex. Although the LMI (2.1) may seem to have a specialized form, it can represent a wide variety of convex constraints on x. In particular, linear inequalities, (convex) quadratic inequalities, and matrix norm inequalities can all be cast in the form of an LMI. For more information on LMIs the reader is referred to [11].

Expressing solutions to problems in terms of LMIs is a common practice these days. Mathematical and software tools capable of efficiently finding x_i satisfying (2.1) are available . The strategy throughout this thesis is to write global stability, robustness, and performance conditions of piecewise linear systems in the form of LMIs.

2.3 The S-procedure

We will often encounter the problem of determining if a quadratic function (or quadratic form) is nonnegative when other quadratic functions (or quadratic forms) are all nonnegative. In some cases, this problem can be expressed as an LMI in the data defining the quadratic functions or forms; in other cases, we can form an LMI that is a conservative but often useful approximation of the original problem using a technique called the *S-procedure* (see [11] and references therein for a complete discussion on the S-procedure).

Let $\sigma_0, \cdots, \sigma_p$ be *quadratic functions* of the variable $x \in \mathbb{R}^n$ given in the form

$$\sigma_i(x) = x'P_ix + 2x'g_i + \alpha_i, \quad i = 0, ..., p$$

where $P_i = P_i'$. We consider the following condition on $\sigma_0, \cdots, \sigma_p$

$$\sigma_0(x) \geq 0 \text{ for all } x \text{ such that } \sigma_i(x) \geq 0, \ i = 1, ..., p \tag{2.2}$$

If there exist $\tau_1 \geq 0, ..., \tau_p \geq 0$ such that

$$\sigma_0(x) - \sum_{i=1}^{p} \tau_i\sigma_i(x) \geq 0$$

for all x, then (2.2) holds. It is a nontrivial fact that when $p = 1$ the converse holds, provided there is some x_0 such that $\sigma_1(x_0) > 0$.

2.4 Dynamic Systems

For completeness, this section contains a brief introduction to dynamic systems. For a complete introduction to dynamic systems the reader is referred to any of the following [48, 38, 19, 36].

In most cases, the evolution of physical systems can be approximately modeled by real ordinary differential equations; that is, the state $x(t) = (x_1(t)\ x_2(t)\ \cdots\ x_n(t))'$ of the physical system at time t is a point along the solution of the coupled first-order ordinary differential equations

$$\dot{x}_i = f_i(t, x, u) \quad i = 1, 2, ..., n \tag{2.3}$$

where $\dot{x}_i$ denotes the derivative of x_i with respect to the time variable t, $u(t) = (u_1(t)\ u_2(t)\ \cdots\ u_p(t))'$ are specified input variables, and the state x passes through the point $x(t_0)$ at time $t = t_0$. Sometimes, we associate with (2.3) another equation

$$y = h(t, x, u) \tag{2.4}$$

which defines a q-dimensional output vector that comprises variables of particular interest in the analysis of the dynamical system, like variables which can be physically measured or variables which are required to behave in a specified manner. We

call (2.4) the output equation and refer to equations (2.3) and (2.4) together as the state space model. In general, the functions $f = (f_1 \ f_2 \ \cdots \ f_n)'$ and h are nonlinear functions of the state variable x.

In closed-loop, a control law $u(t) = g(x(t), t)$ is selected. Thus, the closed-loop dynamics can be written as

$$\dot{x} = f(x, t) \tag{2.5}$$

A special case of (2.5) is when the function f does not depend explicitly on t, that is,

$$\dot{x} = f(x) \tag{2.6}$$

In these cases the system is said to be *autonomous* or *time-invariant*.

For the sake of simplicity in analyzing (2.3) and (2.4), f and h are frequently replaced by linear functions of the form

$$\begin{aligned} \dot{x} &= Ax + Bu \\ y &= Cx + Du \end{aligned}$$

In this case, we say the system is *linear* time-invariant (LTI).

2.4.1 Equilibrium Points

An important concept in dealing with the state equation is the concept of an *equilibrium point*. A point $x = x^*$ in the state space is said to be an equilibrium point of (2.6) if it has the property that whenever the state of the system starts at x^* it will remain at x^* for all future time. The equilibrium points are then the real roots of the equation $f(x) = 0$. An equilibrium point can be isolated (that is, there are no other equilibrium points in its vicinity) or can be part of a continuum of equilibrium points.

Equilibrium points can be characterized as stable, unstable, or asymptotically stable in the sense of Lyapunov.

Definition 2.2 The equilibrium point x^* of (2.6) is

- *stable* if, for each $\epsilon > 0$, there is a $\delta = \delta(\epsilon) > 0$ such that

$$\|x(0) - x^*\| < \delta \Rightarrow \|x(t) - x^*\| < \epsilon, \ \forall t \geq 0$$

- *unstable* if not stable;

- *asymptotically stable* if it is stable and δ can be chosen such that

$$\|x(0) - x^*\| < \delta \Rightarrow \lim_{t \to \infty} x(t) = x^*$$

- *globally asymptotically stable* if it is stable and, for any $x(0)$, $\lim_{t \to \infty} x(t) = x^*$.

2.4.2 Limit Cycles

Oscillation is one of the most important phenomena that occur in dynamical systems. A system oscillates when it has a nontrivial *periodic solution*

$$x(t + t^*) = x(t), \ for\ all\ t \geq 0$$

for some $t^* > 0$ (the period of the oscillation). The word "nontrivial" is used to exclude constant solutions corresponding to isolated equilibrium points. The image set of a periodic solution in the state space is a closed trajectory that is usually called periodic orbit or a closed orbit. *Limit cycles* are special cases of system closed trajectories. A limit cycle is defined as an isolated closed curve. That is, the trajectory has to be both closed (indicating the periodic nature of the motion) and isolated (indicating the limiting nature of the cycle that attracts and/or repels nearby trajectories). Thus, while there may exist many closed trajectories in the state space, only those that are isolated are called limit cycles.

Although linear systems may have closed trajectories, these are never isolated. The truth is that limit cycles are inherent properties of nonlinear systems. This is the reason why limit cycles are so hard to analyze since the existing well developed linear theory cannot be applied. The motivation behind the study of limit cycles in this thesis is based on both the importance of limit cycles in real world applications and the lack of mathematical tools to analyze them.

Periodic motions in $\mathbb{R}^n$ which are described by differential equations or difference equations are exceedingly important in practice. For instance, the motion of planets and the operating of an electric motor or steam engine can all be described by differential equations. This explains the great importance of the theory of periodic motions and the numerous publications in this area. The study of this type of motion is indispensable for understanding many phenomena.

As equilibrium points, limit cycles can be characterized as stable, unstable, or asymptotically stable. Let $\phi(t)$ be a nontrivial periodic solution of the autonomous system (2.6) with period t^*, and let γ be the closed orbit (limit cycle) given by the image set of $\phi(t)$ in the state space, that is,

$$\gamma = \{x \in \mathbb{R}^n |\ x = \phi(t),\ 0 \leq t \leq t^*\}$$

At first, it seems that the right thing to do in order to analyze the stability of the limit cycle, is to make a change of variables $z = x - \phi$ and then study the stability of this system at the equilibrium point $z = 0$ in conformity with definition 2.2. The problem with this approach is that, according to [29, theorem 81.1] or [45, chapter 5], the equilibrium point $z = 0$ is never stable in the sense of definition 2.2. We need then a more suitable definition of stability of limit cycles. Before we present such definition we need to introduce the concept of an ϵ-neighborhood of γ. This is defined by

$$U_\epsilon = \{x \in \mathbb{R}^n |\ dist(x, \gamma) < \epsilon\}$$

where $dist(x, \gamma)$ is the minimum distance from x to a point in γ, that is,

$$dist(x, \gamma) = \inf_{y \in \gamma} \|x - y\|$$

Definition 2.3 The limit cycle γ of (2.6) is

- *stable* if, for each $\epsilon > 0$, there is an $\delta > 0$ such that

$$x(0) \in U_\delta \Rightarrow x(t) \in U_\epsilon, \quad \forall t \geq 0$$

- *asymptotically stable* if it is stable and δ can be chosen such that

$$x(0) \in U_\delta \Rightarrow \lim_{t \to \infty} dist(x(t), \gamma) = 0$$

- *globally asymptotically stable* if it is stable and, for any $x(0)$

$$\lim_{t \to \infty} dist(x(t), \gamma) = 0$$

This definition reduces to definition 2.2 when γ is just an equilibrium point.

Having defined the stability properties of limit cycles, we can now define the stability properties of periodic solutions.

Definition 2.4 A nontrivial periodic solution $\phi(t)$ of (2.6) is

- *orbitally stable* if the limit cycle γ generated by $\phi(t)$ is stable;
- *asymptotically orbitally stable* if the limit cycle γ generated by $\phi(t)$ is asymptotically stable;
- *globally orbitally asymptotically stable* if it is orbitally stable and the limit cycle γ generated by $\phi(t)$ is globally stable.

Notice that different terminology is used depending on whether we are talking about the periodic solution or about the corresponding periodic orbit.

Chapter 3

Piecewise Linear Systems

This chapter is devoted to introduce a class of hybrid systems known as piecewise linear systems (PLS). Such systems arise in many applications like, for example, linear systems with saturating inputs, hopping robots, approximations of nonlinear systems, etc. This chapter gives a rigorous mathematical introduction to PLS. It starts by defining the class of PLS we are interested. Then, sections 3.2 and 3.3 discuss equilibrium points and limit cycles of PLS, respectively. Finally, section 3.4 presents the problem we propose to solve.

3.1 Definitions

Piecewise linear systems (PLS) are characterized by a set of affine linear systems

$$\dot{x} = A_\alpha x + B_\alpha \tag{3.1}$$

where $x \in \mathbb{R}^n$ is the state, together with a switching rule to switch among them

$$\alpha(x) \in \{1, ..., M\} \tag{3.2}$$

that depends on present values of x and possibly also on past values of x. By a solution of (3.1)-(3.2) we mean functions (x, u) satisfying (3.1)-(3.2), where $\alpha(t)$ is piecewise constant. t is a *switching time* of a solution of (3.1)-(3.2) if α is discontinuous at t. We say a trajectory of (3.1)-(3.2) *switches* at some time t if t is a switching time.

In the state space, switches occur at *switching surfaces* consisting of hyperplanes of dimension $n - 1$

$$S_j = \{x |\ C_j x + d_j = 0\}$$

where C_j is a row vector and $j = \{1, ..., N\}$. Define

$$X_i = \{x |\ \alpha(x) = i\}$$

for $i = \{1, ..., M\}$.

The switching rule may or may not be memoryless. In some cases, the value of α depends only on the current state, like linear systems with saturating inputs. In

other cases, the value of α depends also on past values of the state (or on past values of α), like relays with hysteresis. Next, we discuss both cases separately, starting with memoryless switching rules.

When the switching rule has no memory—depends only on the present state x—the state space $\mathbb{R}^n$ is partitioned into M (possibly unbounded) sets called *cells*, such that $X_i \bigcap X_j = \emptyset$, $i \neq j$. In each cell X_i, the system dynamics are given by the affine linear system $\dot{x} = A_i x + B_i$. Define $S_{ji} \subset S_j$ as the boundary of cell i by hyperplane j (see figure 3-1). If the hyperplane j is not part of the boundary of cell i then $S_{ji} = \emptyset$. All together, there are $N \cdot M$ sets S_{ji}, although some of them are the same or empty. For example, in figure 3-1, $S_{11} = S_{12}$, $S_{21} = S_{24}$, $S_{33} = \emptyset$, etc. Here $M = 7$ and $N = 3$.

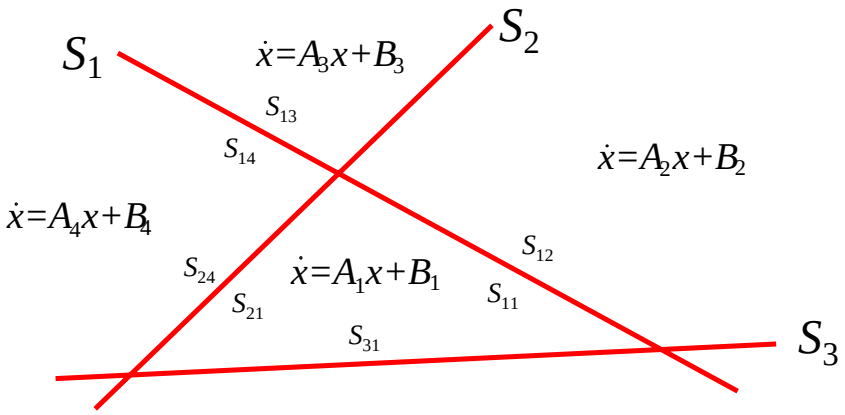

Figure 3-1: Piecewise Linear System with a memoryless switching rule

Example 3.1 A simple example of a PLS with a memoryless switching rule is a saturation system (see the left side of figure 3-2). Basically, an LTI system $\dot{x} = Ax + Bu$, $y = Cx$ is in feedback with a saturation controller of the form

$$u(t) = \begin{cases} -d & \text{if } y(t) < -d \\ y(t) & \text{if } |y(t)| \leq d \\ d & \text{if } y(t) > d \end{cases}$$

In the state space, the system is partitioned in three cells (see the right side of figure 3-2).

In this case, there are 2 hyperplanes ($N = 2$) and 3 linear subsystems ($M = 3$). Also, $S_{ji} = S_j$ since the hyperplanes do not intersect. This class of PLS will be the topic of chapter 7. ■

Another scenario is when the switching rule has memory and the decision of which affine linear system to use may not depend solely on the actual values of the state, but also on its past values. In this case, the intersection of different X_i may not result in an empty set, as the next example shows.

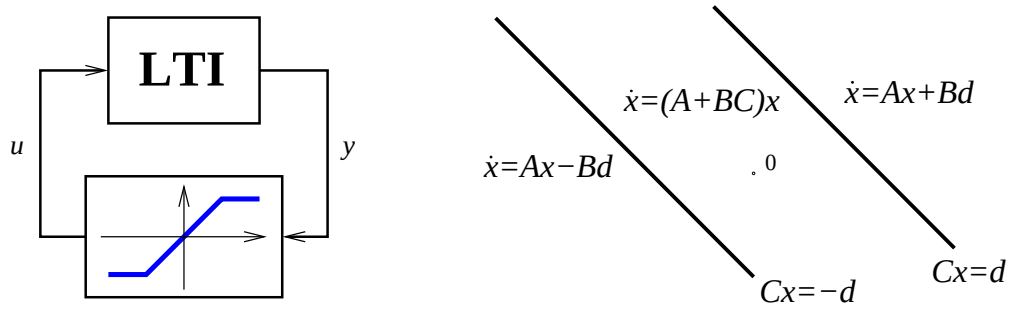

Figure 3-2: Left—Saturation system; Right—state space cells

Example 3.2 A simple class of PLS with a switching rule with memory is relay feedback systems (RFS). Such systems are characterized by a linear system in feedback with an hysteresis (see figure 3-3). This class of PLS will be the topic of chapter 5, and the reader is referred to that chapter for a precise definition of RFS. Basically, u, the input to the LTI system, can take values of 1 or -1 depending not only on the present state but also on past values of the state (or u).

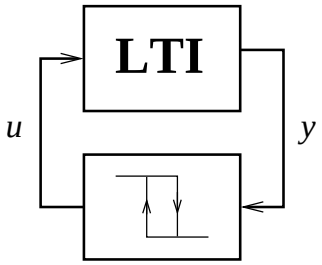

Figure 3-3: Relay Feedback System

Just like in the saturation system, the state space is divided in 3 parts, although, in this case, there are only two affine linear systems, corresponding to X_1 and X_2. In the outer cells, the PLS behaves just like a memoryless switching rule where u is clearly either 1 or -1. In the open inner cell, the value of u depends on its previous value. If $u(t-0) = 1$ then $u(t) = 1$, else $u(t) = -1$. Thus, the inner cell is shared by both affine linear systems and, in order to decide which system to use, it is necessary to know information about the past of the state (or the past of u). The intersection $X_1 \bigcap X_2$ is then exactly the inner cell. ■

In this thesis, we assume existence of solution is always guaranteed for any initial condition. If an initial condition is an interior point[1] of a cell, then existence of solution is guaranteed at least from the initial condition to the first intersection with a switching surface. This follows since the system is affine linear in the cell. When an initial condition belongs to a switching surface, however, there may be a unique, multiple, or no solutions. In figure 3-4, we have an example of each of these three

[1] x is an *interior point* of a set $X \subset \mathbb{R}^n$ if there exists a neighborhood W of x such that $W \subset X$.

situations. On the left, the orientation of the vector field of both systems i and k results in only one alternative for a solution starting at x_0. In this case, the unique trajectory will move downwards, to system k. In the center, the solution is not unique. The trajectory can either move downwards or upwards. In the last case, depicted on the right of figure 3-4, both vector fields point inwards to the switching surface. As before, at x_0 the switching rule (3.2) can take values i or k. As soon as $\alpha(x_0)$ is assigned to either one, it must switch immediately. Since, by definition, $\alpha(t)$ is piecewise constant, arbitrarily fast switches are not possible. Therefore, in this case, no solution exists. Hence, in order to guarantee existence of solutions, throughout this thesis we consider only those PLS that do not exhibit the behavior of the last scenario.

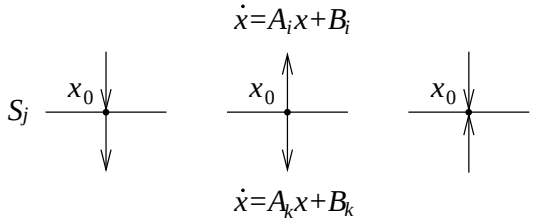

Figure 3-4: Existence of solutions; from left to right: one, multiple, and no solutions

One way to solve the problem of existence of solutions in cases like the one on the right of figure 3-4, is to define a dynamical system on the switching surface S_j, and let the trajectory evolve in this surface until it can "escape" to either side of S_j. This is typically known as *sliding modes*. Hence, the evolution of the trajectory along the switching surface satisfies an $n-1$ dimensional system defined in S_j. Although this thesis does not explicitly address sliding modes, the analysis of such cases is actually not that different from PLS without sliding modes.

In next chapter we will give further remarks about sliding modes.

Unlike linear systems that only have a single equilibrium point, PLS may exhibit multiple equilibrium points and/or limit cycles. We will analyze each of these cases separately in the following two sections, starting with equilibrium points.

3.2 Equilibrium Points

Remember that, by definition, a point is an equilibrium point if whenever the state of the system starts at that point it will remain there for all future. In the case of PLS, these may have none, one, or multiple equilibrium points.

Example 3.3 Consider again the saturation system described in example 3.1 and let

$$A = \begin{pmatrix} -1/2 & 0 \\ 0 & -1 \end{pmatrix} \qquad B = \begin{pmatrix} 1 \\ -\beta \end{pmatrix}$$

where $\beta \in \mathbb{R}$, $C = \begin{pmatrix} 0 & 1 \end{pmatrix}$ and $d = 1$. This means that $CA^{-1}B = \beta$. Let $\beta = 2$. Then the system has a single equilibrium point at the origin. On the other hand, if,

for example, $\beta = -2$, the system has 3 equilibrium points: one at the origin, one at $(\,2 \quad 2\,)'$, and one at $(\,-2 \quad -2\,)'$. ■

In many situations, checking stability of equilibrium points of PLS is not an easy task. In some cases, even showing local stability can be quite challenging. This is not the case, however, if an equilibrium point of some system i is an interior point of cell i. Here, local stability is easily verified just like in linear systems, by checking if the eigenvalues of A_i are in open left half plane.

If an equilibrium point belongs to a switching surface then this is a limit point[2] of two or more cells. In this case, it is not enough to simply check the eigenvalues of all of the A_i matrices of the cells for which the equilibrium point is a limit point. A well known example is the following.

Example 3.4 Let

$$A_1 = \begin{bmatrix} -0.1 & 1 \\ -10 & -0.1 \end{bmatrix}, \qquad A_2 = \begin{bmatrix} -0.1 & 10 \\ -1 & -0.1 \end{bmatrix}$$

and $B_1 = B_2 = 0$. The origin of each system $\dot{x} = A_i x$, $i = 1, 2$, is globally asymptotically stable. However, the switched system using system 1 in the second and fourth quadrants and system 2 in the first and third quadrants is unstable. ■

3.3 Limit Cycles

Limit cycles and stability of limit cycles were defined in section 2.4.2. In this section, we give existence and local stability conditions of limit cycles of PLS.

Assume the PLS (3.1)-(3.2) has a limit cycle γ with period t^*, and that this limit cycle crosses k switching surfaces per cycle. For simplicity, and without loss of generality, assume the trajectory of the limit cycle evolves consecutively from system 1, to system 2, and so forth until it reaches system k, and finally, after completing one cycle, returns to system 1. Assume also the switching surfaces are ordered the same way (see figure 3-5). This means the trajectory $\phi(t)$ of the limit cycle, starting at $x_0^* \in S_k$, satisfies $\phi(t_1^*) = x_1^* \in S_1$. Then system 2 "takes over" until $\phi(t_1^* + t_2^*) = x_2^* \in S_2$, and so on. The last affine linear system k takes the trajectory $\phi(t)$ from $x_{k-1}^* \in S_{k-1}$ to the point $x_k^* \in S_k$, i.e., $\phi(t_1^* + t_2^* + \cdots + t_k^*) = x_k^* = x_0^* \in S_k$. Note that $t^* = t_1^* + t_2^* + \cdots + t_k^*$. Note also that there is no loss of generality in this characterization of a limit cycle. If, for instance, the limit cycle crosses the same switching surface more than once, we simply have $S_i = S_j$ for some i, j.

[2] x is a *limit point* of a set $X \subset \mathbb{R}^n$ if every neighborhood of x contains a point $w \neq x$ such that $w \in X$.

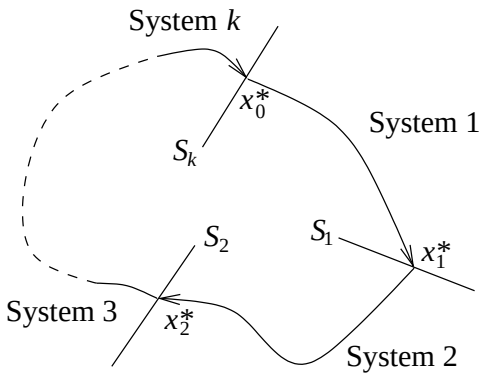

Figure 3-5: Limit cycle γ

3.3.1 Existence of Limit Cycles

Next we present necessary and sufficient conditions for the existence of limit cycles of PLS. For simplicity, we will first study the case where the limit cycle has only two switches per cycle. Then, we extend the result to k switches. For $k = 2$, we have the following result.

Proposition 3.1 *Consider the PLS (3.1)-(3.2). Assume there exists a periodic solution γ with two switches per cycle and with period $t^* = t_1^* + t_2^* > 0$, where t_1^* and t_2^* are defined as above. Define*

$$\begin{aligned} g_1(t_1^*, t_2^*) &= C_1 \left(I - e^{A_1 t_1^*} e^{A_2 t_2^*}\right)^{-1} \left[e^{A_1 t_1^*}(e^{A_2 t_2^*} - I)A_2^{-1}B_2 + (e^{A_1 t_1^*} - I)A_1^{-1}B_1\right] + d_1 \\ g_2(t_1^*, t_2^*) &= C_2 \left(I - e^{A_2 t_2^*} e^{A_1 t_1^*}\right)^{-1} \left[e^{A_2 t_2^*}(e^{A_1 t_1^*} - I)A_1^{-1}B_1 + (e^{A_2 t_2^*} - I)A_2^{-1}B_2\right] + d_2 \end{aligned}$$

Then the following conditions hold

$$\left\{ \begin{array}{rcl} g_1(t_1^*, t_2^*) &=& 0 \\ g_2(t_1^*, t_2^*) &=& 0 \end{array} \right. \tag{3.3}$$

and the periodic solution is governed by system 1 on $[0, t_1^*)$, and by system 2 on $[t_1^*, t^*)$. Furthermore, the periodic solution γ is obtained with either initial conditions

$$\begin{aligned} x_0^* &= \left(I - e^{A_2 t_2^*} e^{A_1 t_1^*}\right)^{-1} \left[e^{A_2 t_2^*}(e^{A_1 t_1^*} - I)A_1^{-1}B_1 + (e^{A_2 t_2^*} - I)A_2^{-1}B_2\right] \\ x_1^* &= \left(I - e^{A_1 t_1^*} e^{A_2 t_2^*}\right)^{-1} \left[e^{A_1 t_1^*}(e^{A_2 t_2^*} - I)A_2^{-1}B_2 + (e^{A_1 t_1^*} - I)A_1^{-1}B_1\right] \end{aligned}$$

Example 3.5 For visualization purposes, consider two affine linear systems in $\mathbb{R}^2$, $\dot{x} = A_i x + B_i$ where

$$A_1 = A_2 = \begin{pmatrix} -1 & 0 \\ 0 & -2 \end{pmatrix}, \quad B_1 = \begin{pmatrix} -3 \\ -2 \end{pmatrix}, \quad \text{and} \quad B_2 = \begin{pmatrix} 2 \\ 2 \end{pmatrix}$$

together with a switching rule with memory that uses system 1 until the trajectory intersects the switching surface S_1, and then uses system 2 until the trajectory in-

tersects the switching surface S_2, and so on. The switching surfaces are given by $C_1 = (-1 \quad 1)$, $d_1 = -1$, $C_2 = (1 \quad 0)$, and $d_2 = -1$. Solving (3.3) numerically we get $t_1^* = 1.24$, $t_2^* = 1.35$, $x_0^* = x_2^* = (1.0000 \quad 0.87)^T$, $x_1^* = (-1.84 \quad -0.84)^T$. The resulting periodic solution γ can be seen in figure 3-6. ■

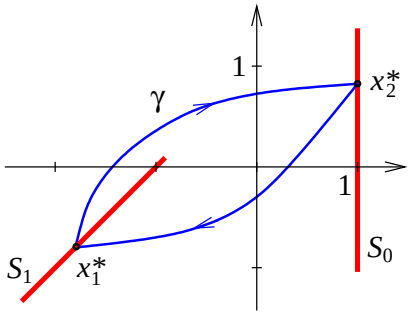

Figure 3-6: Periodic solution of a second-order PLS

Proof of proposition 3.1: Let's first find g_2. Integrating (3.1) for the first system we get

$$x(t) = e^{A_1 t}(x_0 + A_1^{-1}B_1) - A_1^{-1}B_1$$

If $x_0 = x_0^* \in S_2$ is a point in γ then

$$x_1^* = e^{A_1 t_1^*}(x_0^* + A_1^{-1}B_1) - A_1^{-1}B_1$$

where $x_1^* \in S_1$. In a similar way, for the second system

$$x_2^* = e^{A_2 t_2^*}(x_1^* + A_2^{-1}B_2) - A_2^{-1}B_2$$

Replacing x_1^* in the previous equation and noticing that $x_2^* = x_0^*$ we get

$$x_0^* = e^{A_2 t_2^*}\left(e^{A_1 t_1^*}(x_0^* + A_1^{-1}B_1) - A_1^{-1}B_1 + A_2^{-1}B_2\right) - A_2^{-1}B_2$$

which, after solving for x_0^*, yields

$$x_0^* = \left(I - e^{A_2 t_2^*}e^{A_1 t_1^*}\right)^{-1}\left[e^{A_2 t_2^*}(e^{A_1 t_1^*} - I)A_1^{-1}B_1 + (e^{A_2 t_2^*} - I)A_2^{-1}B_2\right]$$

Since $x_0^* \in S_2$, $C_2 x_0^* + d_2 = 0$, and the desired result follows. x_1^* and g_2 can be found in a similar way. ■

This result can be generalized to the case where a periodic solution γ switches among k systems instead of just two. For the remainder of this section, for simplicity of notation, let $E_i = e^{A_i t_i^*}$ and $z_i = A_i^{-1}B_i$. Define

$$g_k(t_1^*, t_2^*, ..., t_k^*) = C_k\left(I - E_k \cdots E_1\right)^{-1}\left[\sum_{i=1}^{k-1} E_k \cdots E_{i+1}(E_i - I)z_i + (E_k - I)z_k\right] + d_k$$

g_k was found based on the switching sequence $\{1, 2, ..., k\}$. To find, g_j, $j = 1, ..., k-1$, consider the switching sequence $\{j+1, ..., k, 1, ..., j\}$, i.e., just replace the indexes of g_k in the following way: 1 by $j+1$, 2 by $j+2$ (or by 1 if $j+2 > k$), up to k by j.

Proposition 3.2 *Consider the PLS (3.1)-(3.2). Assume there exists a periodic solution γ with k switches per cycle and with period $t^* = t_1^* + t_2^* + \cdots t_k^* > 0$. Consider the functions $g_1, g_2, ..., g_k$ defined as above. Then the following conditions hold*

$$\left\{ \begin{array}{rcl} g_1(t_1^*, t_2^*, ..., t_k^*) & = & 0 \\ g_2(t_1^*, t_2^*, ..., t_k^*) & = & 0 \\ \vdots & & \\ g_k(t_1^*, t_2^*, ..., t_k^*) & = & 0 \end{array} \right. \tag{3.4}$$

and the periodic solution is governed by system 1 on $[0, t_1^*)$, and by system i on $[t_1^* + \cdots + t_{i-1}^*, t_1^* + \cdots + t_i^*)$, $i = 2, ..., k$. Furthermore, the periodic solution γ can be obtained with the initial condition $x_0^* \in S_k$

$$x_0^* = (I - E_k \cdots E_1)^{-1} \left[\sum_{i=1}^{k-1} E_k \cdots E_{i+1}(E_i - I)z_i + (E_k - I)z_k \right]$$

Proof: Integrating the linear dynamics between two switching surfaces we get

$$x_i^* = E_i x_{i-1}^* + (E_i - I)z_i$$

To find x_k^* as a function of x_0^* we solve recursively, starting at x_k^*:

$$\begin{array}{rcl} x_k^* & = & E_k x_{k-1}^* + (E_k - I)z_k \\ & = & E_k \left(E_{k-1} x_{k-2}^* + (E_{k-1} - I)z_{k-1} \right) + (E_k - I)z_k \\ & = & E_k E_{k-1} x_{k-2}^* + E_k(E_{k-1} - I)z_{k-1} + (E_k - I)z_k \\ & = & E_k \cdots E_1 x_0^* + E_k \cdots E_2(E_1 - I)z_1 + \cdots + E_k E_{k-1}(E_{k-2} - I)z_{k-2} \\ & & \qquad + E_k(E_{k-1} - I)z_{k-1} + (E_k - I)z_k \end{array}$$

The desired result can be obtained by knowing $x_0^* = x_k^*$ and solving for x_k^*. g_k can be found by computing $g_k = C_k x_k^* + d_k = 0$, since $x_k^* \in S_k$. The rest of the proof follows in a similar way. ■

As in the case where $k = 2$, (3.4) is a set of transcendental equations. Closed form solutions can be given only for very special cases and, even numerically, this is a hard problem. An alternative is to simulate the system for some time and get approximate values for $t_1^*, t_2^*, ..., t_k^*$. Then, use some numerical algorithm to compute $t_1^*, t_2^*, ..., t_k^*$.

3.3.2 Local Stability

Consider the PLS (3.1)-(3.2). Assume there exists a periodic solution γ with period t^*. Let $x_0^* \in S_k$ be the initial state that generates the periodic motion. Consider the

map T from some point in a small neighborhood of x_0^* in S_k, to the point when the trajectory returns to S_k. Local stability of a limit cycle can be checked by looking at the poles of the linear part of T. Stability follows if the poles are inside the unit disk. The following proposition gives conditions for local stability of limit cycles of PLS.

Proposition 3.3 *Consider the PLS (3.1)-(3.2). Assume there exists a limit cycle γ with period t^* as described above. Assume also the limit cycle is transversal*[3] *to the switching surfaces $S_1, ..., S_k$ at $x_1^*, ..., x_k^*$, respectively. The Jacobian of the map T defined above is given by $W = W_k W_{k-1} \cdots W_2 W_1$ where*

$$W_i = \left(I - \frac{v_i C_i}{C_i v_i} \right) e^{A_i t_i^*}$$

with $v_i = A_i x_i^* + B_i$, $i = 1, ..., k$. The limit cycle γ is locally stable if W has all its eigenvalues inside the unit disk. It is unstable if at least one of the eigenvalues of W is outside the unit disk.

Proof: Consider a trajectory with initial condition $x(0) = x_0^*$. Then, the solution at time t_1^* is $x(t_1^*) = x_1^* = e^{A_1 t_1^*}(x_0^* + A_1^{-1}B_1) - A_1^{-1}B_1$. Now, let $x(0) = x_0^* + \delta_1 x_0^*$ where $\delta_1 x_0^*$ is chosen so that $x(0)$ is on the switching surface plane, i.e., such that $C_k(x_0^* + \delta_1 x_0^*) + d_k = 0$. The solution to this initial condition is $x(t) = e^{A_1 t}(x_0^* + \delta_1 x_0^* + A_1^{-1}B_1) - A_1^{-1}B_1$. Assuming the solution reaches the switching surface S_1 at time $t_1^* + \delta_1 t_1^*$ we have

$$x(t_1^* + \delta_1 t_1^*) = e^{A_1(t_1^* + \delta_1 t_1^*)} \left(x_0^* + \delta_1 x_0^* + A_1^{-1} B_1 \right) - A_1^{-1} B_1$$

Making a series expansion in $\delta_1 x_0^*$ and $\delta_1 t_1^*$ we get

$$\begin{aligned} x(t_1^* + \delta_1 t_1^*) &= x_1^* + e^{A_1 t_1^*} \delta_1 x_0^* + e^{A_1 t_1^*} \left(A_1 x_0^* + B_1 \right) \delta_1 t_1^* + O(\delta_1^2) \\ &= x_1^* + e^{A_1 t_1^*} \delta_1 x_0^* + v_1 \delta_1 t_1^* + O(\delta_1^2) \end{aligned} \tag{3.5}$$

where we use the fact that $e^{A_1 t_1^*} \left(A_1 x_0^* + B_1 \right) = A_1 x_1^* + B_1 = v_1$. Since $x(t_1^* + \delta_1 t_1^*)$ is on the switching surface S_1, we have $C_1 x(t_1^* + \delta_1 t_1^*) + d_1 = 0$. Neglecting high-order terms gives

$$C_1 x_1^* + C_1 e^{A_1 t_1^*} \delta_1 x_0^* + C_1 v_1 \delta_1 t_1^* + d_1 = 0$$

and since $C_1 x_1^* + d_1 = 0$ we have

$$C_1 v_1 \delta_1 t_1^* = -C_1 e^{A_1 t_1^*} \delta_1 x_0^*$$

Since, by assumption, the limit cycle is transversal to S_1 at x_1^*, $C_1 \dot{x}(t_1^*) \neq 0$. Thus, $C_1(A_1 x_1^* + B_1) \neq 0$ or $C_1 v_1 \neq 0$, which means that

$$\delta_1 t_1^* = -\frac{C_1 e^{A_1 t_1^*}}{C_1 v_1} \delta_1 x_0^*$$

[3] ϕ is *transversal* to $S = \{x |\ Cx = d\}$ at $p = \phi(t) \in S$ if $C\dot{\phi}(t-0) \neq 0$.

replacing in (3.5) yields

$$\begin{aligned} x(t_1^* + \delta_1 t_1^*) &= x_1^* + \left(I - \frac{v_1 C_1}{C_1 v_1}\right) e^{A_1 t_1^*} \delta_1 x_0^* + O(\delta_1^2) \\ &= x_1^* + W_1 \delta_1 x_0^* + O(\delta_1^2) \end{aligned}$$

Similarly, we get

$$x(t_2^* + \delta_2 t_2^*) = x_2^* + W_2 \delta_2 x_1^* + O(\delta_2^2)$$

with initial condition $x_1^* + \delta_2 x_1^* = x_1^* + W_1 \delta_1 x_0^* + O(\delta_1^2)$. Neglecting high-oder terms, we get $\delta_2 x_1^* = W_1 \delta_1 x_0^*$. Replacing in the above equality yields

$$x(t_2^* + \delta_2 t_2^*) = x_2^* + W_2 W_1 \delta_1 x_0^* + O(\delta_1^2)$$

Repeating this procedure $k-2$ times, we get to the last system, system k. Letting the initial condition to system k be $x_{k-1}^* + \delta_k x_{k-1}^* = x_{k-1}^* + W_{k-1} \cdots W_2 W_1 \delta_1 x_0^* + O(\delta_1^2)$ leads to

$$\begin{aligned} x(t_k^* + \delta_k t_k^*) &= x_k^* + W_k \delta_k x_{k-1}^* + O(\delta_k^2) \\ &= x_0^* + W_k W_{k-1} \cdots W_2 W_1 \delta_1 x_0^* + O(\delta_1^2) \end{aligned}$$

where we used the fact $x_k^* = x_0^*$. This proves the proposition. ■

Example 3.6 Coming back to example 3.5, we can compute W from W_1 and W_2. Replacing the values we get

$$W = 10^{-3} \begin{pmatrix} 0 & 0 \\ -0.29 & 0.32 \end{pmatrix}$$

which has all its eigenvalues inside the unit disk. Therefore the limit cycle in example 3.5 is locally stable. ■

3.4 Problem Statement

After defining PLS and discussing equilibrium points and limit cycles of PLS, the natural question is how to analyze such trajectories. Like in the example in figure 3-7, PLS may have equilibrium points, limit cycles, or some combination of both of these trajectories. One may ask: is the limit cycle stable? Or one of the equilibrium points? Or both? Or all of these trajectories? If they are not unstable, what are their regions of attraction? And, what if we are looking for global analysis? For instance, if a PLS has a single equilibrium point or a single limit cycle, how can we guarantee such trajectory is global asymptotically stable? That it meets certain performance criteria? That it is robust to unmodeled dynamics? These are the sort of questions we propose to answer with the results in this thesis.

The main purpose of this thesis is to develop an entirely new constructive global analysis methodology. This methodology consists in inferring global properties of

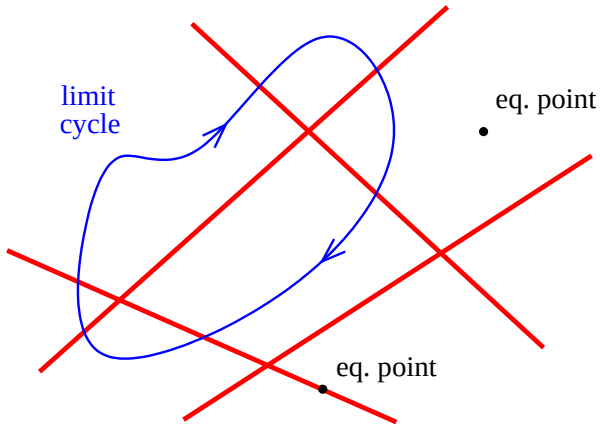

Figure 3-7: PLS with limit cycles and equilibrium points

PLS solely by studying their behavior at switching surfaces. The main idea is to analyze impact maps, i.e., maps from one switching surface to the next switching surface. These maps are proven globally stable by constructing quadratic Lyapunov functions on switching surfaces associated with PLS. Impact maps are known to be "unfriendly" maps in the sense that they are highly nonlinear, multivalued, and not continuous. Thus, the first step is to find a representation of impact maps that allows us to use them to conclude about stability, performance, and robustness of PLS.

Although analysis of nonlinear systems at switching surfaces has been studied by others (e.g., Poincaré), with the exception of very simple systems, no one really knew how to use impact maps to study global analysis of hybrid systems. The reason why in this thesis we are able use impact maps in global analysis of certain classes of hybrid systems is based on the discovery that impact maps can be written in an "nice", analytical way. We found that impact maps can be represented as a linear transformation analytically parametrized by a scalar parameter of the state. This parameter is simply the switching time associated with the impact map. When the switching time is fixed, it turns out the impact map is linear along a subset of a linear manifold of dimension smaller than the dimension of the switching surface. Writing matrix inequalities that guarantee quadratic stability of impact maps is then straightforward.

In the first part of this thesis we will mainly focus on global asymptotic stability analysis of PLS with either a single limit cycle or a single equilibrium point. We will analyze several classes of PLS: relay feedback systems, on/off systems, and saturation systems. Then, in the second part of the thesis we show that performance analysis of PLS can also be checked using the very same ideas: global analysis of impact maps using surface quadratic Lyapunov functions. We show this can be done by applying the results to on/off systems.

To summarize, we propose to develop a new methodology to analyze stability, robustness, and performance of PLS. The main ideas will be presented in the next chapter.

Chapter 4

Main Results

This chapter includes the main contributions of this thesis. In the next section, we motivate the need for better and more efficient analysis tools for PLS. We explain how available methods are inefficient or even useless to analyze many important PLS. Such analysis tools are mainly based on constructing quadratic Lyapunov functions in the state space. Alternatively, we propose the construction of quadratic Lyapunov functions in the switching surfaces. In section 4.2, we introduce the notion of impact maps, which are simply maps between two switching surfaces. We show that impact maps induced by an LTI flow can be represented as linear transformations analytically parametrized by a scalar function of the state. This, in turn, allows us to reduce the problem of quadratic stability of impact maps to solving a set of LMIs, as explained in section 4.3. Then, section 4.4 briefly discusses how these results can be used in the analysis of equilibrium points and limit cycles of PLS. Basically, section 4.4 gives an overview of the following three chapters. In these chapters, different and specific issues of PLS are separately addressed in detail. This will be done by studying three different classes of PLS: relay feedback systems, on-off systems, and saturation systems.

4.1 Motivation

As discussed in introduction, there exist several tools to analyze PLS. One of the most important [50, 34, 30], is based on constructing piecewise quadratic Lyapunov functions in the state space. There are, however, several drawbacks with this approach. These include:

- Lyapunov functions in the state space cannot be constructed to analyze limit cycles.
- Partitioning of the state-space is the key of the approach proposed in [50, 34, 30]. For most PLS, construction of piecewise quadratic Lyapunov functions is only possible after a more refined partition of the state space, in addition to the already existent natural state space partition of the PLS. As a consequence, the analysis method is efficient only when the number of partitions required

to prove stability is small. The following example shows that even for second order systems, the construction of piecewise quadratic Lyapunov functions can be computationally intractable due to the large number of partitions in the state space required for the analysis.

Example 4.1 In this simple example, we are interested in showing the origin of a second order PLS is globally asymptotically stable. Consider the PLS in figure 4-1 composed of two linear systems. On the left side of the vertical axis—x_2 axes—we have an unstable linear system and on the right side we have a stable linear system parametrized by $\epsilon > 0$.

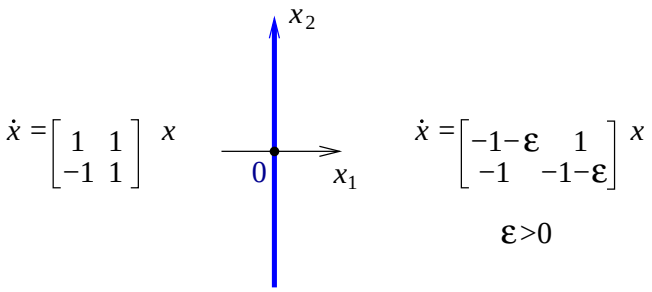

Figure 4-1: PLS composed of an unstable and a stable linear systems

First, we show there is no global quadratic Lyapunov function for the system. By contradiction, assume $V(x) = x'Qx$ is a Lyapunov function of the system, where $Q > 0$ has the following block partition

$$Q = \begin{pmatrix} q_1 & q \\ q & q_2 \end{pmatrix}$$

Consider the level set $x'Qx = q_2$. It must be true that for any initial condition x_0 such that $x_0'Qx_0 \leq q_2$, the solution $x(t)$ satisfies $x'(t)Qx(t) \leq q_2$ for all $t \geq 0$. Let $x_0 = (0 \quad -1)'$. x_0 belongs to the level set since $x_0'Qx_0 = q_2$. Then, $x(\pi) = e^{\pi}(0 \quad 1)'$ and $x'(\pi)Qx(\pi) = q_2 e^{2\pi} > q_2$, which is a contradiction. Thus, there is no global quadratic Lyapunov function for the system.

We then turn to find piecewise quadratic Lyapunov functions. As seen in the figure, the PLS divides the state space in two equal partitions. However, as we will see, in order to construct piecewise quadratic Lyapunov functions, a much larger number of partitions is required to prove stability of the origin.

We start with just the natural partition of the system. Using the software developed by [34], no piecewise quadratic Lyapunov functions can be found this way. This was expected from the above proof.

A more refined partition of the state space is then required. This refinement must be supplied to the software. We decided to partition the state space with lines through the origin, including the x_2 axes, and with each separated by an

angle of $2\pi/k$ radius, where k is a positive integer. This resulted in k equally sized partitions. Table 4.1 shows the number of required partitions for the analysis of the system as a function of ϵ.

ϵ	k
≥ 0.2	> 8
$0.05 \leq \epsilon < 0.2$	> 16
< 0.05	$> ?$

Table 4.1: Number of required partitions as a function of ϵ

This table clearly shows that as ϵ decreases, the required number of partitions for the analysis of the PLS increases. For $\epsilon < 0.05$, the number of required partitions is very high and it becomes computationally intractable to prove stability of the origin using this method. Note that even for large values of ϵ, the number of required partitions is always greater than 8, although the original system is only divided in 2 partitions. ■

- Stability of equilibrium points using the approach proposed in [50, 34, 30] requires the state space to be divided in simplex partitions. For high-order systems, it is extremely hard to obtain a refinement of partitions in the state-space to efficiently analyze the PLS. In other words, the method does not scale well with the dimension of the system.

The construction of piecewise quadratic Lyapunov functions for PLS proposed in [50, 34, 30] imposes continuity of the the Lyapunov functions along the switching surfaces. This means that the intersection of two Lyapunov functions with a switching surface—one from each side—defines a unique quadratic Lyapunov function on the switching surface. Therefore, we conclude that if there are piecewise quadratic Lyapunov functions for a certain PLS, then there are also quadratic Lyapunov functions on the switching surfaces for that PLS. Note that the converse is not true. For instance, piecewise quadratic Lyapunov functions cannot be constructed to analyze limit cycles. However, as we will see in chapter 5, quadratic Lyapunov functions on switching surfaces exist and can be efficiently constructed to analyze limit cycles. It is then enough to look for Lyapunov functions on the switching surfaces instead of in the state space.

The purpose of this thesis is to show how Lyapunov functions on switching surfaces can be efficiently constructed. We call these Lyapunov functions *Quadratic Surface Lyapunov Functions*. Properties of many PLS can be inferred just by analyzing the behavior of the system at switching surfaces. Since a PLS behaves linearly inside a cell, only one of the following three things can happen to a trajectory entering a cell at some point x_0 on a switching surface:

1. The cell is unbounded and there exists a trajectory that will grow unbounded without ever switching. In this case, x_0 belongs to an unstable region and, if the PLS only has one equilibrium point or limit cycle, then these can never be globally stable.

2. There is a locally stable equilibrium point in the cell and the trajectory will asymptotically converge to it without switching. If this is the case, the initial point x_0 belongs to a stable region of that equilibrium point.

3. The trajectory will switch in finite time.

There are several ways to check if scenario 1 can happen or not. Some will be discussed in later sections and chapters. For now, assume that scenario 1 does not happen. Then, we are left with 2 and 3. If scenario 2 happens, we are done, i.e., the initial point x_0 is a stable point and so it does not require any further analysis. So, we are left with scenario 3. We can then ask several questions, like: what happens to the trajectory after it switches? Will it switch again? And, will it converge to some equilibrium point or some limit cycle? These are the sort of questions we propose to answer in this thesis. The idea is to start by analyzing individual maps from one switching surface to the next switching surface. This is the topic of this chapter. Then, in the next chapters, we show that the analysis of PLS can be reduced to the analysis of different maps from one switching surface to another switching surface.

Analysis of nonlinear systems at manifolds has been used by many researchers for a while now. The so-called *Poincaré map* was introduced in order to reduce the study of an n-dimensional system to a discrete $n-1$-dimensional system in a manifold (see, for example, [36] for an introduction to Poincaré maps). With the exception of small and specific classes of PLS, the problem is that no one really knew until now how to use these maps to globally analyze PLS. This thesis explains how it can be done and shows that our results really work in the sense that a large number of examples of certain classes of PLS, that could not be analyzed by any other method, was successfully proven globally stable.

As explained by Poincaré, there are several advantages in analyzing systems along manifolds, or, in our case, switching surfaces. First, it is a natural way to prove stability of limit cycles. In fact, that's how local stability of limit cycles was proven in section 3.3, similar to what Åström and Hagglund [5, 3] had done for relay feedback systems back in 1984. Second, an analysis method based on quadratic surface Lyapunov functions scales well with the increase of the dimension of the system. And finally, systems like the one in example 4.1 are easily analyzed using quadratic surface Lyapunov functions. This can be seen next.

Example 4.2 Consider again example 4.1. There, we showed that as ϵ goes to zero it becomes extremely hard to find piecewise quadratic Lyapunov functions to prove stability of the system. However, there are quadratic surface Lyapunov functions for Poincaré maps, for any $\epsilon > 0$, and these are easily found (see figure 4-2).

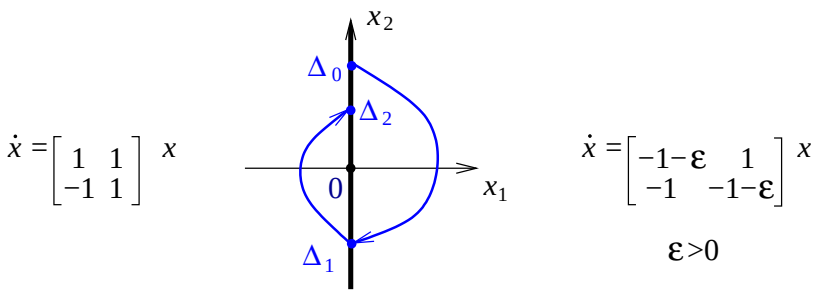

Figure 4-2: Maps from one switching surface to the next switching surface

Let A_1 be the linear matrix for the stable system and A_2 for the unstable one. For a given $\epsilon > 0$, both maps around the origin can be expressed as

$$\begin{aligned} \Delta_1 &= H_1(t_1)\Delta_0 \\ \Delta_2 &= H_2(t_2)\Delta_1 \end{aligned}$$

where $H_i(t_i) = e^{A_i t_i}$, for $i = 1, 2$. Since Δ_i belong to the x_2 axis, these can be parametrized by $\Delta_i = \Pi'\delta_i$, where $\Pi' = \begin{pmatrix} 0 & 1 \end{pmatrix}$ and $\delta_i \in \mathbb{R}$. Let

$$F_i(t_i) = \Pi' H_i(t_1)\Pi$$

Global asymptotic stability of the origin follows if there exist $p_0 > 0$ and $p_1 > 0$ such that

$$\begin{aligned} F_1'(t_1)p_1F_1(t_1) &< p_0 \qquad \text{for all expected switching times } t_1 \\ F_2'(t_2)p_0F_2(t_2) &< p_1 \qquad \text{for all expected switching times } t_2 \end{aligned}$$

Let $q = p_1/p_0 > 0$. Since the switching times are always $t_i = \pi$ for any initial condition on the switching surface, stability follows if there exists a $q > 0$ such that

$$\begin{aligned} \left[F_1(\pi)\right]^2 q &< 1 \\ \left[F_2(\pi)\right]^2 &< q \end{aligned}$$

or

$$\left[F_2(\pi)\right]^2 < q < \frac{1}{\left[F_1(\pi)\right]^2}$$

Since, for any $\epsilon > 0$, $\left[F_2(\pi)F_1(\pi)\right]^2 < 1$, the following q

$$q = \frac{\left[F_2(\pi)F_1(\pi)\right]^2 + 1}{2\left[F_1(\pi)\right]^2}$$

satisfies the stability conditions. Therefore, the origin is globally asymptotically stable. ■

This simple example serves not only to demonstrate some of the advantages of quadratic surface Lyapunov functions but also to illustrate some of the ideas we will use to analyze more complex PLS. In the example, no quadratic Lyapunov function exists for the system and piecewise quadratic Lyapunov functions are extremely hard or even impossible to construct when ϵ is small. However, quadratic Lyapunov functions on the switching surface are easily constructed for any $\epsilon > 0$. This, in turn, shows the origin is globally asymptotically stable for all $\epsilon > 0$.

4.2 Impact Maps

In order to analyze PLS using quadratic surface Lyapunov functions, we first need to understand the behavior of the system as this flows from one switching surface to the next switching surface. A useful notion that we will be using throughout this thesis is that of *impact map*. An impact map is simply a map from one switching surface to the next switching surface. Only after we understand the nature of a single impact map can we look at a PLS as a whole, by combining all impact maps associated with the PLS, to conclude about stability, robustness, and performance properties of the system.

Consider the following affine linear time-invariant system

$$\dot{x} = Ax + B \tag{4.1}$$

where $x \in \mathbb{R}^n$, $A \in \mathbb{R}^{n \times n}$, and $B \in \mathbb{R}^n$. Note that we are not imposing any kind of restrictions on A. At this point, A is allowed to have stable, unstable, and pure imaginary eigenvalues. Assume (4.1) is part of some PLS, and that (4.1) is defined on some open set $X \subset \mathbb{R}^n$. Assume also a trajectory just arrived to a boundary[1] of X

$$S_0 = \{x \in \mathbb{R}^n : \ C_0 x = d_0\}$$

and the system switches to (4.1). In this chapter, we are interested in studying the impact map from some subset of S_0 to some subset of

$$S_1 = \{x \in \mathbb{R}^n : \ C_1 x = d_1\}$$

also in the boundary of X. In this scenario, some subsets of S_0 and S_1 are switching surfaces of the PLS.

By a solution of (4.1) we mean a function x defined on $[0, t]$, with $x(0) \in S_0$, $x(t) \in S_1$, $x(\tau) \in \bar{X}$ on $[0, t]$[2], and satisfying (4.1). In this case, t is a *switching time* of the solution x of (4.1) and we say a *switch* occurs at $x(t)$.

Let S_0^d be some polytopical subset of S_0 where any trajectory starting at S_0^d satisfies $x(t) \in S_1$, for some finite $t \geq 0$, and $x(\tau) \in \bar{X}$ on $[0, t]$. Let also $S_1^a \subset S_1$ be the set of those points $x_1 = x(t)$. The set S_1^a can be seen as the image set of S_0^d. We

[1] The *boundary* of X is the set of all limit points p of X such that $p \notin X$.

[2] $\bar{X}$ denotes the *closure* of X, i.e, the set $\bar{X} = X \cup \{p | \ p \text{ is a limit point of } X\}$.

call S_0^d the *departure set* in S_0 and S_1^a the *arrival set* in S_1.

We are interested in studying the impact map, induced by (4.1), from $x_0 \in S_0^d$ to $x_1 \in S_1^a$. Since both x_0 and x_1 belong to switching surfaces, they can be parametrized in their respective hyperplanes. For that, let

$$\begin{aligned} x_0 &= x_0^* + \Delta_0 \\ x_1 &= x_1^* + \Delta_1 \end{aligned}$$

where $x_0^* \in S_0$, $x_1^* \in S_1$, and Δ_0, Δ_1 are any vectors such that $C_0\Delta_0 = C_1\Delta_1 = 0$. Define also $x_0^*(t)$ as the trajectory of (4.1), starting at x_0^*, for all $t \geq 0$. The impact map of interest reduces to the map from Δ_0 to Δ_1 (see figure 4-3).

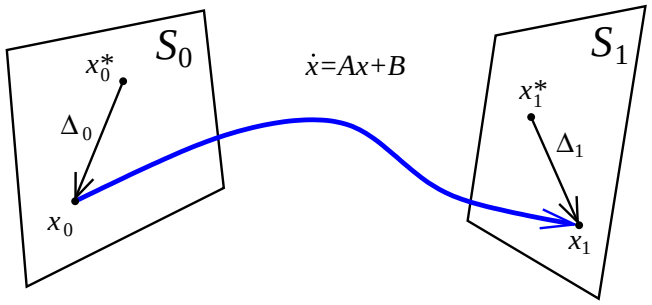

Figure 4-3: Impact map from $\Delta_0 \in S_0^d - x_0^*$ to $\Delta_1 \in S_1^a - x_1^*$

Note that the impact map from $\Delta_0 \in S_0^d - x_0^*$ to $\Delta_1 \in S_1^a - x_1^*$ defined above is not continuous and it is multivalued. This is illustrated in the following example.

Example 4.3 Consider a 3[rd]-order system given by

$$\dot{x} = \begin{pmatrix} -1 & 0 & 0 \\ 0 & -2 & 0 \\ 0 & 0 & -3 \end{pmatrix} x + \begin{pmatrix} 1 \\ 1 \\ 1 \end{pmatrix}$$

with the switching surfaces defined above given by $C_0 = C_1 = [-2 \;\; 2 \;\; 1]$, and $d_0 = 0.5$, $d_1 = -0.5$. Let $X = \{x |\, d_1 < C_1 x(t) < d_0\}$. In the state space, the switching surfaces are parallel to each other. Let $x(0) \approx [-52 \;\; 80 \;\; -63]^T \in S_0$. The resulting $C_1 x(t)$ can be seen in figure 4-4.

When $t \approx 0.47$, $C_1 x(t) = d_1$ and $\dot{y}(t-0) = 0$. At this point, the trajectory can return to X (dash trajectory), or it can switch. This means that a switch can occur at either $t = 0.47$ or $t = 2.85$.

Let $x_0^* = x(0)$ and $x_1^* = x(0.47)$. The impact map from Δ_0 to Δ_1, as defined above, is also not continuous since in a small enough neighborhood $\mathcal{W} \subset S_1$ of x_1^*, there is no neighborhood $\mathcal{W}_0 \subset S_0$ of x_0^* such that every point in $\mathcal{W}_0$ is mapped in $\mathcal{W}$ (see figure 4-5). In this figure, we have two initial conditions in a small neighborhood of x_0^*. One of these (in the figure, the one on the left) switches "close" to x_1^* while the other (the one of the right) switches "far" from x_1^*. ■

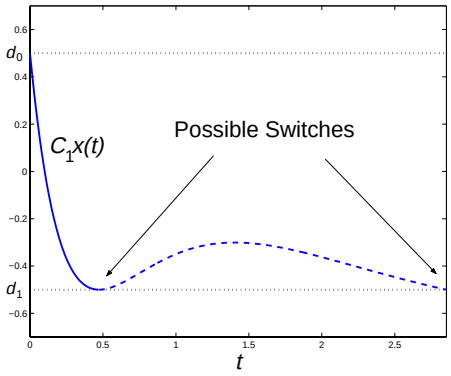

Figure 4-4: Existence of multiple solutions

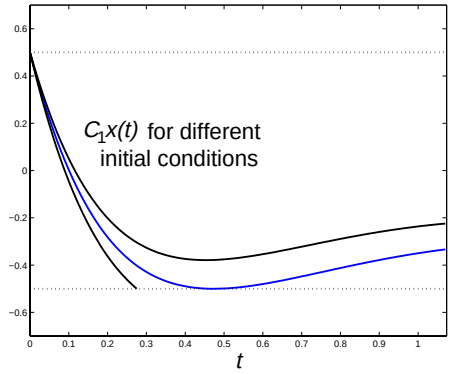

Figure 4-5: Map from Δ_0 to Δ_1 is not continuous

Definition 4.1 Let $x(0) = x_0^* + \Delta_0$. Define t_{Δ_0} as the set of all times $t_i \geq 0$ such that the trajectory $x(t)$ with initial condition $x(0)$ satisfies $C_1 x(t_i) = d_1$ and $x(t) \in \bar{X}$ on $[0, t_i]$. Define also the set of *expected switching times* of the impact map from $\Delta_0 \in S_0^d - x_0^*$ to $\Delta_1 \in S_1^a - x_1^*$ as

$$\mathcal{T} = \left\{ t |\ t \in t_{\Delta_0},\ \Delta_0 \in S_0^d - x_0^* \right\}$$

For instance, in the last example, $t_{\Delta_0} = \{0.47, 2.85\}$ for the initial condition $x(0)$.

As seen, the impact map is nonlinear, multivalued, and not continuous. Once an initial condition in S_0^d is given, the first step is to find an associated switching time t. However, solving for t involves solving a transcendental equation. Solution to such equations cannot, in general, be written in a closed form, and numerical procedures are typically the only way to solve for t. Once a switching time is found, we can finally find the corresponding Δ_1.

The "non-friendly" nature of the impact map from Δ_0 to Δ_1 has been the main reason why global analysis of PLS has not been done using quadratic surface Lyapunov functions. The following result, however, shows that this map is not as "bad" as it looks, and opens the door to analysis of PLS in switching surfaces.

Theorem 4.1 *Assume $C_1 x_0^*(t) \neq d_1$ for all $t \in \mathcal{T}$. Define*

$$w(t) = \frac{C_1 e^{At}}{d_1 - C_1 x_0^*(t)}$$

and let

$$H(t) = e^{At} + (x_0^*(t) - x_1^*)\, w(t)$$

Then, for any $\Delta_0 \in S_0^d - x_0^*$ there exists a $t \in \mathcal{T}$ such that the impact map is given by

$$\Delta_1 = H(t)\Delta_0 \tag{4.2}$$

Such $t \in t_{\Delta_0}$ is the switching time associated with Δ_1.

This theorem says that maps between switching surfaces, induced by an LTI flow, can be represented as linear transformations analytically parametrized by a scalar function of the state. At first, equation (4.2) may not seem of great help in analyzing the impact map from Δ_0 to Δ_1. There, Δ_1 is a linear function of Δ_0 and a nonlinear function of t, the switching time associated with Δ_0 and Δ_1. The switching time, however, is a function of Δ_0. A transcendental equation needs to be solved in order to find t. Thus, by this reasoning, it seems (4.2) is saying that Δ_1 is a nonlinear function of Δ_0. But, that we already knew.

This is, however, just one way of thinking about (4.2). Fortunately, there are other ways to approach equation (4.2). Assume, for a second, the switching time t is fixed. The result: the impact map (4.2) would be linear! But, what does it mean to have the switching time t is fixed? In other words, what are the set of points $x_0^* + \Delta_0$ in the switching surface S_0 such that every point in that set has a switching time of t? In that set, the impact map (4.2) is linear.

It turns out that the set of points in S_0^d that have a switching time of t is a convex subset of a linear manifold of dimension $n-2$ (see figure 4-6). Let S_t be that set, that is, the set of points $x_0^* + \Delta_0 \in S_0^d$ such that $t \in t_{\Delta_0}$. In other words, a trajectory starting at $x_0 \in S_t$ satisfies both $x(\tau) \in \bar{X}$ on $[0, t]$, and $C_1 x(t) = d_1$. Note that since the impact map is multivalued, a point in S_0^d may belong to more than one set S_t. In fact, in example 4.3, there existed a point in S_0^d that belonged to both $S_{0.47}$ and $S_{2.85}$.

Note also that, as $t \in \mathcal{T}$ changes, S_t covers every single point of S_0^d, i.e., $S_0^d = \{x |\ x \in S_t,\ t \in \mathcal{T}\}$. This follows since every point $\Delta_0 \in S_0^d - x_0^*$ can switch for the first time at S_1^a, and therefore t_{Δ_0} is always a nonzero set. These results can all be summarized in the following corollary.

Corollary 4.1 *Under the assumptions of theorem 4.1, for a given $t \in \mathcal{T}$, the impact map from $\Delta_0 \in S_t - x_0^*$ to $\Delta_1 \in S_1 - x_1^*$, given by $\Delta_1 = H(t)\Delta_0$, is a linear map. Moreover, S_t is a subset of a linear manifold of dimension $n-2$, and $S_0^d = \{x |\ x \in S_t,\ t \in \mathcal{T}\}$.*

As we will see in section 4.3 and succeeding chapters, this result is fundamental in the analysis of PLS using quadratic surface Lyapunov functions. It allows us to find

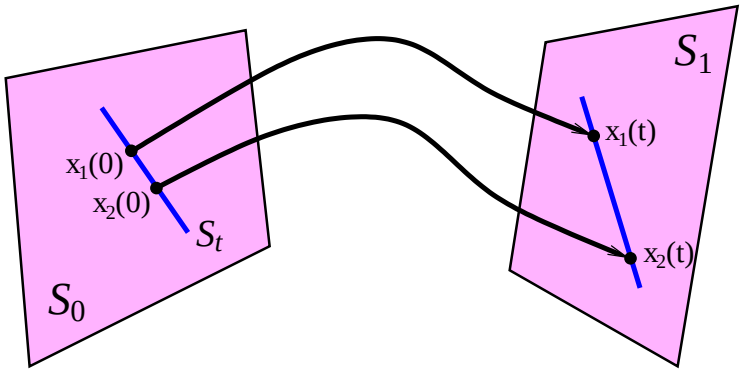

Figure 4-6: Every point in S_t has a switching time of t

conditions in the form of LMIs that, when satisfied, guarantee stability, robustness, and performance of PLS.

Before moving onto the proofs of the above results, it is important to understand the meaning of the assumption in theorem 4.1. This says the trajectory $x_0^*(t)$ cannot intersect the switching surface S_1 for all $t \in \mathcal{T}$. With a careful choice of $x_0^* \in S_0$ (the initial condition of $x_0^*(t)$), there are many cases when this assumption is always satisfied. The details on how this is done can be found in both chapters 6 and 7, and are, therefore, omitted here.

There are, however, cases where no choice of $x_0^* \in S_0$ satisfies the assumption. Or, in other cases, x_0^* is fixed a priori, and it may not satisfy the assumption (like in chapter 5, where the location of x^* in S_0 cannot be freely chosen). In these worst case scenarios, there is at least one $t_s \in \mathcal{T}$ such that $w(t_s)$ is unbounded. This does not mean we cannot obtain the desired linear representation for the impact map. For some PLS, like RFS, at some $t = t_s$ the map is defined via continuation, and the theorem follows. If this is not the case, the theorem needs to be slightly modified. Basically, at $t = t_s$, the impact map can still be written as a linear transformation but parametrized by another variable at t_s, i.e., $\Delta_1 = H_s(t_s, \delta)\Delta_0$, with $\Delta_0 \in S_{t_s}$.

4.2.1 Proof of Results

Proof of theorem 4.1: We start by expressing Δ_1 as function of Δ_0 and t, the switching time associated with Δ_1. Let $x(0) = x_0 \in S_0^d$. Integrating the differential equation (4.1) gives

$$x_1 = e^{At}x_0 + \int_0^t e^{A(t-\tau)}Bd\tau$$

Since $x_i = x_i^* + \Delta_i$, $i = 0, 1$,

$$\begin{aligned}\Delta_1 &= e^{At}\Delta_0 + e^{At}x_0^* + \int_0^t e^{A(t-\tau)}Bd\tau - x_1^* \\ &= e^{At}\Delta_0 + x_0^*(t) - x_1^*\end{aligned}$$

From the fact $C_1\Delta_1 = 0$ and $C_1 x_1^* = d_1$ we get

$$C_1 e^{At}\Delta_0 = d_1 - C_1 x_0^*(t) \tag{4.3}$$

Since, by assumption, $C_1 x_0^*(t) \neq d_1$ for all $t \in \mathcal{T}$, the last expression can be written as

$$w(t)\Delta_0 = 1 \tag{4.4}$$

which means Δ_1 reduces to

$$\Delta_1 = e^{At}\Delta_0 + (x_0^*(t) - x_1^*)\, w(t)\Delta_0$$

which proves the desired result. ■

Note that if A is invertible, $x_0^*(t)$ is given by $x_0^*(t) = e^{At}(x_0^* + A^{-1}B) - A^{-1}B$.

Proof of corollary 4.1: The only thing left to prove is that S_t is a subset of a linear manifold of dimension $n-2$. Let $x_0 = x_0^* + \Delta_0 \in S_t$. Since $C_1 x(t) = d_1$, Δ_0 must satisfy equation (4.3), and $C_0\Delta_0 = 0$ since $\Delta_0 \in S_0 - x_0^*$, which are both linear equalities. Δ_0 also satisfies a set of linear inequalities from the fact that $x_0 \in S_0^d$, $x(t) \in S_1^a$, and $x(\tau) \in \bar{X}$ on $[0, t]$. Therefore, $S_t - x_0^*$ has at the most dimension $n-2$ and is linear. ■

4.3 Quadratic Surface Lyapunov Functions

Construction of Lyapunov functions for nonlinear systems is, and has been, a difficult, and sometimes, frustrating task. As explained before, there has been some results in constructing piecewise quadratic Lyapunov functions for PLS. Although these results are able to analyze equilibrium points of certain classes of PLS, many important PLS cannot be analyzed this way because either they have limit cycles or the method is computationally too expensive.

An alternative to constructing Lyapunov functions in the state space is to construct Lyapunov functions on switching surfaces. Define then two quadratic Lyapunov functions on the switching surfaces S_0^d and S_1^a. Respectively, let V_0 and V_1 be given by

$$V_i(x) = x' P_i x - 2x' g_i + \alpha_i \tag{4.5}$$

where $P_i > 0$, for $i = 0, 1$. These are Lyapunov candidates defined of the switching surfaces with parameters $P_i > 0$, g_i, and α_i, to be found.

Next, we want to show an impact map from $S_0^d \subset S_0$ to $S_1^a \subset S_1$ is contracting in some sense. In particular, an impact map is quadratically stable if there exist $P_i > 0$, g_i, α_i such that

$$V_1(\Delta_1) < V_0(\Delta_0) \quad \text{for all } \Delta_0 \in S_0^d - x_0^* \tag{4.6}$$

Let $P > 0$ on S stand for $x'Px > 0$ for all nonzero $x \in S$. As a short hand, we will be using H_t for $H(t)$ and w_t for $w(t)$. The following theorem uses the results from section 4.2 to derive a set of matrix inequalities equivalent to condition (4.6).

Theorem 4.2 *Define*

$$R(t) = P_0 - H_t' P_1 H_t - 2\left(g_0 - H_t' g_1\right) w_t + w_t' \alpha w_t$$

where $\alpha = \alpha_1 - \alpha_2$. *The impact map from* $\Delta_0 \in S_0^d - x_0^*$ *to* $\Delta_1 \in S_1^a - x_1^*$ *is a contraction if there exist* $P_0, P_1 > 0$ *and* g_0, g_1, α *such that*

$$R(t) > 0 \quad \text{on } S_t - x_0^* \tag{4.7}$$

for all expected switching times $t \in \mathcal{T}$.

Basically, all this theorem does is substitute (4.2) in (4.6), and use both facts that the map Δ_0 to Δ_1 is linear in S_t and that, as t ranges over $\mathcal{T}$, S_t covers every point in S_0^d.

4.3.1 Approximation to a Set of LMIs

There are many ways to approximate condition (4.7) with a set of LMIs, which can be efficiently solved using available software. A trivial one is to relax the constraints on Δ_0 in theorem 4.2. On one hand, this results in a more conservative condition. On the other hand, such conditions are computationally efficient.

Corollary 4.2 *The impact map from* $\Delta_0 \in S_0^d - x_0^*$ *to* $\Delta_1 \in S_1^a - x_1^*$ *is a contraction if there exist* $P_0, P_1 > 0$ *and* g_0, g_1, α *such that*

$$R(t) > 0 \quad \text{on } S_0 - x_0^* \tag{4.8}$$

for all expected switching times $t \in \mathcal{T}$.

This result uses the ideas from the previous section to show that the problem of quadratic stability of an impact map reduces to the solution of a infinite dimensional set of LMIs. As we will see in later chapters, although condition (4.8) is more conservative than condition (4.7), in many situations it is enough to successfully and efficiently analyze PLS.

(4.8) for all $t \in \mathcal{T}$ forms an infinite set of LMIs. Computationally, to overcome this difficulty, we grid this set to obtain a finite subset of expected switching times. This grid consists of a finite sequence of switching times $t_0 < t_1 < \cdots < t_k$. In other words, $P_i > 0$, g_i, and α are found by solving a finite set of LMIs consisting of (4.8) on $t = \{t_i\}$, $i = 0, 1, ..., k$. For a large enough k, it can be shown that (4.8) is also satisfied for all $t \in \mathcal{T}$. The idea here is to find bounds on the derivative of the minimum eigenvalue of $R(t)$ over (t_i, t_{i+1}), and to use these bounds to show that nothing can go wrong in the intervals (t_i, t_{i+1}), i.e., that (4.8) is also satisfied on each interval (t_i, t_{i+1}).

$n-1$ Dimensional Map

Next, we show that condition (4.8) can in fact be written as an an equivalent set of LMIs. Note that although the vectors Δ_0 and Δ_1 are n-dimensional, the solution

generated by the impact map is restricted to the $n-1$-dimensional hyperplanes S_0 and S_1 (see figure 4-7). Thus, the impact map is actually a map from $\mathbb{R}^{n-1}$ to $\mathbb{R}^{n-1}$. Let $\Pi_0 \in C_0^{\perp}$ be a map from $\mathbb{R}^{n-1}$ to S_0, where $C_0^{\perp}$ are the *orthogonal complements* to C_0, i.e., matrices with a maximal number of column vectors forming an orthonormal set such that $C_0 C_0^{\perp} = 0$.

Condition to (4.8) is equivalent to

$$\Delta_0' R(t) \Delta_0 > 0 \quad \text{for all } \Delta_0 \in S_0 - x_0^*$$

Since $C_0 \Delta_0 = 0$, we can write $\Delta_0 = \Pi_0 \delta_0$, where $\delta_0 \in \mathbb{R}^{n-1}$. Hence, the last matrix inequality is equivalent to

$$\Pi_0' R(t) \Pi_0 > 0$$

which is an infinite dimensional set of LMIs.

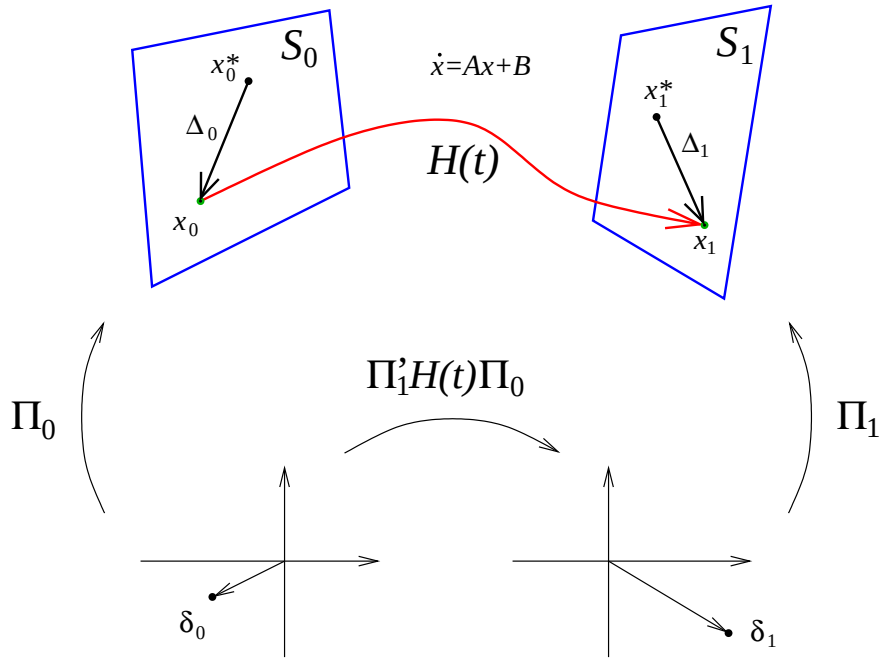

Figure 4-7: $n-1$ dimensional map

Meaning of condition (4.7)

It is possible to make condition (4.8) less conservative at a cost of an increase in computations. This condition takes only into account that $\Delta_0 \in S_0 - x_0^*$. The remaining of this section, explains how to approximate condition (4.7) with a set of LMIs.

Let's first see what exactly is condition (4.7). For every $t \in \mathcal{T}$, we want

$$\Delta_0' R(t) \Delta_0 > 0$$

for all Δ_0 such that $\Delta_0 \in S_t$, or equivalently, that

$$\begin{cases} \Delta_0 \in \{x \in S_0 |\ x \text{ can be reached by some trajectory of the PLS}\} - x_0^* \\ C_1 H(t) \Delta_0 = 0 \\ x(\tau) \in \bar{X}, \text{ for all } \tau \in [0, t] \end{cases} \tag{4.9}$$

Next, we explain in detail each constraint in (4.9), starting with the first inclusion. The switching surfaces S_0 and S_1, together with (4.1), are part of some PLS. The set S_0^d can exclude those points in S_0 that cannot be reached by a trajectory of the PLS starting somewhere in $\mathbb{R}^n \setminus S_0$.

Example 4.4 Figure 4-8 shows a PLS with both switching surfaces S_0 and S_1, and X defined between them. Above the switching surface S_0 we have system $\dot{x} = A_1 x + B_1$. In the figure we see the vector fields of systems 1 and (4.1) along the switching surface S_0 (above and below, respectively), and the vector field of (4.1) along the switching surface S_1. The points $\bar{x}_0$, $\bar{x}_1$, and $\bar{x}_2$ are the points where $C_0(A_1\bar{x}_0 + B_1) = 0$, $C_0(A\bar{x}_1 + B) = 0$, and $C_1(A\bar{x}_2 + B) = 0$. Note that $\bar{x}_1$ must be to the left of $\bar{x}_0$ in order to guarantee existence of solutions.

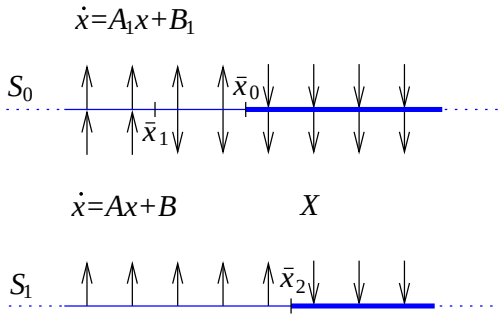

Figure 4-8: $S_0^d \subset S_0$ and $S_1^a \subset S_1$ are some sets defined to the right of $\bar{x}_0$ and $\bar{x}_2$, respectively

As seen in the figure, points in S_0 between $\bar{x}_0$ and $\bar{x}_1$ cannot be reached by any trajectory starting somewhere in $\mathbb{R}^n \setminus S_0$. Points to the left of $\bar{x}_1$ do not belong to the domain of the impact map from S_0 to S_1. Thus, only points to the right of $\bar{x}_0$ can belong to S_0^d. Note that those are exactly the points that can be reached by system 1. Similarly, only some points to the right of $\bar{x}_2$ can be reached by (4.1). Hence, $S_1^a \subset S_1$ is some set defined to the right of $\bar{x}_2$. ■

The first inclusion of (4.9) is then composed of a linear equality together with a set of linear inequalities. The equality, $C_0\Delta_0 = 0$, comes from the fact that $\Delta_0 \in S_0 - x_0^*$. As seen before, all it is needed here is a change of variables $\Delta_0 = \Pi_0 \delta_0$, where $\delta_0 \in \mathbb{R}^{n-1}$. As for the inequalities, they are necessary to ensure that every point in S_0^d can be reached by some trajectory of the PLS, starting somewhere in $\mathbb{R}^n \setminus S_0$ (see example 4.4 and figure 4-9). So, for each system i that shares a boundary with X through S_0, consider those points in S_0 for which the vector field along S_0 points

inward (see figure 4-9). The set of points in S_0 where the vector field of system i is parallel to S_0 are those where $C_0\dot{x} = 0$, i.e., $C_0(A_ix + B_i) = 0$, $x \in S_0$. As in the left of figure 4-9, assume C_0' orientation points towards X (if this is not the case, just consider $-C_0'$ and $-d_0$). The set of points in S_0 that can be reached by system i is some subset of the set of points such that $C_0(A_ix + B_i) > 0$, $x \in S_0$.

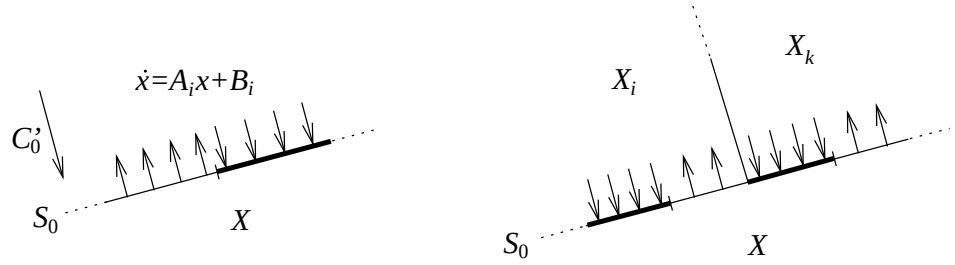

Figure 4-9: Sets in S_0 where S_0^d can be defined, for two different PLS

The equality in (4.9) arises from the fact that $\Delta_1 \in S_1 - x_1^*$, i.e., $C_1\Delta_1 = 0$. In terms of Δ_0, we have equality (4.3), that we repeat here

$$C_1 e^{At}\Delta_0 = d_1 - C_1 x_0^*(t) \tag{4.10}$$

This equality automatically excludes those points in S_0 that do not intersect S_1, since such points do not have a finite solution $t > 0$ satisfying (4.10). Note that (4.10) depends on $t \in \mathcal{T}$, contrasting with the first equality $C_0\Delta_0 = 0$, which is independent of t.

The last inclusion in (4.9) ensures that a trajectory $x(\tau)$, starting at some point in S_0, stays in the closure of X, i.e., in $\bar{X}$, for all $\tau \in [0, t]$. Thus, the first switch must occur at S_1 (see figure 4-10). The inclusion consists of several infinite dimensional sets of linear inequalities, one for each boundary of X. For instance, in figure 4-10, it must be true that $C_jx(\tau) \geq d_j$, $j = 0, 1, 2$, for all $\tau \in [0, t]$, assuming C_j' orientations point towards X, as in the figure.

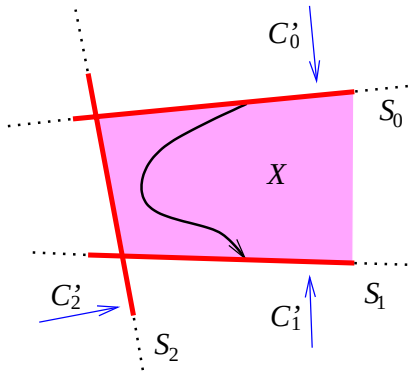

Figure 4-10: Trajectories starting at S_0 must remain in X

Less conservative conditions: equality plus one inequality

It was clear from the above description of the set S_t why condition (4.7) cannot, in general, be written as a equivalent set of LMIs. Basically, the characterization of the set S_t is too complicated. A straightforward transformation of (4.7) into a set of LMIs was to use only the equality $C_0\Delta_0 = 0$. This resulted in a more conservative condition (4.8). As for the others equality and inequalities, that is a different story. To date, there is no non-conservative way to incorporate several linear and quadratic inequality constraints and reduce the problem to a set of LMIs. Application of the S-procedure, introduced in section 2.3, results in equivelent, and therefore non-conservative, conditions, only when a quadratic function is subject to a single quadratic constraint. However, this is not the case here.

In this subsection, we show how equality (4.10) plus one inequality can be used to approximate (4.7) with a set of LMIs, resulting in conditions less conservative than (4.8). In the next subsection, we briefly discuss how to include other inequalities using the S-procedure.

First, we are going to approximate S_t with a larger set. For a given $t \in \mathcal{T}$, let $\tilde{S}_t \supset S_t$ be the set of points in S_0 where $C_1x(t) = d_1$. This can be obtained from (4.10), yielding

$$\tilde{S}_t = \left\{ x_0^* + \Delta_0 \in S_0 : \; C_1 e^{At}\Delta_0 = d_1 - C_1 x_0^*(t) \right\}$$

To see the differences between S_t and $\tilde{S}_t$, consider again example 4.3. Figure 4-11 shows the solution $C_1x(t)$ for two different initial conditions in S_0^d.

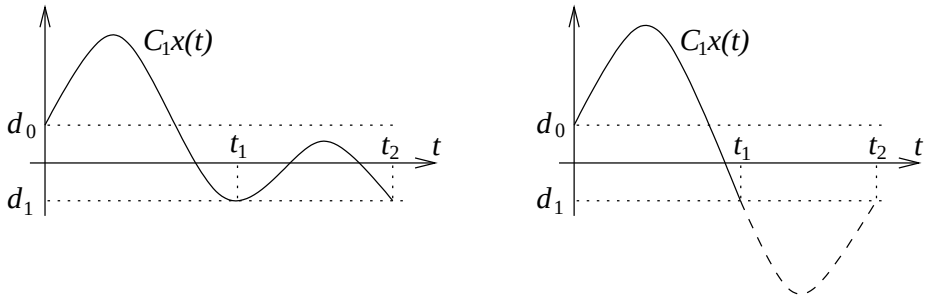

Figure 4-11: On the left: $C_1x(t) \geq d_1$ for $0 \leq t \leq t_2$; on the right: $C_1x(t) < d_1$ for $t_1 < t < t_2$

On the left of figure 4-11, $t_{\Delta_0} = \{t_1, t_2\}$. This means $x_0^* + \Delta_0$ belongs to both S_{t_1}, and S_{t_2}. The right side of figure 4-11 shows what would happen to $C_1x(t)$ if the trajectory had not switched at $t = t_1$ (dashed curve). In that case, it would have intersected S_1 again at $t = t_2$. This means that although t_2 is a solution of (4.10), it is not a switching time since $C_1x(t) < 0$ for $t_1 < t < t_2$. In other words, the switching time t_2 does not satisfy the inequality $C_1x(t) \geq d_1$ on $[0, t_2]$. Although both t_1 and t_2 satisfy (4.10), only t_1 is a valid switching time, i.e., $t_{\Delta_0} = \{t_1\}$. Thus, $x_0^* + \Delta_0$ belongs to $\tilde{S}_{t_1}$, S_{t_1}, and $\tilde{S}_{t_2}$, but it does not belong to S_{t_2}.

Since $S_t \subset \tilde{S}_t$, condition (4.7) holds if there exist $P_1, P_2 > 0$, g_1, g_2, α such that

$$R(t) > 0 \quad \text{on } \tilde{S}_t - x_0^* \tag{4.11}$$

for all expected switching times $t \in \mathcal{T}$.

In order to transform the last matrix inequality into a set of LMIs, we need to better characterize the set $\tilde{S}_t$. For that, we are going to use one inequality from (4.9) together with equality (4.10). As discussed above, there are many inequalities to choose from. For the purpose of demonstrating how this is done, just assume we choose one of these inequalities, represented here by some L and m such that $L\Delta_0 > m$. A less conservative condition than (4.11) is then

$$R(t) > 0 \quad \text{on } \left(\tilde{S}_t \bigcap \{x_0^* + \Delta_0 |\ L\Delta_0 > m\}\right) - x_0^* \tag{4.12}$$

for all expected switching times $t \in \mathcal{T}$ (see figure 4-12).

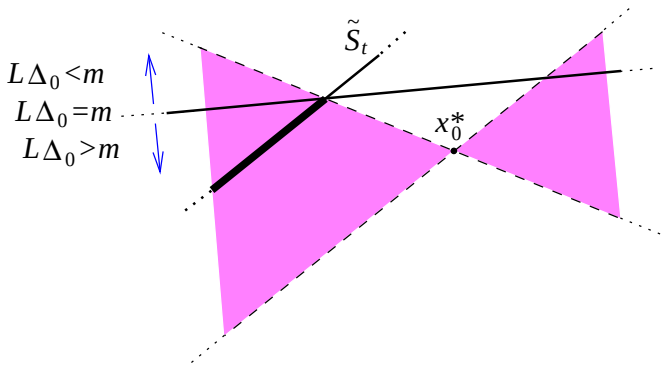

Figure 4-12: Region in S_0 defined by equality (4.10) and the inequality $L\Delta_0 > m$ satisfies a conic relation

As seen in figure 4-12, $\Delta_0 \in \left(\tilde{S}_t \bigcap \{x_0^* + \Delta_0 |\ L\Delta_0 > m\}\right) - x_0^*$ satisfies a conic relation

$$\Delta_0' \beta_t \Delta_o > 0$$

for some matrix β_t (the construction of this matrix will be addressed in section 4.5). Using the S-procedure, condition (4.12) is equivalent to

$$R(t) - \tau_t \beta_t > 0 \quad \text{on } S_0 - x_0^* \tag{4.13}$$

for some scalar function $\tau_t > 0$, and for all expected switching times $t \in \mathcal{T}$. Note that, for each t, (4.13) is now an LMI.

Less conservative conditions: other inequalities

It is still possible to improve conditions (4.13) further more. They do not take advantage of all other inequalities, including all of those arising from the last inclusion in (4.9). In this subsection, we show how to incorporate other linear constraints,

and will also discuss tradeoffs between less conservative and computationally efficient conditions.

In order to guarantee, for instance, that $x(\tau) \in \bar{X}$ on $[0, t]$, it is necessary that the trajectory $x(\tau)$ stays to the correct side of all switching surfaces that compose the boundary X. In particular, it must be true that $C_1 x(\tau) \geq d_1$ for all $\tau \in [0, t]$, i.e.,

$$C_1 \left(e^{A\tau} \Delta_0 + x_0^*(\tau) \right) \geq d_1$$

for all $\tau \in [0, t]$. This is an infinite dimensional set of linear inequalities. To overcome this difficulty, we consider a finite number of values of τ in $[0, t]$. For example, if $\tau = t/2$, we could have the following linear constraint on Δ_0

$$C_1 e^{At/2} \Delta_0 \geq d_1 - C_1 x_0^*(t/2)$$

As before, this inequality, together with $\tilde{S}_t$ satisfies a conic relation $\Delta_0' \gamma_{t/2} \Delta_0 > 0$ in which (4.12) would be improved to

$$R(t) - \tau_t \beta_t - \tau_{1t} \gamma_{t/2} > 0 \quad \text{ on } S_0 - x_0^* \tag{4.14}$$

for some scalar function $\tau_{1t} > 0$, and for all expected switching times $t \in \mathcal{T}$.

There is an infinite number of constraints that can be added to condition (4.14) in order to further reduce the level of conservatism. On one hand, the more constraints, the less conservative conditions we get and, in turn, better chances of finding quadratic surface Lyapunov functions (4.5). On the other hand, increasing the number of constraints will eventually make the problem computationally intractable. In spite of this, and as we will see later on, it is interesting to notice that many important PLS can be analyzed with just conditions of the form (4.8), the most conservative of all the ones presented.

4.3.2 Proof of Results

Proof of theorem 4.2: From (4.6) and using theorem 4.1, we have

$$\begin{aligned} & \Delta_1' P_1 \Delta_1 - 2\Delta_1' g_1 + \alpha_1 < \Delta_0' P_0 \Delta_0 - 2\Delta_0' g_0 + \alpha_0 \\ \Leftrightarrow \quad & \Delta_0' H_t' P_1 H_t \Delta_0 - 2\Delta_0' H_t' g_1 + \alpha_1 < \Delta_0' P_0 \Delta_0 - 2\Delta_0' g_0 + \alpha_0 \\ \Leftrightarrow \quad & \Delta_0' \left(P_0 - H_t' P_1 H_t \right) \Delta_0 - 2\Delta_0' \left(g_0 - H_t' g_1 \right) + \alpha > 0 \end{aligned}$$

Finally, using (4.4) we have

$$\Delta_0' \left(P_0 - H_t' P_1 H_t \right) \Delta_0 - 2\Delta_0' \left(g_0 - H_t' g_1 \right) w_t \Delta_0 + \Delta_0' w_t' \alpha w_t \Delta_0 > 0$$

Condition (4.7) follows from corollary 4.1, which proofs the desired result. ■

Proof of corollary 4.2: The proof follows since $S_0 \supset S_t$. ■

4.4 Classes of PLS

We have seen how global analysis of a single impact map can be done using quadratic Lyapunov functions defined on switching surfaces. The following chapters will answer the question: how to combine different impact maps associated with a PLS to globally analyze the system? Basically, for a general PLS, analysis of a single impact map is not enough to conclude about global stability and performance properties of the system. As we will see, the combination of several impact maps to globally analyze PLS is straightforward in some cases, and more complex in others.

We will analyze several well known and very distinct classes of PLS by increasing order of complexity. These are: relay feedback system (chapter 5), on/off systems (chapter 6), and saturation systems (chapter 7). Next, we explain the reasons why we analyze these particular classes of PLS, and what are the main difficulties we will encounter in each one of them.

- Relay Feedback Systems (RFS). This is one of the simplest, if not the simplest, class of PLS. But, make no mistake: this is already a very hard class of PLS to analyze. To prove it are the many attempts by researchers to analyze RFS over the last decades. In spite of all the efforts, no general global analysis methodologies resulted from all this research. In other words, the problem of rigorous global analysis of RFS is still open.

  In the state space, RFS consist of two affine linear systems together with two parallel switching surfaces. In between the switching surfaces, the choice of the affine linear system is based on past values of the state. In chapter 5, we will analyze symmetric unimodal limit cycles[3], although the results there can be generalized to study other classes of limit cycles.

  The reason why we start with this class of systems is that there is only a single impact map that needs to be analyzed. In fact, RFS are simple enough that the results developed in this chapter can almost be directly applied. This gives a chance to prove that the ideas in this chapter have great potential in globally analyzing PLS. If the methodology introduced in this chapter would fail to analyze RFS, most likely there would be no reason to expect it to successfully analyze other more complex classes of PLS. As we will see in the next chapter, this was not the case, and we successfully proved global asymptotic stability of a large number of RFS analyzed.

- On/Off Systems (OFS). After successfully globally analyzing limit cycles of RFS, the question is if we can use the same ideas to prove global asymptotically stability of equilibrium points of PLS. The analysis of limit cycles at switching surfaces was natural since we were simply checking if an impact map was getting close to the intersection of the limit cycle with the switching surface. In case of PLS with equilibrium points that do not belong to the switching surface, the

[3] A limit cycle is *unimodal* if it only switches twice per cycle.

analysis of the corresponding impact maps is not as straightforward as in the case of RFS.

OFS are characterized by an LTI system in feedback with a nonlinear static controller that switches between closed loop (on) and open loop (off) depending on the value of the output of the LTI system. In the state space, the system is composed of two affine linear systems separated by a single switching surface that may or may not include the equilibrium point being analyzed. The two most important contributions of chapter 6 are (1) to show that the ideas from chapter 4 can be used to globally analyze equilibrium points and (2) to explain how more than one impact map is simultaneously analyzed.

Although several classic analysis methodologies exist to globally analyze OFS, all fail when OFS have unstable nonlinearity sectors. We will show, however, that this is no problem in our case. Even those OFS can be globally analyzed using impact maps and quadratic surface Lyapunov functions.

- The last class of PLS that we will analyze is saturation systems (SAT). SAT are characterized by an LTI system in feedback with a saturation controller. In the state space they consist of three different affine linear systems, separated by two switching surfaces. They are, therefore, perfect to show how the ideas introduced in chapter 4 can be applied to globally analyze equilibrium points of PLS with more than one switching surface. How to deal with multiple switching is then the main contribution of this chapter.

4.5 Technical Details: Construction of Conic Relations

We now describe how to construct the cones β_t introduced in section 4.3.1. Remember that for each $t > 0$, the cone is defined by two hyperplanes in S_0: one is the hyperplane parallel to $\tilde{S}_t$ containing x_0^* and the other is the hyperplane defined by the intersection of $\mathcal{M} = \{x_0^* + \Delta_0 \in S_0 |\ L\Delta_0 = m\}$ and $\tilde{S}_t$, and containing the point x_0^* (see figure 4-12). Let $\Pi_0 l_t$ and $\Pi_0 s_t$, respectively, be vectors in S_0 perpendicular to each hyperplane. Once these vectors are known, the cone can easily be characterized. This is composed of all the vectors $\Delta_0 \in S_0 - x_0^*$ such that $\Delta_0' \Pi_0 (s_t l_t' + l_t s_t') \Pi_0' \Delta_0 \geq 0$. The symmetric matrix β_t introduced in (4.13) is just $\beta_t = \Pi_0 \bar{\beta}_t \Pi_0'$ where $\bar{\beta}_t = s_t l_t' + l_t s_t'$. Remember that the cone is centered at x_0^* and note that after l_t is chosen, s_t must have the right direction in order to guarantee $(\tilde{S}_t \cap \{x_0^* + \Delta_0 |\ L\Delta_0 > m\}) \subset \{x_0^* + \Delta_0 \in S_0 |\ \Delta_0' \beta_t \Delta_0 > 0\}$.

We first find $\Pi_0 l_t$, the vector perpendicular to $\tilde{S}_t$. Looking back at the definition of $\tilde{S}_t$, l_t is given by

$$l_t = \frac{(C_1 e^{At} \Pi_0)'}{\|C_1 e^{At} \Pi_0\|^2} (d_1 - C_1 x_0^*(t))$$

The derivation of s_t is not as trivial as l_t. We actually need to introduce a few extra

variables. The first one is $\Pi_0 l_0$, the vector perpendicular to the set $\mathcal{M}$, given by

$$l_0 = \frac{(L\Pi_0)'}{\|L\Pi_0\|^2} m$$

Proposition 4.1 *The hyperplane defined by the intersection of $\mathcal{M}$ and $\tilde{S}_t$, and containing the point x_0^* is perpendicular to the vector*

$$\frac{\Pi_0 l_t}{\|l_t\|}\|l_0\| - \frac{\Pi_0 l_0}{\|l_0\|}\|l_t\|$$

Proof: $\mathcal{M}$ can be parameterize the following way

$$\mathcal{M} = \left\{ x_0^* + \Delta_0 \in S_0 |\ \Delta_0 = \Pi_0(l_0 + l_0^{\perp} z),\ z \in \mathbb{R}^{n-2} \right\}$$

and $\tilde{S}_t$

$$\tilde{S}_t = \left\{ x_0^* + \Delta_0 \in S_0 |\ \Delta_0 = \Pi_0(l_t + l_t^{\perp} w),\ w \in \mathbb{R}^{n-2} \right\}$$

The intersection of $\mathcal{M}$ and $\tilde{S}_t$ occurs at points in S_0 such that $l_0 + l_0^{\perp} z = l_t + l_t^{\perp} w$. Multiplying on the left by l_t' we have $l_t' l_0 + l_t' l_0^{\perp} z = l_t' l_t$ or

$$l_t' l_0^{\perp} z = \|l_t\|^2 - l_t' l_0 \tag{4.15}$$

We want to show that

$$\left(\frac{l_t}{\|l_t\|}\|l_0\| - \frac{l_0}{\|l_0\|}\|l_t\| \right)' \left(l_0 + l_0^{\perp} z \right) = 0$$

Using (4.15) we have

$$\begin{aligned} \left(\frac{l_t}{\|l_t\|}\|l_0\| - \frac{l_0}{\|l_0\|}\|l_t\| \right)' \left(l_0 + l_0^{\perp} z \right) &= \frac{l_t' l_0}{\|l_t\|}\|l_0\| + \frac{l_t' l_0^{\perp} z}{\|l_t\|}\|l_0\| - \frac{l_0' l_0}{\|l_0\|}\|l_t\| \\ &= \frac{l_t' l_0}{\|l_t\|}\|l_0\| + \frac{\|l_t\|^2 - l_t' l_0}{\|l_t\|}\|l_0\| - \|l_0\|\|l_t\| \\ &= 0 \end{aligned}$$

■

The characterization of s_t is not complete yet. The orientation of s_t must be carefully chosen to guarantee that the cone $\mathcal{C}_t$ contains $\tilde{S}_t \cap \{x_0^* + \Delta_0 |\ L\Delta_0 > m\}$.

Proposition 4.2 *If*

$$s_t = m \left(\frac{l_0}{\|l_0\|}\|l_t\| - \frac{l_t}{\|l_t\|}\|l_0\| \right)$$

then the cone $\{x_0^* + \Delta_0 \in S_0 |\ \Delta_0' \beta_t \Delta_0 > 0\}$ contains $\tilde{S}_t \cap \{x_0^* + \Delta_0 |\ L\Delta_0 > m\}$.

The proof, omitted here, is based on taking a point $\Delta_0 \in (\tilde{S}_t \cap \{x_0^* + \Delta_0 |\ L\Delta_0 > m\}) - x^*$ and showing that $\Delta_0' \beta_t \Delta_0 > 0$.

Chapter 5

Relay Feedback Systems

This chapter is dedicated to study *relay feedback systems* (RFS). We consider relays with hysteresis in feedback with LTI stable systems. There are basically two main reasons why we study RFS. First, RFS are one of simplest classes of PLS. Thus, their study and understanding are essential before analyzing more complex classes of PLS. Second, RFS have been widely used in many real life applications, dating at least to the beginning of the last century. The interest in such systems is clearly demonstrated by the large number of publications on the topic.

RFS are indeed one of the simplest classes of PLS. Unfortunately, even for such a simple class of PLS, not much is known about their global stability. It is well known that for a large class of RFS there will be limit cycle oscillations. Conditions to check existence and *local* stability of limit cycles for these systems are well known. *Global* stability conditions, however, are practically nonexistent. This chapter presents conditions in the form of linear matrix inequalities (LMIs) that, when satisfied, guarantee *global* asymptotic stability of limit cycles induced by RFS. Following the ideas introduced in chapter 4, the analysis is based on finding quadratic surface Lyapunov functions for maps from one switching surface to the next switching surface, by solving a set of LMIs.

5.1 Introduction

Analysis of RFS is an old problem. The early work was motivated by relays in electromechanical systems and simple models of dry friction. Applications of relay feedback range from stationary control of industrial processes to control of mobile objects as used, for example, in space research. A vast collection of applications of relay feedback can be found in the first chapter of [64]. More recent examples include the delta-sigma modulator (as an alternative to conventional A/D converters) and the automatic tuning of PID regulators. In the delta-sigma modulator, a relay produces a bit stream output whose pulse density depends on the applied input signal amplitude (see, for example, [2]). Various methods were applied to the analysis of delta-sigma modulators. In most situations, however, none allowed to verify global stability of nonlinear oscillations. As for the automatic tuning of PID regulators, implemented

in many industrial controllers, the idea is to determine some points on the Nyquist curve of a stable open loop plant by measuring the frequency of oscillation induced by a relay feedback (see, for example, [6]). One problem that needs to be solved here is the characterization of those systems that have unique global attractive unimodal limit cycles. This problem is important because it gives the class of systems where relay tuning can be used.

Some important questions can be asked about RFS: do they have limit cycles? If so, are they locally stable or unstable? And if there exist a unique locally stable limit cycle, is it also globally stable? Over many years, researchers have been trying to answer these questions. [8] and [64] are references that survey a number of analysis methods. Rigorous results on existence and *local* stability of limit cycles of RFS can be found in [3, 33, 66]. [3] presents necessary and sufficient conditions for local stability of limit cycles. [33] emphasizes fast switches and their properties and also proves volume contraction of RFS. In [23], reasonably large regions of stability around limit cycles were characterized. For second-order systems, convergence analysis can be done in the phase-plane [60, 28]. Stable second-order non-minimum phase processes can in this way be shown to have a globally attractive limit cycle. In [41] it is proved that this also holds for processes having an impulse response sufficiently close, in a certain sense, to a second-order non-minimum phase process. Many important RFS, however, are not covered by this result. It is then clear that the problem of rigorous *global* analysis of relay-induced oscillations is still open.

In this chapter, we prove *global* asymptotic stability of symmetric unimodal[1] limit cycles of RFS by finding quadratic surface Lyapunov functions for associated Poincaré maps.[2] These results are based on the discovery in the last chapter that Poincaré maps can be represented as linear transformations parametrized by a scalar function of the state. Quadratic stability can then be easily checked by solving a set of linear matrix inequalities (LMIs), which can be efficiently done using available computational tools. Although this analysis methodology yields only a sufficient criterion of stability, it has proved very successful in globally analyzing a large number of examples with a unique locally stable symmetric unimodal limit cycle. In fact, it is still an open problem whether there exists an example with a globally stable symmetric unimodal limit cycle that could not be successfully analyzed with this new methodology. Examples analyzed include minimum-phase systems, systems of relative degree larger than one, and of high dimension. Such results lead us to believe that globally stable limit cycles of RFS frequently have quadratic surface Lyapunov functions.

It is important to point out that the main ideas behind the results in this chapter can be used in the analysis of more general PLS. In particular, although the stability analysis in this chapter focuses on symmetric unimodal limit cycles, similar ideas can

[1]Symmetric unimodal limit cycles are those that are symmetric about the origin and switch only twice per cycle.

[2]Poincaré maps play the same role here as impact maps did in the previous chapter. It turns out that in the analysis of symmetric unimodal limit cycles, Poincaré maps and impact maps are equivalent notions. In this chapter, we choose to use the terminology of Poincaré map since this may be more familiar to the reader.

be applied to prove stability of other types of limit cycles. As we will see, analysis of symmetric unimodal limit cycles can be done by analyzing a single map from one switching surface to the other switching surface. Other types of limit cycles require a simultaneous analysis of several of such maps. However, as we will see in the next two chapters, multiple maps have been shown to work as well as the single map described in this chapter.

This chapter is organized as follows. Section 5.2 gives some background on RFS followed by the main result of this chapter in section 5.3. There, we first show that Poincaré maps can be represented as linear transformations, and then use this result to demonstrate that quadratic stability of Poincaré maps can be easily checked by solving sets of LMIs. Section 5.4 contains some illustrative examples. Improvements of the stability conditions presented in section 5.3 are discussed in section 5.5. Finally, section 5.6 considers computationally issues associated with bounds on switching times of RFS.

5.2 Background

In this section, we start by defining RFS and talking about some of their properties. Then, we present some relevant results from the literature on existence and local stability of limit cycles of RFS. Finally, we define Poincaré maps for RFS.

5.2.1 Definitions

Consider a SISO LTI system satisfying the following linear dynamic equations

$$\left\{ \begin{array}{rcl} \dot{x} & = & Ax + Bu \\ y & = & Cx \end{array} \right. \tag{5.1}$$

where $x \in \mathbb{R}^n$ and A is a Hurwitz matrix, in feedback with a relay (see figure 5-1)

$$u = \mathrm{rel}_d(y) \tag{5.2}$$

where $d \geq 0$ is the hysteresis parameter. By a solution of (5.1)-(5.2) we mean functions (x, y, u) satisfying (5.1)-(5.2), where $u(t)$ is piecewise constant and

$$\mathrm{rel}_d(y(t)) \in \left\{ \begin{array}{ll} \{-1\} & \text{if } y(t) > d, \text{ or } y(t) > -d \text{ and } u(t-0) = -1 \\ \{1\} & \text{if } y(t) < -d, \text{ or } y(t) < d \text{ and } u(t-0) = 1 \\ \{-1, 1\} & \text{if } y(t) = -d \text{ and } u(t-0) = -1, \text{ or } y(t) = d \text{ and } u(t-0) = 1 \end{array} \right.$$

t is a *switching time* of a solution of (5.1)-(5.2) if u is discontinuous at t. We say a trajectory of (5.1)-(5.2) *switches* at some time t if t is a switching time.

In the state space, the *switching surfaces* S_0 and S_1 of the RFS are the surfaces of dimension $n-1$ where y is equal to d and $-d$, respectively. More precisely,

$$S_0 = \{x \in \mathbb{R}^n : \ Cx = d\}$$

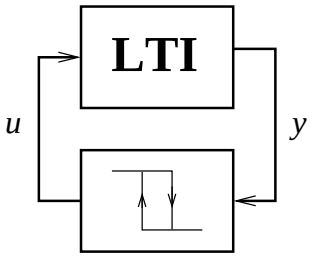

Figure 5-1: Relay Feedback System

and

$$S_1 = \{x \in \mathbb{R}^n : \ Cx = -d\}$$

Consider a subset S_0^d of S_0 given by

$$S_0^d = \{x \in S_0 : \ CAx + CB \geq 0\}$$

This set is important since it characterizes those points in S_0 that can be reached by any trajectory starting at S_1. We call it the *departure set* in S_0 (see figure 5-2). Similarly, define S_1^a as

$$S_1^a = \{x \in S_1 : \ CAx - CB \leq 0\}$$

This is the *arrival set* in S_1. It is easy to see that $S_0 = -S_1$ and $S_0^d = -S_1^a$ where $-X$ stands for the set $\{-x | x \in X\}$.

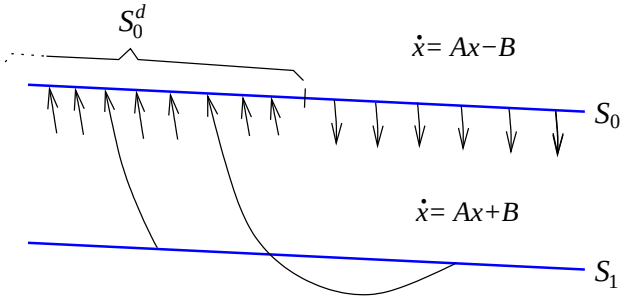

Figure 5-2: The arrival set S_0^d

5.2.2 Existence of Solutions

If an initial condition does not belong to a switching surface then existence of solution is guaranteed at least from the initial condition to the first intersection with a switching surface. This follows since in that region the system is affine linear. When an initial condition belongs to a switching surface, however, depending on the RFS, a solution may or may not exist. If $d > 0$ then existence of solution is always guaranteed since there is a "gap" between both switching surfaces. This gap allows a trajectory

to evolve according to an affine linear system.

In the case of the ideal relay, i.e., when $d = 0$, for some RFS there are initial conditions for which no solution exists. In figure 5-3, we have two examples of ideal RFS. The figure shows the vector field along both sides of the unique switching surface $S = \{x|\ Cx = 0\}$. Above, the vector field is given by $\dot{x} = Ax - B$, and below by $\dot{x} = Ax + B$. p_+ and p_- are those points in S such that $C(Ax \pm CB) = 0$, respectively. On the left in figure 5-3, $CB < 0$, and on the right $CB > 0$. When $CB < 0$, every point in S has at least one solution. For an initial condition on the left of p_-, the trajectory moves downwards, and on the right of p_+ it moves upwards. In between p_- and p_+, the trajectory can either move upwards or downwards. When $CB > 0$, however, there is no solution if a trajectory starts between p_+ and p_-. The reason for this is that the vector field on both sides of the switching surface points towards the switching surface. In these situations, one of the following two alternatives is typically used to guarantee existence of solutions: (1) an hysteresis with $d > 0$ is introduced to avoid chattering or (2) the definition of relay in (5.2) is slightly modified to allow trajectories to evolve in the switching surface, leading to the so-called sliding modes. Here, we consider the first case. Although sliding modes are not studied in this thesis, we expect that such systems can be analyzed using the same ideas described here. Sliding modes are currently under investigation and will be the topic of future publications.

Hence, according to the definition of relay in (5.2), existence of solutions is guaranteed if $d > 0$, or if $d = 0$ and $CA^kB < 0$, where $k \in \{0, 1, ..., n-1\}$ is the smallest number such that $CA^kB \neq 0$ (see [33] for details).

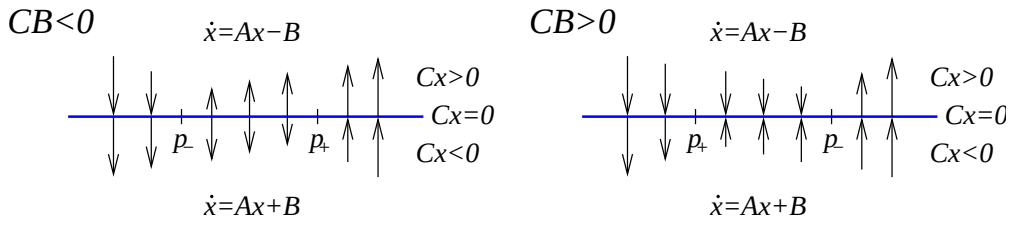

Figure 5-3: Existence of solutions when $d = 0$

Note that trajectories of $\dot{x} = Ax - B$ starting at any point $x_0 \in S_0$ will converge to the equilibrium point $A^{-1}B$. When connected in feedback with a relay, one of the following two possible scenarios will occur for a certain trajectory starting at x_0: this will either cross S_1 at some time, or it will never cross S_1. The last situation is not interesting to us since it does not lead to limit cycle trajectories. One way to ensure a switch is to have $CA^{-1}B + d < 0$, although this is not a necessary condition for the existence of limit cycles. However, if we are looking for globally stable limit cycles, it is in fact necessary to have $CA^{-1}B + d < 0$. Otherwise a trajectory starting at $A^{-1}B$ would not converge to the limit cycle. Throughout this chapter, it is assumed $CA^{-1}B + d < 0$.

As mentioned before, for a large class of processes, there will be limit cycle oscillations. Let $\xi(t)$ be a nontrivial periodic solution of (5.1)-(5.2) with period $2t^*$, and

let γ be the limit cycle defined by the image set of $\xi(t)$. The limit cycle γ is called *symmetric* if $\xi(t + t^*) = -\xi(t)$. It is called *unimodal* if it only switches twice per cycle. A class of limit cycles of RFS we are particularly interested in is the class of symmetric unimodal limit cycles.

The next proposition, proven in [3], gives necessary and sufficient conditions for the existence of symmetric unimodal limit cycles. This proposition is a special case of proposition 3.2, with $k = 1$.

Proposition 5.1 *Consider the RFS (5.1)-(5.2). Assume there exists a symmetric unimodal limit cycle γ with period $2t^*$. Then the following conditions hold*

$$g(t^*) := C(e^{At^*} + I)^{-1}(e^{At^*} - I)A^{-1}B - d = 0 \tag{5.3}$$

and

$$y(t) = C\left[e^{At}(x^* - A^{-1}B) + A^{-1}B\right] \geq -d \quad for \quad 0 \leq t < t^*$$

Furthermore, the periodic solution γ is obtained with the initial condition $x^* \in S_0^d$ given by

$$x(0) = x^* = (e^{At^*} + I)^{-1}(e^{At^*} - I)A^{-1}B$$

5.2.3 Poincaré Maps of RFS

Before defining Poincaré maps, it is important to notice an interesting property of linear systems in relay feedback: their symmetry around the origin (see figure 5-4).

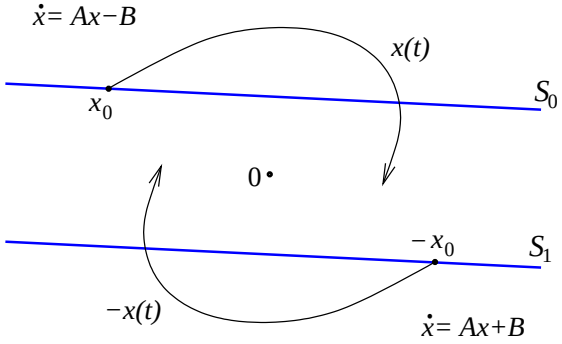

Figure 5-4: Symmetry around the origin

Proposition 5.2 *Consider a trajectory $x(t)$ of $\dot{x} = Ax - B$ starting at $x_0 \in S_0$. Then $-x(t)$ is a trajectory of $\dot{x} = Ax + B$ starting at $-x_0 \in S_1$.*

Proof: Assume $x_0 \in S_0$. Since

$$\begin{aligned} -\dot{x}(t) &= -(Ax(t) - B) \\ &= A(-x(t)) + B \end{aligned}$$

$-x(t)$ is a trajectory of $\dot{x} = Ax + B$ starting at $-x_0 \in S_1$. ■

This property tells us that, in terms of stability analysis, a limit cycle only needs to be studied from one switching surface (say S_0) to the other switching surface (S_1). In other words, for analysis purposes, it is equivalent to consider the trajectory from $x_1 \in S_0$ to the next switch $x_2 \in S_1$, or the trajectory starting at $-x_1 \in S_1$ and switching at $-x_2 \in S_0$. We then focus our attention on trajectories from S_0 to S_1.

Next, we define Poincaré maps for RFS. Typically, such maps are defined from one switching surface and back to the same switching surface. In the case of RFS, however, a Poincaré map only needs to be defined as the map from one switching surface to the other switching surface, due to the symmetry of the system. Note that, as mention before, Poincaré maps play the same role here as impact maps did in the previous chapter. In this chapter, the Poincaré map we consider is defined from one switching surface to the other switching surface, just like impact maps were defined before.

Consider a symmetric unimodal limit cycle γ, with period $2t^*$, obtained with the initial condition $x^* \in S_0^d$. This means that a trajectory $x(t)$ starting at x^* crosses the switching surface S_1 at $-x^* = x(t^*) \in S_1^a$ (see figure 5-5).

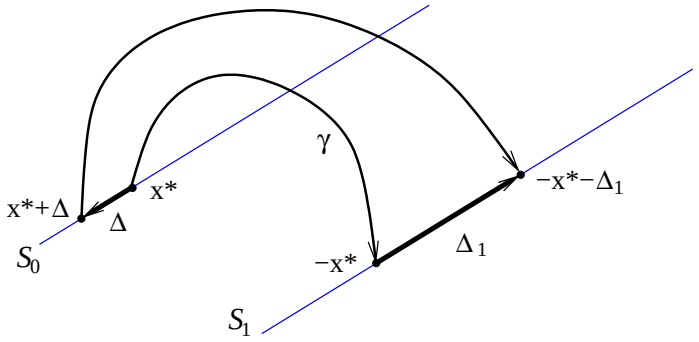

Figure 5-5: Definition of a Poincaré map for a RFS

To study the behavior of the system around the limit cycle we perturb x^* by Δ such that $x^* + \Delta \in S_0^d$. Consider a solution of (5.1)-(5.2) with initial condition $x^* + \Delta$ and let $-x^* - \Delta_1 \in S_1$ be its first switch. We are interested in studying the map from Δ to Δ_1 (see figure 5-5). As seen in example 4.3, this map is not continuous and is multivalued. In general, there exist $\Delta \in S_0^d$ such that Δ_1 is not unique. This is illustrated in the next example. Note that this is the same as example 4.3, but now applied to a RFS.

Example 5.1 Consider the RFS (5.1)-(5.2) where the LTI system is given by

$$H(s) = -\frac{s^2 + s - 4}{(s+1)(s+2)(s+3)}$$

and the hysteresis parameter is $d = 0.5$. Let $u(0) = -1$, $y(0) = d$, $\dot{y}(0) \approx -6.36$, and $\ddot{y}(0) \approx 31.67$. The resulting $y(t)$ can be seen in figure 5-6.

When $t \approx 0.47$, $y(t) = -d$ and $\dot{y}(t-0) = 0$. At this point, the trajectory can return to the region where $Cx > -d$ and $u(t+0) = u(t-0) = -1$ (dash trajectory),

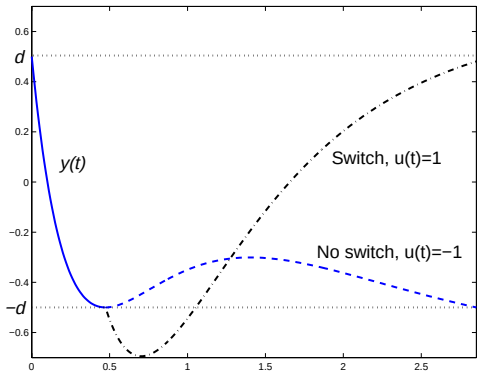

Figure 5-6: Existence of multiple solutions

or it can move into the region where $Cx < -d$ with $u(t+0) = 1$ (dash-dot trajectory). This means that a switch can occur at either $t = 0.47$ or $t = 2.85$. ■

Let $x(0) = x^* + \Delta \in S_0^d$. Define t_Δ as the set of all times $t_i \geq 0$ such that $y(t_i) = -d$ and $y(t) \geq -d$ on $[0, t_i]$. For the initial condition considered in the previous example, $t_\Delta = \{0.47, 2.85\}$. Let $-x^* - \Delta_1 \in x(t_\Delta)$. Since $-x^* - \Delta_1 \in S_1^a$ then $x^* + \Delta_1 \in S_0^d$. Consider the multivalued Poincaré map $T_0 : S_0^d \to S_0^d$ defined by $x^* + \Delta_1 \in T_0(x^* + \Delta)$. Since x^* is fixed, the Poincaré map can be redefined as the map $T : S_0^d - x^* \to S_0^d - x^*$ given by $\Delta_1 \in T(\Delta)$, where $T(\Delta) = T_0(x^* + \Delta) - x^*$. In result, $\Delta = 0$ is an equilibrium point of the discrete-time system

$$\Delta_{k+1} \in T(\Delta_k) \tag{5.4}$$

The following proposition, proven in [3], gives conditions for local stability of symmetric unimodal limit cycles. This result, based on the linearization of the Poincaré map around the origin, is a special case of proposition 3.3, with $k = 1$.

Proposition 5.3 *Consider the RFS (5.1)-(5.2). Assume there exists a symmetric unimodal limit cycle γ with period $2t^*$, obtained with the initial condition $x^* \in S_0$. Assume also the limit cycle is transversal[3] to S_0 at x^*. The Jacobian of the Poincaré map T at $\Delta = 0$ is given by*

$$W = \left(\frac{vC}{Cv} - I\right) e^{At^*}$$

where $v = -Ax^* - B$. The limit cycle γ is locally stable if W has all its eigenvalues inside the unit disk. It is unstable if at least one of the eigenvalues of W is outside the unit disk.

Define $\mathcal{T}$, the set of expected switching times of the Poincaré map T, as in definition 4.1, i.e.,

$$\mathcal{T} = \left\{ t |\ t \in t_\Delta,\ \Delta \in S_0^d - x^* \right\}$$

[3] ϕ is *transversal* to S_0 at $p = \phi(t) \in S_0$ if $C\dot{\phi}(t-0) \neq 0$.

Note that $t^* \in \mathcal{T}$.

In this chapter, we are interested in those systems that have a unique locally stable unimodal limit cycle. For such systems, the idea is to construct a quadratic Lyapunov function on the switching surface S_0 to prove that the Poincaré map is globally stable. This, in turn, shows that the limit cycle is globally asymptotically stable. The next section shows that a Poincaré map from one switching surface to the other switching surface can be represented as a linear transformation analytically parametrized by the switching time. This representation will then allow us to reduce the problem of checking quadratic stability to the solution of a set of LMIs.

5.3 Poincaré Map Decomposition and Stability

This section contains the main results of this chapter. First, we show that Poincaré maps induced by an LTI flow between the switching surfaces S_0 and S_1 can be represented as linear transformations analytically parametrized by a scalar function of the state. This proposition is similar to theorem 4.1.

Proposition 5.4 *Consider the Poincaré map T defined above. Let*

$$v_t = \left(e^{At} - e^{At^*}\right)\left(x^* - A^{-1}B\right)$$

and assume $|Cv_t| \geq K\|v_t\|$, for some $K > 0$ and all $t \in \mathcal{T}$. Define

$$H(t) = \left(\frac{v_t C}{Cv_t} - I\right) e^{At}$$

for all $t \in \mathcal{T}$ (for $t = t^*$, $H(t)$ is defined by the limit as $t \to t^*$). Then, for any $\Delta \in S_0^d - x^*$ and $\Delta_1 \in T(\Delta)$ there exists a $t \in \mathcal{T}$ such that

$$\Delta_1 = H(t)\Delta \tag{5.5}$$

Such $t \in t_\Delta$ is the switching time associated with Δ_1.

This result says that Poincaré maps induced by an LTI flow between two hyperplanes can be represented as linear transformations analytically parametrized by a scalar function of the state. The advantage of expressing such maps this way is to have all nonlinearities depending only on one parameter t. Although t depends on Δ, once t is fixed, the map becomes linear in Δ. Note that $H(t)$ defined above is continuous in $t \in \mathcal{T}$.

The assumption in proposition 5.4 is somehow similar to the assumption in theorem 4.1. Here it is slightly different since at $t = t^*$, $Cv_{t^*} = 0$ and $v_{t^*} = 0$. By continuation, the quotient $v_t/(Cv_t)$ (and, in turn, $H(t)$) is well defined at $t = t^*$. What the assumption in the proposition says is that the trajectory $x^*(t)$ of $\dot{x} = Ax - B$ starting at x^* does not intersect S_1 for $t > t^*$. As we have mentioned in section 4.2, however, even if this assumption is not satisfied for some $t_s \in \mathcal{T}$, it is still possible to obtain a

linear representation of the Poincaré map for all $t \in \mathcal{T}$. Such linear transformation would be parametrized by another variable at t_s, i.e., $\Delta_1 = H_s(t_s, \delta)\Delta_0$.

Proof: The proof is similar to the proof of theorem 4.1. Let $x(0) = x_0 \in S_0^d$. Integrating the differential equation (5.1) gives

$$\begin{aligned} x(t) &= e^{At}x_0 - \int_0^t e^{A(t-\tau)}Bd\tau \\ &= e^{At}(x_0 - A^{-1}B) + A^{-1}B \end{aligned}$$

If $x(0) = x^*$ and $t = t^*$ then $x(t^*) = -x^*$, i.e.,

$$-x^* = e^{At^*}(x^* - A^{-1}B) + A^{-1}B \tag{5.6}$$

Now, let $x(0) = x^* + \Delta \in S_0^d$ and $\Delta_1 \in T(\Delta)$. Let also $t \in t_\Delta$ be the switching time associated with Δ_1. Then

$$-x^* - \Delta_1 = e^{At}(x^* + \Delta - A^{-1}B) + A^{-1}B$$

Using (5.6), the last equality can be written as

$$\begin{aligned} -\Delta_1 &= e^{At}(x^* - A^{-1}B + \Delta) - e^{At^*}(x^* - A^{-1}B) \\ &= e^{At}\Delta + v_t \end{aligned}$$

Since $-x^* - \Delta_1 \in S_1$, $C(-x^* - \Delta_1) = -d$, or $C\Delta_1 = 0$, that is,

$$Ce^{At}\Delta + Cv_t = 0 \tag{5.7}$$

Therefore, it is also true that $v_tCe^{At}\Delta + v_tCv_t = 0$. Since, by assumption, $|Cv_t| \geq K\|v_t\|$, for some $K > 0$ and all $t \in \mathcal{T}$,

$$v_t = -\frac{v_tC}{Cv_t}e^{At}\Delta$$

is well defined for $t \in \mathcal{T}$ (for $t = t^*$ it is defined via continuation). Replacing above we get

$$\Delta_1 = \left(\frac{v_tC}{Cv_t} - I\right)e^{At}\Delta$$

for all $t \in \mathcal{T}$. ■

This result agrees with proposition 5.3. Via continuation, $H(t)$ at $t = t^*$ is given by

$$H(t^*) = \left(\frac{vC}{Cv} - I\right)e^{At^*}$$

where $v = e^{At^*}(Ax^* - B)$. Using equality (5.6), v can be written as $v = e^{At^*}(Ax^* - B) = -Ax^* - B$. This means $H(t^*)$ is exactly the Jacobian of the Poincaré map T at $\Delta = 0$.

As explained in chapter 4, based on this theorem it is possible to reduce the problem of checking quadratic stability of Poincaré maps to solving a set of LMIs. The Poincaré map T defined above is quadratically stable if there exists a symmetric matrix $P > 0$ such that

$$T'(\Delta)PT(\Delta) < \Delta' P \Delta \ , \quad \forall \Delta \in S_0^d - x^*, \ \Delta \neq 0 \tag{5.8}$$

Success in finding $P > 0$ satisfying (5.8) is then sufficient to prove global asymptotic stability of the limit cycle γ.

A sufficient condition for the quadratic stability of a Poincaré map can easily be obtained by substituting (5.5) in (5.8):

$$\Delta' \left(P - H'(t)PH(t) \right) \Delta > 0 \tag{5.9}$$

for some $P > 0$ and for all $\Delta \in S_0^d$, with associated switching times $t \in t_\Delta$.

There are several alternatives to transform (5.9) into a set of LMIs. A simple sufficient condition is

$$P - H'(t)PH(t) > 0 \quad \text{ on } S_0 - x^* \tag{5.10}$$

for some $P > 0$ and for all $t \in \mathcal{T}$. In the next section, using some illustrative examples, we will see that although this condition is more conservative than (5.9), it can prove global asymptotic stability of many important RFS. Other less conservative conditions are considered and discussed in section 5.5. These are based on the fact that T is a map from S_0^d to S_0^d, and that the set of points in S_0^d with the same switching time t is a convex subset of a linear manifold of dimension $n-2$.

Before moving into the examples, it is important to notice that condition (5.10) can be relaxed. Since A is Hurwitz and $u = \pm 1$ is a bounded input, there is a bounded set such that any trajectory will eventually enter and stay there. This will lead to bounds on the difference between any two consecutive switching times. Let t_- and t_+ be bounds on the minimum and maximum switching times of trajectories in that bounded invariant set. The expected switching times $\mathcal{T}$ can, in general, be reduced to a smaller set $[t_-, t_+]$. Condition (5.10) can then be relaxed to be satisfied on $[t_-, t_+]$ instead of on $t \in \mathcal{T}$. See section 5.6 for details.

5.4 Examples

The following examples were processed in `matlab` code. The latest version of this software is either available at [27] or upon request. Before presenting the examples, it is important to understand these `matlab` functions. Overall, the user provides an LTI system, together with d, the hysteresis parameter. If the RFS is proven globally asymptotically stable, the `matlab` functions return a matrix $P > 0$ that is guaranteed to satisfy (5.10) on $t \in [t_-, t_+]$, where t_- and t_+, found as explained in section 5.6, are bounds of the expected switching times.

In more detail, after providing the software with an LTI system and an hysteresis

parameter d, this confirms that certain necessary conditions are met. Then, it checks if there exists a unique locally stable symmetric unimodal limit cycle. This is done by first finding t_i^*, the zeros of (5.3). A symmetric unimodal limit cycle exists if, for some i, $y(t) + d > 0$ for all $t \in (0, t_i^*)$, and is unique if this is true for only one i.

As explained in section 4.3.1, although the vectors Δ and Δ_1 are n-dimensional, the solution generated by the Poincaré map T is restricted to the $n-1$-dimensional hyperplane S_0 (see figure 5-7). Therefore, the map T is actually a map from $\mathbb{R}^{n-1}$ to $\mathbb{R}^{n-1}$. Let $\Pi \in C^\perp$ be a map from $\mathbb{R}^{n-1}$ to S_0, where $C^\perp$ are the *orthogonal complements* to C, i.e., matrices with a maximal number of column vectors forming an orthonormal set such that $CC^\perp = 0$. An equivalent condition to (5.10) is then

$$Q - F'(t)QF(t) > 0 \tag{5.11}$$

for some symmetric $(n-1) \times (n-1)$ matrix $Q > 0$ and all expected switching times $t \in [t_-, t_+]$, where $F(t) = \Pi' H(t) \Pi$. $P > 0$ in (5.10) can be obtained by letting $P = \Pi Q \Pi'$.

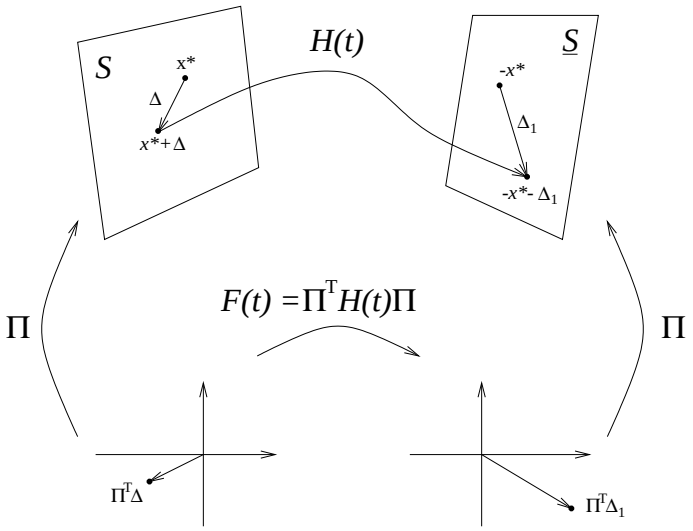

Figure 5-7: T is a $n-1$-dimensional map

(5.11) on $[t_-, t_+]$ forms an infinite set of LMIs. Computationally, to overcome this difficulty, we grid this set to obtain a finite subset of expected switching times $t_- = t_0 < t_1 < \cdots < t_k = t_+$. In other words, $Q > 0$ is found by solving a finite set of LMIs consisting of (5.11) on $t = \{t_i\}$, $i = 0, 1, ..., k$. For a large enough k, it can be shown that (5.11) is also satisfied for all $t \in [t_-, t_+]$. The idea here is to find bounds on the derivative of the minimum eigenvalue of $Q - F'(t)QF(t)$ over (t_i, t_{i+1}), and to use these bounds to show that nothing can go wrong in the intervals (t_i, t_{i+1}), i.e., that (5.11) is also satisfied on each interval (t_i, t_{i+1}).

Solving a set of LMIs allows us to find $Q > 0$ in (5.11). In the examples below, once $Q > 0$ is found, we confirm (5.11) is satisfied for all switching times $[t_-, t_+]$ by plotting the minimum eigenvalue of $Q - F'(t)QF(t)$ on $[t_-, t_+]$, and showing that this

in indeed positive in that interval.

Example 5.2 Consider the RFS on the left of figure 5-8. Since for this system any state-space realization of the LTI system in relay feedback results in $CB < 0$, it is possible to consider the ideal relay, i.e., $d = 0$. Although very simple, this system has never been proved globally stable.

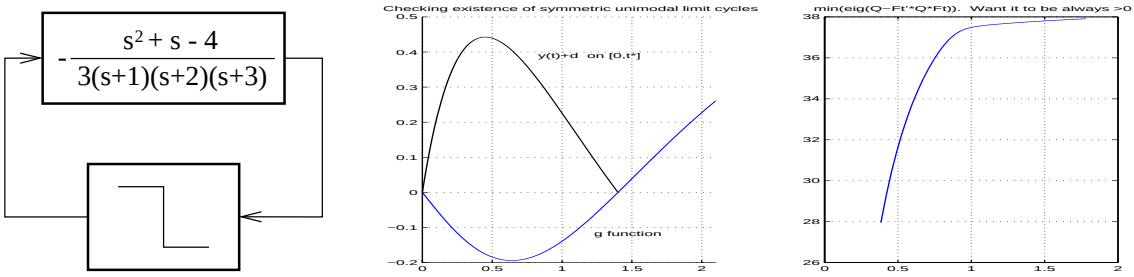

Figure 5-8: 3^{rd}-order non-minimum phase system

From the center of figure 5-8 it is easy to see the RFS has one unimodal symmetric limit cycle with period approximately equal to 2×1.4. We have analyzed this same RFS in [23]. There, we characterized a reasonably large region of stability around the limit cycle. Using the software described above, however, we were able to find a $Q > 0$ satisfying (5.11) for all switching times $[t_-, t_+]$, showing, this way, that the RFS is actually globally asymptotically stable. The right side of figure 5-8 confirms the result. ■

Example 5.3 Consider the RFS in figure 5-9. Let $d = 0.25$. As seen in figure 5-9, the RFS has one unimodal symmetric limit cycle with period approximately equal to 2×0.94.

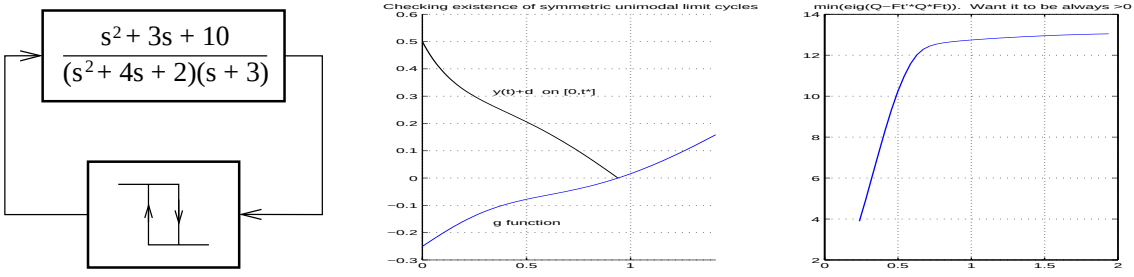

Figure 5-9: 3^{rd}-order minimum phase system

Again, a $Q > 0$ satisfying (5.11) for all switching times $[t_-, t_+]$ exists, which means the limit cycle is globally asymptotically stable. This is confirmed from the right side of figure 5-9. ■

Example 5.4 Consider the 6^{th}-order RFS in figure 5-10. In this case, sliding modes occur if $d = 0$ ($CB = 1$). However, stability was proven for d as low as 0.061.

Figure 5-10 shows the result to $d = 0.061$. Note that, in the figure on the right, the function depicted is always positive although, due the bad resolution, it may seem otherwise. This is due to the fact that $d = 0.061$ is the lowest value for which we can still prove global stability.

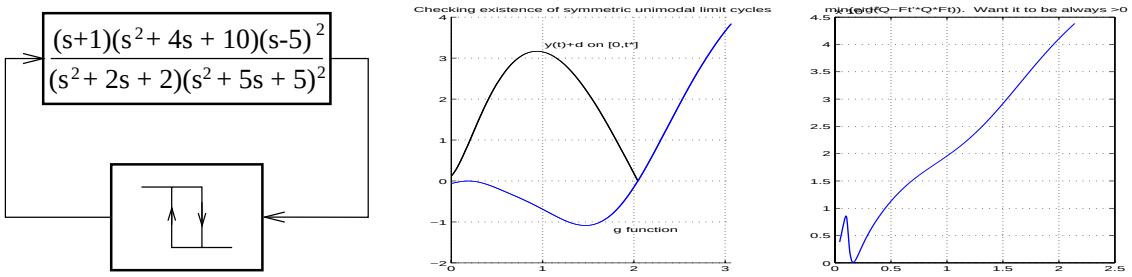

Figure 5-10: 6^{th}-order system

It is interesting to notice that more than one limit cycle exists for $0 < d < 0.061$. Thus, for this example, condition (5.10) is not conservative. ■

Example 5.5 Consider the RFS in figure 5-11 consisting of an LTI system with relative degree 7 in feedback with an hysteresis, where $d = 0.1$. As seen in the center of figure 5-11, this RFS has a symmetric unimodal limit cycle with period $2t^*$, where $t^* \approx 6.89$. Note how the period of the limit cycle is much larger than the hysteresis parameter d.

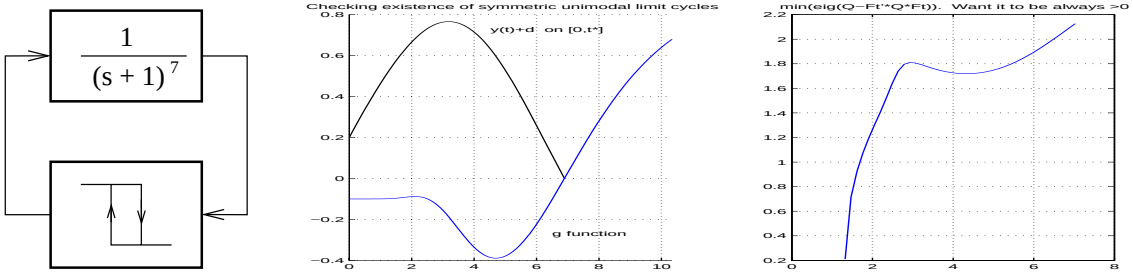

Figure 5-11: System with relative degree 7

Again, from the right side of figure 5-11 we conclude that the limit cycle is globally asymptotically stable ■

5.5 Improvement of Stability Condition

As mentioned before, there are several alternatives to transform (5.9) into a set of LMIs. Here, we explore some of these alternatives to derive less conservative conditions than (5.10). Since many of the ideas in this section were discussed in section 4.3.1, we will skip some of the details.

The Poincaré map T is a map from S_0^d to S_0^d and, for each point in S_0^d, there is at least one associated switching time t. An interesting property of this map is that the set of points in S_0^d with the same switching time t forms a convex subset of a linear manifold of dimension $n-2$. Let S_t be that set, i.e., let S_t be the set of points $x^* + \Delta \in S_0^d$ that have t as a switching time, i.e., $t \in t_\Delta$ (see figure 5-12). In other words, a trajectory starting at $x_0 \in S_t$ satisfies both $y(t) \geq -d$ on $[0,t]$, and $y(t) = -d$. Note that since T is a multivalued map, a point in S_0^d may belong to more than one set S_t. In fact, in example 5.1, there existed a point in S_0^d that belonged to both $S_{0.47}$ and $S_{2.85}$.

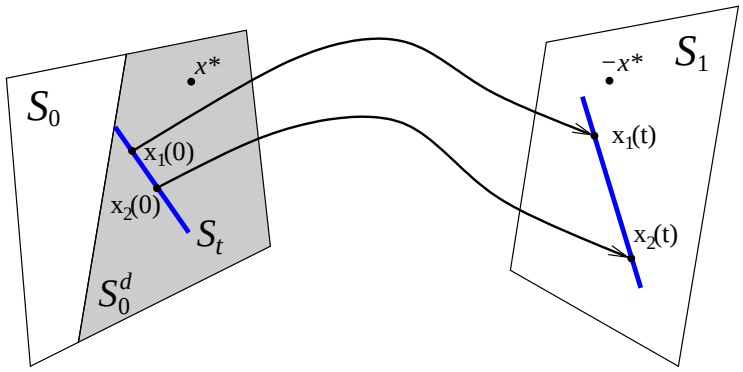

Figure 5-12: Example of a set S_t (in $\mathbb{R}^3$, both S_t and its image in S_1 are segments of lines)

Condition (5.10) can then be improved to

$$P - H'(t)PH(t) > 0 \quad \text{on } S_t - x^* \tag{5.12}$$

for some $P > 0$ and for all expected switching times $t \in \mathcal{T}$.

The problem with condition (5.12) is that, in general, the sets S_t are not easily characterized. An alternative is to consider the sets $\tilde{S}_t \supset S_t$ obtained from equation (5.7), given by

$$\tilde{S}_t = \left\{ x^* + \Delta \in S_0^d : Ce^{At}\Delta = -Cv_t \right\}$$

To see the difference between S_t and $\tilde{S}_t$, refer to figure 4-11 and the discussion following this figure.

Since $S_t \subset \tilde{S}_t$, condition (5.12) holds if there exists a $P > 0$ such that

$$P - H'(t)PH(t) > 0 \quad \text{on } \tilde{S}_t - x^* \tag{5.13}$$

for all expected switching times.

As seen in figure 5-13, $\Delta \in \tilde{S}_t - x^*$ satisfies a conic relation

$$\Delta' \beta_t \Delta > 0$$

for some matrix β_t (section 4.5 explains how this matrix is constructed). Let

$$\mathcal{C}_t = \{x^* + \Delta \in S_0 : \Delta' \beta_t \Delta > 0\}$$

It is important to notice that it is equivalent to say that some matrix M satisfies $M > 0$ on $\tilde{S}_t - x^*$ or that $M > 0$ on $\mathcal{C}_t - x^*$. This has to do with the fact that quadratic forms are homogeneous. To see this, assume $\Delta' M \Delta > 0$ for all $\Delta \in \tilde{S}_t - x^*$. Let $x = \lambda\Delta$ where $\lambda \in \mathbb{R}\backslash\{0\}$. Then $x'Mx = \lambda^2 \Delta' M \Delta > 0$, which is to say $M > 0$ on $\mathcal{C}_t - x^*$. The converse follows since $\tilde{S}_t \subset \mathcal{C}_t$.

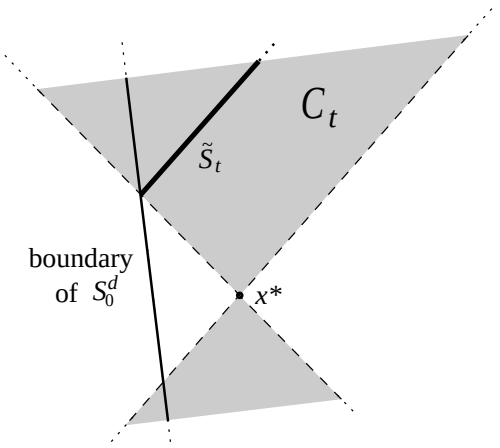

Figure 5-13: View of the cone $\mathcal{C}_t$ in the S_0 plane

Condition (5.13) is then equivalent to:

$$P - H'(t)PH(t) > 0 \quad \text{ on } \mathcal{C}_t - x^*$$

for some $P > 0$ and for all expected switching times t. Using the S-procedure, condition (5.13) is again equivalent to

$$P - H'(t)PH(t) - \tau_t \beta_t > 0 \quad \text{ on } S_0 - x^* \tag{5.14}$$

for some $P > 0$, some scalar function $\tau_t > 0$, and for all expected switching times $t \in \mathcal{T}$. Note that, for each t, (5.14) is an LMI .

Example 5.6 Consider again the system with relative degree 7 analyzed in example 5.5. For small values of $d > 0$ there is no $P > 0$ satisfying condition (5.10). Using condition (5.14), however, a $P > 0$ and a positive function τ_t satisfying (5.14) are known to exist for values of d as small as 0.00404. Figure 5-14 shows the result to $d = 0.00404$. Again, the function depicted on the right in the figure is always positive although, due to bad resolution, it may seem otherwise.

Note that the g function on the left of the figure has 3 zeros. However, only one corresponds to a limit cycle.

Although condition (5.10) was not able to prove global stability of the RFS for small values of d, the less conservative condition (5.14) proved that the limit cycle

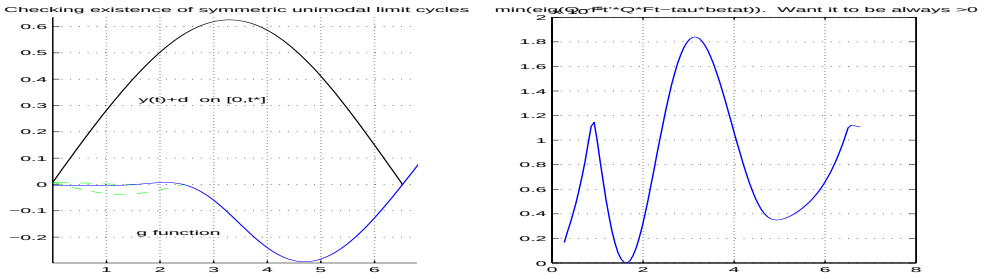

Figure 5-14: System of relative order 7 with $d = 0.00404$

is globally asymptotically stable for small values of d. An interesting fact is that for $0 < d < 0.00378$ there is more than one limit cycle. ■

It is possible to improve condition (5.14) furthermore. This condition does not take advantage that a trajectory starting at $x^* + \Delta \in \tilde{S}_t$ must satisfy $y(\tau) \geq -d$ on $[0, t]$. This is captured by condition (5.12) but not by (5.14) since $\tilde{S}_t \supset S_t$. Constraint $y(\tau) \geq -d$ on $[0, t]$ can be expressed as

$$Ce^{A\tau}\Delta \geq -Cv_\tau \tag{5.15}$$

for all $[0, t]$. However, this last inequality would lead to an infinite dimensional set of LMIs. One way to transform the problem into a finite set of LMIs is to consider certain samples of time in $(0, t)$. For instance, if $\tau = t/2$ then we would have the following constraint on Δ

$$Ce^{A\frac{t}{2}}\Delta \geq -Cv_{t/2}$$

This, together with $\Delta \in S_0^d$, satisfies a conic relation $\Delta'\gamma_{t/2}\Delta > 0$ in which case (5.14) could be improved to

$$P - H'(t)PH(t) - \tau_t\beta_t - \tau_{1t}\gamma_{t/2} > 0 \quad \text{on } S_0 - x^* \tag{5.16}$$

for some scalar function $\tau_{1t} > 0$

There is an infinite number of constraints that can be added to condition (5.16) in order to further reduce the level of conservatism. On one hand, the more constraints, the better chances to find surface Lyapunov functions. On the other hand, increasing the number of constraints will eventually make the problem computationally intractable. In spite of this, it is interesting to notice that many important RFS were proven globally stable with just conditions (5.10) (the most conservative of all presented in this chapter).

We want to point out that the value of all these results lie in the fact that they work well. In fact, we have not been able to find a RFS with a globally stable symmetric unimodal limit cycle that could not be successfully analyzed with this new methodology. This lead us to believe that globally stable limit cycles of RFS frequently have quadratic surface Lyapunov functions.

5.6 Computational Issues: Bounds on Expected Switching Times

In this section we will talk about computational aspects related to finding $P > 0$ in (5.10) and (5.14). First, we show that since A is Hurwitz and $u = \pm 1$ is a bounded input, there is a bounded and invariant set such that any trajectory will eventually enter. This will lead to bounds on the difference between any two consecutive switching times. This way, the search for $P > 0$ in (5.10) and (5.14) becomes restricted to $0 < t_- \leq t \leq t_+ < \infty$.

For a fixed $t \in \mathcal{T}$, condition (5.10) is an LMI with respect to P, while (5.14) is an LMI with respect to P and τ_t. We want to show that it is sufficient that conditions (5.10) or (5.14) are satisfied in some carefully chosen interval $[t_-, t_+]$, instead of requiring them to be satisfied for all expected switching times $t \in \mathcal{T}$. In order to do so, one must guarantee there exists a t_0 such that the difference between any two consecutive switching times of a trajectory $x(t)$ for $t > t_0$ is higher than t_- but lower than t_+. Before we find such bounds, we need to show there is a particular bounded set such that any trajectory will eventually enter and stay there (i.e., will not leave the set). Remember that, by definition, $\|Fe^{At}B\|_{\mathcal{L}_1}$ is given by

$$\|Fe^{At}B\|_{\mathcal{L}_1} = \int_0^\infty \left|Fe^{At}B\right| dt$$

Proposition 5.5 *Consider the system $\dot{x} = Ax + Bu$, $y = Fx$, where A is Hurwitz, $u(t) = \pm 1$, and F is a row vector. Then, for any fixed $\bar{t} \geq 0$,*

$$\limsup_{t\to\infty} |Fe^{A\bar{t}}x(t)| \leq \int_{\bar{t}}^\infty \left|Fe^{A\tau}B\right| d\tau \leq \|Fe^{At}B\|_{\mathcal{L}_1}$$

Proof: At time t, $x(t)$ is given by

$$x(t) = e^{At}x_0 + \int_0^t e^{A(t-\tau)}Bu(\tau)d\tau$$

Therefore

$$\begin{aligned}
\limsup_{t\to\infty} \left|Fe^{A\bar{t}}x(t)\right| &= \limsup_{t\to\infty} \left|Fe^{A\bar{t}}\left(e^{At}x_0 + \int_0^t e^{A(t-\tau)}Bu(\tau)d\tau\right)\right| \\
&\leq \limsup_{t\to\infty} \left|Fe^{A\bar{t}}e^{At}x_0\right| + \limsup_{t\to\infty} \left|Fe^{A\bar{t}}\int_0^t e^{A(t-\tau)}Bu(\tau)d\tau\right| \\
&\leq 0 + \limsup_{t\to\infty} \int_0^t \left|Fe^{A(t+\bar{t}-\tau)}Bu(\tau)\right| d\tau \\
&\leq \limsup_{t\to\infty} \int_0^t \left|Fe^{A(t+\bar{t}-\tau)}B\right| d\tau \\
&= \int_{\bar{t}}^\infty \left|Fe^{A\tau}B\right| d\tau \\
&\leq \int_0^\infty \left|Fe^{A\tau}B\right| d\tau
\end{aligned}$$

which is equal to $\|Fe^{At}B\|_{\mathcal{L}_1}$. ■

We now focus our attention in finding an upper bound for t_+. First, remember from the proof of theorem 5.4 that a trajectory $x(t)$ starting at $x_0 \in S_0^d$ is given by $x(t) = e^{At}(x_0 - A^{-1}B) + A^{-1}B$. Then the output $y(t) = Cx(t)$ is given by

$$y(t) = Ce^{At}(x_0 - A^{-1}B) + CA^{-1}B$$

By definition of S_0^d, $y(t) > -d$ at least in some interval $(0, \epsilon)$, where $\epsilon > 0$. However, since we are assuming $CA^{-1}B < -d$, and A Hurwitz, it is easy to see that $y(t)$ cannot remain larger than $-d$ for all $t > 0$ (see figure 5-15). For any initial condition x_0, $Ce^{At}(x_0 - A^{-1}B) \to 0$ as $t \to \infty$. Hence, since for sufficiently large time t, $x(t)$ is bounded (from the above proposition), an upper bound t_+ on the expected switching times can be obtained.

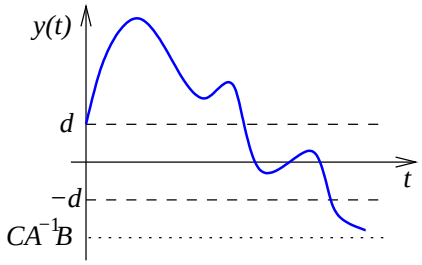

Figure 5-15: If there were no switches, $y(t) \to CA^{-1}B$

Proposition 5.6 *Let $t_+ > 0$ be the smallest solution of*

$$\int_{t_+}^{\infty} \left|Ce^{A\tau}B\right| d\tau + |Ce^{At_+}A^{-1}B| \leq -(CA^{-1}B + d) \tag{5.17}$$

If t_a and t_b are sufficiently large consecutive switching times then $|t_a - t_b| \leq t_+$.

Proof: Assume that after a sufficiently large time the trajectory is at $x_0 \in S_0^d$. Without loss of generality, assume $x(0) = x_0$. Then $y(t)$ will be positive in some interval $(0, \epsilon)$. We are interested in finding an upper bound on the time it takes to switch. That is, we would like to find an upper bound $t_+ > 0$ of those $t > 0$ such that $y(t) = -d$, i.e.,

$$Ce^{At_+}(x_0 - A^{-1}B) = -(CA^{-1}B + d) > 0$$

Using proposition 5.5 with $F = C$ and $\bar{t} = t_+$, we can get a bound on the left side of the inequality

$$\begin{aligned} \left|Ce^{At_+}x_0 - Ce^{At_+}A^{-1}B\right| &\leq |Ce^{At_+}x_0| + |Ce^{At_+}A^{-1}B| \\ &\leq \int_{t_+}^{\infty} \left|Ce^{A\tau}B\right| d\tau + |Ce^{At_+}A^{-1}B| \end{aligned}$$

Therefore, $t_+ > 0$ must satisfy (5.17). ■

Remember that if $x_0 \in S_0^d$, $y(t)$ will be positive at least in some interval $(0, \epsilon)$. The next result shows that in the bounded invariant set characterized in proposition 5.5, ϵ cannot be made arbitrarily small. Basically, for sufficiently large time t, $x(t)$ is bounded, and a lower bound on the time it takes between two consecutive switches can be obtained.

Proposition 5.7 *Let* $k_d = -2CB$, $k_{dd} = \|CA^2e^{At}B\|_{\mathcal{L}_1} + \max_{t\geq 0} |Ce^{At}AB|$, *and* $k_{dl} = \|CAe^{At}B\|_{\mathcal{L}_1} + \max_{t\geq 0} |Ce^{At}B|$ *and define*

$$t_1 = \frac{k_d + \sqrt{k_d^2 + 4k_{dd}d}}{k_{dd}}$$

and

$$t_2 = \frac{2d}{k_{dl}}$$

Also, let $t_- = \max\{t_1, t_2\}$. *If* t_a *and* t_b *are sufficiently large consecutive switching times then* $|t_a - t_b| \geq t_-$.

Proof: There are many ways to find bounds on t_-. We will show two here: t_1 and t_2. Since they are found independently of each other, we are interested in the larger one. We start with t_1.

Assume again that after a sufficiently large time the trajectory is at $x_0 \in S_0^d$. Without loss of generality, assume $x(0) = x_0$. This means that right before the switch (at $t = 0^-$), $\dot{y}(0^-) \geq 0$, i.e., $CAx_0 + CB \geq 0$. Therefore, after the switch at $t = 0^+$, $\dot{y}(0^+) = CAx_0 - CB = CAx_0 + CB - 2CB \geq -2CB$. That is, $\dot{y}(0^+) \geq k_d$.

We also need bounds on the second derivative of y for $t > 0$. From $y(t)$ we get $\dot{y}(t) = CAe^{At}(x_0 - A^{-1}B)$, and $\ddot{y}(t) = CA^2e^{At}(x_0 - A^{-1}B)$. This means that

$$\begin{aligned} |\ddot{y}(t)| &= \left|CA^2e^{At}(x_0 - A^{-1}B)\right| \\ &\leq |CA^2e^{At}x_0| + |Ce^{At}AB| \\ &\leq \|CA^2e^{At}B\|_{\mathcal{L}_1} + \max_{t\geq 0} |Ce^{At}AB| \\ &= k_{dd} \end{aligned}$$

So, $-k_{dd} \leq \ddot{y}(t) \leq k_{dd}$. In order to find a lower bound on the switching time, we consider the worst case scenario, that is, we consider the case when $\ddot{y}(t) = -k_{dd}$ and $\dot{y}(0) = k_d$. This implies that $\dot{y}(t) = -k_{dd}t + k_d$. Integrating once more and knowing that $y(0) = d$, yields

$$y(t) = -\frac{k_{dd}}{2}t^2 + k_dt + d$$

We are looking for values of $t = t_1$ such that $y(t_1) = -d$ and $t_1 > 0$. $y(t_1) = -d$ has two solutions

$$t_1 = \frac{k_d \pm \sqrt{k_d^2 + 4k_{dd}d}}{k_{dd}}$$

However, only one is positive (the one with the + sign) since $\ddot{y}(t) < 0$ for all t and either $y(0) > 0$ (if $d > 0$) or $\dot{y}(0) > 0$ (if $d = 0$ and $CB < 0$).

To find t_2 we find a bound on the first derivative of y for $t > 0$

$$\begin{aligned} |\dot{y}(t)| &= \left|CAe^{At}(x_0 - A^{-1}B)\right| \\ &\leq |CAe^{At}x_0| + |Ce^{At}B| \\ &\leq \|CAe^{At}B\|_{\mathcal{L}_1} + \max_{t\geq 0} |Ce^{At}B| \\ &= k_{dl} \end{aligned}$$

So, $-k_{dl} \leq \dot{y}(t) \leq k_{dl}$. The worst case scenario is the case when $\dot{y}(t) = -k_{dl}$ (with $y(0) = d$). Therefore, $y(t) = -k_{dl}t + d$. Again, we are looking for values of $t = t_2$ such that $y(t_2) = -d$ and $t_2 > 0$, i.e., the solution of $-k_{dl}t_2 + d = -d$. ■

Chapter 6

On/Off Systems

This chapter addresses the problem of global stability analysis of *on/off systems* (OFS) using quadratic surface Lyapunov functions. In the last chapter, quadratic surface Lyapunov functions were successfully applied to prove global asymptotic stability of limit cycles of relay feedback systems. Here, we show that similar ideas can be used to prove global asymptotic stability of equilibrium points of piecewise linear systems (PLS). We consider OFS which are characterized by an LTI system in feedback with a nonlinear static controller that switches between closed loop (on) and open loop (off), depending on the output of the LTI system. We present conditions in the form of LMIs that, when satisfied, guarantee *global* asymptotic stability of an equilibrium point. A large number of examples was successfully proven globally stable, including systems with unstable nonlinearity sectors, for which classical methods like small gain theorem, Popov criterion, Zames-Falb criterion, IQCs, fail to analyze. The main contribution of this chapter is to show that the tools developed in chapter 4 can be used to not only analyze limit cycles (as seen in chapter 5), but also equilibrium points, even when these do not belong to a switching surface. This opens the door to the possibility that more general PLS can be systematically globally analyzed using quadratic surface Lyapunov functions.

6.1 Introduction

The ideas introduced in chapter 5 were very successful in proving global stability of limit cycles of RFS. On the switching surfaces we found quadratic Lyapunov functions that were used to prove that the impact map, i.e., the map from one switching surface to the other switching surface, was contracting in some norm. Such contraction, in turn, proved the limit cycle to be global asymptotically stable. This lead to the discovery that quadratic surface Lyapunov functions can be used in the stability analysis of limit cycles of RFS.

In chapter 5 there was an obvious choice on how the stability problem needed to be setup since the fixed point, consisting of the intersection of the limit cycle with a switching surface, belonged to the switching surface. Therefore, all we needed was to show that consecutive switches were getting closer in some norm to the fixed point.

This could even be done by just analyzing a single impact map due to the symmetry of RFS. In this chapter, we show that the approach introduced in chapter 4 can also be used to efficiently prove global asymptotic stability of equilibrium points, even when these equilibrium points do not belong to the switching surface. In case an equilibrium point belongs to the switching surface, the problem is similar to the one in chapter 5 , with the added difficulty that now we have to simultaneously analyze two impact maps, instead of just one. If an equilibrium points does *not* belong to the switching surface, setting up the stability problem on the switching surface is not so straightforward. This particular aspect, together with the problem of analyzing simultaneously more than one impact map, will be the main focus of this chapter. We show that even in the case where equilibrium points do not belong to the switching surface, analysis using quadratic surface Lyapunov functions can still be applied. When quadratic surface Lyapunov functions are appropriately selected, they can be used to show contraction of impact maps, that, in turn, prove global asymptotic stability of equilibrium points.

To demonstrate these ideas, we chose a class of PLS known as on/off systems (OFS). An OFS can be thought of as an LTI system that switches between open and closed loop. The switches are determined by the values of the output of the LTI system. OFS can be found in many engineering applications. In electronic circuits, diodes can be approximated by on/off controllers. Transient behavior of logical circuits that involve latches/flip-flops performing very fast on/off switching can be modeled using on/off circuits and saturations. In general, on/off circuits have many applications in electronics and circuit design. Another area of application of OFS is aircraft control. For instance, in [12], a *max* controller is designed to achieve good tracking of the pilot's input without violating safety margins.

We are interested in checking if a unique locally stable equilibrium point of an OFS is also globally stable. The idea is to construct quadratic Lyapunov functions on the switching surface of the system to show contraction in some sense of impact maps. Under certain easily verifiable conditions, quadratic stability of impact maps implies globally asymptotically stability of OFS. The search for quadratic surface Lyapunov functions is efficiently done by solving a set of LMIs.

As in relay feedback systems, a large number of examples was successfully proven globally stable. These include systems with an unstable affine linear subsystem, systems of relative degree larger than one and of high dimension, and systems with unstable nonlinearity sectors, for which classical methods like small gain theorem, Popov criterion, Zames-Falb criterion, and integral quadratic constraints [68, 35, 16, 42, 44], fail to analyze. In fact, it is still an open problem whether there exists an example with a globally stable equilibrium point that could not be successfully analyzed with this new methodology.

This chapter is organized as follows. Section 6.2 starts by formulating the problem. Section 6.3 presents the main results of this chapter followed by some illustrative examples in section 6.4. In section 6.5 we show a way to improve the stability conditions presented in section 6.3. Section 6.6 presents a special case of OFS where the switching surface includes the origin. Finally, section 6.7 discusses some technical details.

6.2 Problem Formulation

The main purpose of this section is to introduce the problem we plan to solve. We start by defining OFS followed by some necessary conditions for the global stability of a unique locally stable equilibrium point. We then talk about some of the properties of this class of systems.

An OFS is defined as follows. Consider a SISO LTI system satisfying the following linear dynamic equations

$$\begin{cases} \dot{x} &= Ax + Bu \\ y &= Cx \end{cases} \tag{6.1}$$

where $x \in \mathbb{R}^n$, in feedback with a on/off controller (see figure 6-1) given by

$$u(t) = \max\{0, y(t) - d\} \tag{6.2}$$

where $d \in \mathbb{R}$. By a solution of (6.1)-(6.2) we mean functions (x, y, u) satisfying (6.1)-(6.2). Since u is continuous and globally Lipschitz, $Ax + B\max\{0, Cx - d\}$ is also globally Lipschitz. Thus, the OFS has a unique solution for any initial state.

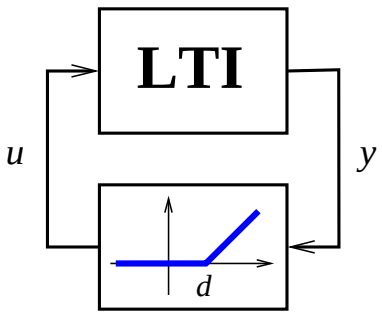

Figure 6-1: On/Off System

In the state space, the on/off controller introduces a switching surface composed of an hyperplane of dimension $n - 1$

$$S = \{x \in \mathbb{R}^n : \ Cx = d\}$$

On one side of the switching surface ($Cx < d$), the system is given by $\dot{x} = Ax$. On the other side ($Cx > d$) the system is given by $\dot{x} = Ax + B(Cx - d) = A_1 x + B_1$, where $A_1 = A + BC$ and $B_1 = -Bd$. Note that the vector field is continuous along the switching surface since for any $x \in S$, $A_1 x + B_1 = Ax$.

An OFS has either zero, one, or two equilibrium points. We are interested in those cases where the system has a unique locally stable equilibrium point. Only here can an OFS have a globally stable equilibrium point. Next, we give necessary conditions for the existence of a single locally stable equilibrium point for different values of d.

If $d > 0$ there is at least one equilibrium point at the origin. In this case, it is necessary that A is Hurwitz to guarantee the origin is locally stable. It is also necessary that A_1 is invertible or otherwise there would exist a continuum of equi-

librium points. The affine linear system $\dot{x} = A_1 x + B_1$ has an equilibrium point at $-A_1^{-1}B_1$. In order to guarantee an OFS has only the origin as an equilibrium point, it is necessary that $-CA_1^{-1}B_1 < d$. It is also necessary that A_1 has no real unstable eigenvalues or, otherwise, the system will have trajectories that grow unbounded[1]. To see this, let λ be a real unstable eigenvalue of A_1 with associated eigenvalue v. Let $x_0 = \alpha v - A_1^{-1}B_1$, where α is chosen such that $Cx_0 > d$. The trajectory starting at x_0 is given by $x(t) = \alpha e^{\lambda t} v - A_1^{-1}B_1$. Hence, the trajectory will grow unbounded without switching since $Cx(t) = \alpha e^{\lambda t} Cv - CA_1^{-1}B_1 \geq \alpha Cv - CA_1^{-1}B_1 > d$, for all $t \geq 0$. Note that $\alpha Cv > d + CA_1^{-1}B_1 > d - d = 0$.

When $d = 0$, the origin is the only equilibrium point. For the same reasons as above, it is necessary that both A and A_1 do not have real unstable eigenvalues. Note that in this case, there is no "easy" way to check if the origin is locally stable or not.

When $d < 0$, it must be true that $-CA_1^{-1}B_1 > d$ or otherwise the system will have no equilibrium point. It is also necessary that A_1 is Hurwitz and A has no real unstable poles.

We can assume without loss of generality that $d \geq 0$. If $d < 0$ and all necessary conditions are met, with an appropriate change of variables ($x_{new} = -(x + A_1^{-1}B_1)$), the problem can be transformed to one of analyzing the origin with $d_{new} \geq 0$. In this case, $A_{new} = A_1$, $A_{1new} = A$, $B_{1new} = AA_1^{-1}B_1$, and $d_{new} = -d - CA_1^{-1}B_1 \geq 0$.

Consider a subset S_+ of S given by

$$S_+ = \{x \in S : \ CAx \geq 0\}$$

This set is important since it tells us which points in S can be reached by trajectories starting at any x_0 such that $Cx_0 < d$ (see figure 6-2). Similarly, define $S_- \subset S$ as

$$S_- = \{x \in S : \ CAx \leq 0\}$$

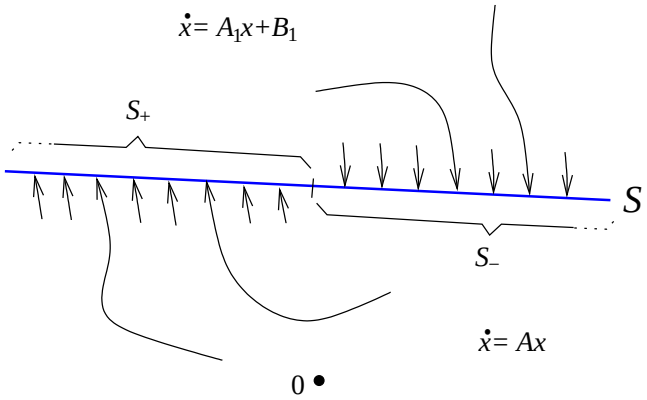

Figure 6-2: Both sets S_+ and S_- in S

[1]Possible exceptions occur when the eigenvector associated with the unstable real eigenvalue is perpendicular to C'.

Note that $S = S_+ \bigcup S_-$ and $S_+ \bigcap S_- = \{x \in S : CAx = 0\}$. From here on, we assume $d > 0$. In terms of stability analysis, $d = 0$ is a special case of when $d > 0$, and will be considered separately in section 6.6.

Since A must be Hurwitz, there is a set of points in S_- such that any trajectory starting in that set will never switch again and will converge asymptotically to the origin. In other words, let $S^* \subset S_-$ be the set of points x_0 such that the following equation

$$Ce^{At}x_0 = d$$

does not have a solution for any $t > 0$. Note that this set S^* is not empty. To see this, let $P > 0$ satisfy $PA + A'P = -I$. Then, an obvious point in S^* is the point x_1^* obtained from the intersection of S with the level set $x'Px = k$, where $k \geq 0$ is chosen such that the ellipse $x'Px = k$ is tangent to S (see figure 6-3).

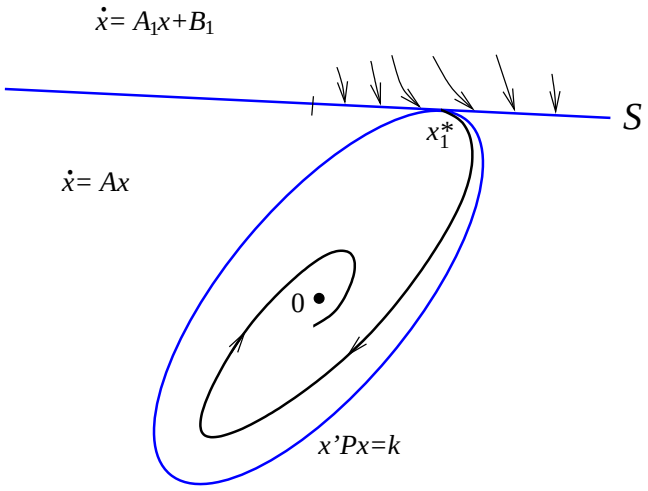

Figure 6-3: How to obtain x_1^*

The problem we propose to solve here is to give sufficient conditions that, when satisfied, prove the origin of an OFS is globally asymptotically stable. The strategy of this proof is a follows. Consider a trajectory starting at some point $x_0 \in S_+$ (see figure 6-4). Since A_1 has no unstable real poles, the trajectory $x(t)$ will eventually switch at some time $t_1 > 0$, i.e., $Cx(t_1) = d$ and $Cx(t) \geq d$ for $t \in [0, t_1]$. Let $x_1 = x(t_1) \in S_-$. If $x_1 \in S^*$, the trajectory will not switch again and converge asymptotically to the origin. Since we already know S^* is a stable set, we need to concentrate on those points in $S_- \backslash S^*$ since those are the ones that may lead to potentially unstable trajectories. So, assume the trajectory switches again at time $t_2 > t_1$, and let $x_2 = x(t_2) \in S_+$. Again, we would switch at $x(t_3) = x_3$ and so on. The idea is to check if x_3 is closer in some sense to S^* than x_1. If so, this would mean that eventually $x(t_{2N-1}) \in S^*$, for some positive integer N, and prove that the origin is globally asymptotically stable. This is the idea behind the results in the next section.

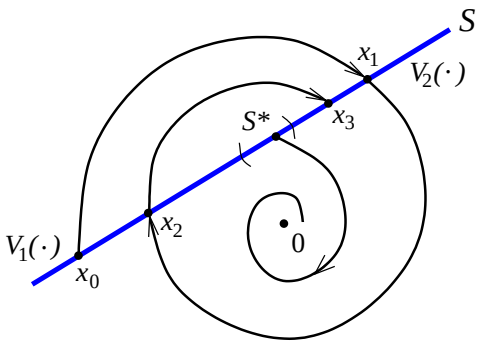

Figure 6-4: Trajectory of an OFS

Before presenting the main results, it is convenient to notice that $x_0, x_1, x_2 \in S$ can be parametrized. Let $x_0 = x_0^* + \Delta_0$, $x_1 = x_1^* + \Delta_1$, and $x_2 = x_0^* + \Delta_2$, where $x_0^*, x_1^* \in S$, and $C\Delta_0 = C\Delta_1 = C\Delta_2 = 0$. Also, define $x_0^*(t)$ $(x_1^*(t))$ as the trajectory of $\dot{x} = A_1 x + B_1$ $(\dot{x} = Ax)$, starting at x_0^* (x_1^*), for all $t > 0$. Since x_i^* can be any points in S, we chose them to be such that $Cx_i^*(t) < d$ for all $t > 0$. As explained in section 6.7.1, this is always possible, even when A_1 is unstable (as long as it has at least one stable eigenvalue with an associated eigenvector that is not perpendicular to C'). The reason for this particular choice of x_0^* and x_1^* is so that $Cx_i^*(t) - d \neq 0$ for all $t > 0$. This will be necessary in proposition 6.1.

As in RFS, impact maps associated with OFS are multivalued. Define the expected switching times $\mathcal{T}_1$ and $\mathcal{T}_2$ as in chapter 4.

6.3 Global Asymptotic Stability of On/Off Systems

Before presenting the main result of this chapter, we first show that each impact map associated with the OFS can be represented as a linear transformation analytically parametrized by the correspondent switching time. This result is similar to theorem 4.1.

Proposition 6.1 *Define*

$$w_1(t) = \frac{Ce^{A_1 t}}{d - Cx_0^*(t)}$$

and

$$w_2(t) = \frac{Ce^{At}}{d - Cx_1^*(t)}$$

Let $H_1(t) = e^{A_1 t} + (x_0^*(t) - x_1^*)w_1(t)$ *and* $H_2(t) = e^{At} + (x_1^*(t) - x_0^*)w_2(t)$. *Then, for any* $\Delta_0 \in S_+ - x_0^*$ *there exists a* $t_1 \in \mathcal{T}_1$ *such that*

$$\Delta_1 = H_1(t_1)\Delta_0$$

Such t_1 *is the switching time associated with* Δ_1. *Similarly, for any* $\Delta_1 \in S_- \backslash S^* - x_1^*$

there exists a $t_2 \in \mathcal{T}_2$ *such that*

$$\Delta_2 = H_2(t_2)\Delta_1$$

Such t_2 *is the switching time associated with* Δ_2*.*

Next, define two quadratic Lyapunov functions V_1 and V_2 on the switching surface S

$$V_i(x) = x'P_ix - 2x'g_i + \alpha_i \tag{6.3}$$

where $P_i > 0$, for $i = 1, 2$. Global asymptotically stability of the origin follows if both impact maps are quadratically stable, i.e., if there exist $P_i > 0$, g_i, α_i such that

$$V_2(\Delta_1) < V_1(\Delta_0) \quad \text{for all } \Delta_0 \in S_+ - x_0^* \tag{6.4}$$

$$V_1(\Delta_2) < V_2(\Delta_1) \quad \text{for all } \Delta_1 \in S_- \backslash S^* - x_1^* \tag{6.5}$$

The next theorem is an extension of theorem 4.2 for the case where we have to simultaneously prove contraction of two impact maps. Let $P > 0$ on S stand for $x'Px > 0$ for all $x \in S$. As a short hand, in the following result we use $H_{it} = H_i(t)$ and $w_{it} = w_i(t)$.

Theorem 6.1 *Define*

$$\begin{aligned} R_1(t) &= P_1 - H_{1t}'P_2H_{1t} - 2\left(g_1 - H_{1t}'g_2\right)w_{1t} + w_{1t}'\alpha w_{1t} \\ R_2(t) &= P_2 - H_{2t}'P_1H_{2t} - 2\left(g_2 - H_{2t}'g_1\right)w_{2t} - w_{2t}'\alpha w_{2t} \end{aligned}$$

where $\alpha = \alpha_1 - \alpha_2$*. The origin of the OFS is globally asymptotically stable if there exist* $P_1, P_2 > 0$ *and* g_1, g_2, α *such that*

$$\begin{cases} R_1(t_1) > 0 & \text{on } S_+ - x_0^* \\ R_2(t_2) > 0 & \text{on } S_- \backslash S^* - x_1^* \end{cases}$$

for all expected switching times $t_1 \in \mathcal{T}_1$ *and* $t_2 \in \mathcal{T}_2$*.*

A relaxation of the constraints on Δ_0 and Δ_1 in the previous theorem results in computationally efficient conditions.

Corollary 6.1 *The origin of the OFS is globally asymptotically stable if there exist* $P_1, P_2 > 0$ *and* g_1, g_2, α *such that*

$$\begin{cases} R_1(t_1) > 0 & \text{on } S - x_0^* \\ R_2(t_1) > 0 & \text{on } S - x_1^* \end{cases} \tag{6.6}$$

for all expected switching times $t_1 \in \mathcal{T}_1$ *and* $t_2 \in \mathcal{T}_2$*.*

For each t_1, t_2 these conditions are LMIs for which we can solve for $P_1, P_2 > 0$ and g_1, g_2, α using efficient available software. As we will see in the next section, although

these conditions are more conservative than the ones in theorem 6.1, they are already enough to prove global asymptotic stability of many important OFS.

Each condition in (6.6) depends only on a single scalar parameter, i.e., R_1 depends only on t_1 and not on t_2, and, similarly, R_2 depends only on t_2. Computationally, this means that when we grid each set of expected switching times, this will only affect one of the conditions in (6.6). Thus, if we need m_1 samples of $\mathcal{T}_1$ and m_2 samples of $\mathcal{T}_2$, we end up with a total of $m_1 + m_2$ LMIs. Note that a less conservative condition than those in theorem 6.1 could be obtained. Such condition, of the form $R(t_1, t_2) > 0$, would, however, lead to $m_1 \times m_2$ LMIs, and the analysis problem would easily become computationally intractable. This difference in complexity is even more obvious in the analysis of other, more complex classes of PLS that may require the simultaneous analysis of a large number of impact maps.

Proof of proposition 6.1: This proof is similar to the proof of theorem 4.1. If $x(0) = x_0 + \Delta_0 \in S_+$, integrating the dynamic equations (6.1) with $u = Cx - d$ yields

$$\Delta_1 = e^{A_1 t}\Delta_0 + x_0^*(t) - x_1^*$$

From the fact that $C\Delta_1 = 0$ we get $Ce^{A_1 t}\Delta_0 = d - Cx_0^*(t)$. Since x_0^* was chosen such that $d - Cx_0^*(t) > 0$ for all $t > 0$ we rewrite the last expression as

$$w_1(t)\Delta_0 = 1 \tag{6.7}$$

which means that Δ_1 can be written as

$$\Delta_1 = e^{A_1 t}\Delta_0 + \left(x_0^*(t) - x_1^*\right) w_1(t)\Delta_0$$

The same way, we can find Δ_2 as a function of Δ_1 and t, the switching time associated with Δ_2. The dynamic equations now are simply $\dot{x} = Ax$. Therefore, $x_2 = e^{At}x_1$. Since $x_2 = x_0^* + \Delta_2$,

$$\Delta_2 e^{At}\Delta_1 + x_1^*(t) - x_0^*$$

Again, from the fact that $C\Delta_2 = 0$ we get $Ce^{At}\Delta_1 = d - Cx_1^*(t)$. Since x_1^* was chosen such that $d - Cx_1^*(t) > 0$ for all $t > 0$ we rewrite the last expression as

$$w_2(t)\Delta_1 = 1 \tag{6.8}$$

leading to

$$\Delta_2 = e^{At}\Delta_1 + \left(x_1^*(t) - x_0^*\right) w_2(t)\Delta_1$$

which proves the desired result. ■

Note that equations (6.7) and (6.8) tell us that for a given switching time t, Δ_0 and Δ_1 are restricted to $n-2$-dimensional sets consisting of the intersection of $S_+ - x_0^*$ with the set of Δ_0 that satisfy (6.7) and the intersection of $S_- \backslash S^* - x_0^*$ with the set of Δ_1 that satisfy equation (6.8), respectively.

Proof of theorem 6.1: From (6.4) and using proposition 6.1, we have

$$\begin{aligned} & \Delta_1' P_2 \Delta_1 - 2\Delta_1' g_2 + \alpha_2 < \Delta_0' P_1 \Delta_0 - 2\Delta_0' g_1 + \alpha_1 \\ \Leftrightarrow \quad & \Delta_0' H_{1t}' P_2 H_{1t} \Delta_0 - 2\Delta_0' H_{1t}' g_2 + \alpha_2 < \Delta_0' P_1 \Delta_0 - 2\Delta_0' g_1 + \alpha_1 \\ \Leftrightarrow \quad & \Delta_0' \left(P_1 - H_{1t}' P_2 H_{1t}\right) \Delta_0 - 2\Delta_0' \left(g_1 - H_{1t}' g_2\right) + \alpha > 0 \end{aligned}$$

Finally, using (6.7) we have

$$\Delta_0' \left(P_1 - H_{1t}' P_2 H_{1t}\right) \Delta_0 - 2\Delta_0' \left(g_1 - H_{1t}' g_2\right) w_{1t} \Delta_0 + \Delta_0' w_{1t}' \alpha w_{1t} \Delta_0 > 0$$

which is the desired result. $R_2(t)$ can be obtained in a similar way. ■

6.4 Examples

The following examples were processed in `matlab` code. The latest version of this software is either available at [27] or upon request. Before presenting the examples, we briefly explain the `matlab` function we developed. The inputs to this function are a transfer function of an LTI system together with the displacement of the nonlinearity switch d. If the OFS is proven to be globally stable, the function returns the values of the parameters of the Lyapunov functions (6.3). The `matlab` function also returns a graphic showing the minimum eigenvalues of each $R_i(t_i)$ in (6.6), which must be positive for all expected switching times t_i.

For most OFS, the expected switching times include $t_i = 0$ and large values of t_i. Thus, before moving into the examples, it is important to explain how the analysis is done when t_i is close to zero and when t_i is very large. We start with the analysis near zero.

Zero switching time corresponds to points in S such that $CAx = 0$. At those points, the Lyapunov functions (6.3) must be continuous since this is the only way

$$\begin{cases} V_2(\Delta_1) \leq V_1(\Delta_0) \\ V_1(\Delta_2) \leq V_2(\Delta_1) \end{cases}$$

can be satisfied simultaneously, for all $\Delta_0, \Delta_1, \Delta_2 = \Delta_0$ such that $x_0^* + \Delta_0 = x_1^* + \Delta_1 = x$ and $CAx = 0$. Therefore, we need $V_1(\Delta_0) = V_2(\Delta_1)$. This imposes certain restrictions on $P_1, P_2 > 0$, g_1, g_2, and α. The details can be found in section 6.7.2.

Just like in RFS, we would like to obtain bounds on the expected switching times. With the exception of 3^{rd}-order systems, however, finding upper bounds t_{imax} on switching times is, in general, not an easy task. The idea is to first guarantee conditions (6.6) are satisfied in some intervals $(0, t_{imax})$ and then check if they are also valid for all $t_i > t_{imax}$. This is considered in section 6.7.3.

Note that for 3^{rd}-order systems, at least one of the upper bounds of the expected switching times is easily calculated since the switching surface is an hyperplane of dimension 2, which can be visualized.

Example 6.1 Consider the OFS on the left of figure 6-5 with $d = 1$. It is easy to

see that the origin of this system is locally stable.

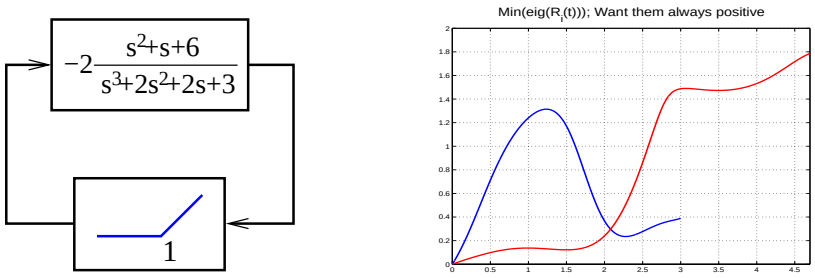

Figure 6-5: 3^{rd}-order system with unstable nonlinearity sector

Using conditions (6.6), we show that the origin is in fact globally asymptotically stable. The right side of figure 6-5 illustrates this fact: the minimum eigenvalue of each condition (6.6) is positive on its respective set of expected switching times. The expected switching times in this example are approximately $\mathcal{T}_1 = (0, 1.85)$ and $\mathcal{T}_2 = (0, 4.7)$. For instance, if $t_1 \geq 1.85$, there is no point in S_+ with switching time equal to t_1.

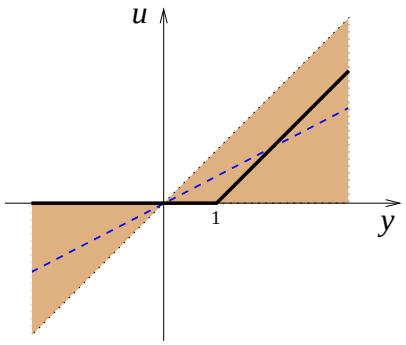

Figure 6-6: On/off controller versus constant gain of 1/2 (dashed)

Note that this system has an unstable nonlinearity sector. If the on/off nonlinearity is replaced by a linear constant gain of 1/2, the system becomes unstable (see figure 6-6). This is very interesting since it tells us that analysis tools like small gain theorem, Popov criterion, Zames-Falb criterion, and integral quadratic constraints, would all fail to analyze OFS of this nature. ■

Example 6.2 Consider the OFS on the left of figure 6-7 with $d = 1$ and $k > 0$. Once again, it is easy to see that the origin of this system is locally stable for any $k > 0$.

Note that $\|Ce^{At}B\|_{\mathcal{L}_1} = k$. Thus, the small gain theorem can be applied whenever $k \leq 1$. When $k > 1$, however, the small gain theorem fails to analyze the system.

Let $k = 2$. Using conditions (6.6), we show the origin is globally asymptotically stable. The right side of figure 6-7 shows how conditions (6.6) are satisfied in some intervals $(0, t_{imax})$, $i = 1, 2$. The intervals $(0, t_{imax})$ are bounds on the expected

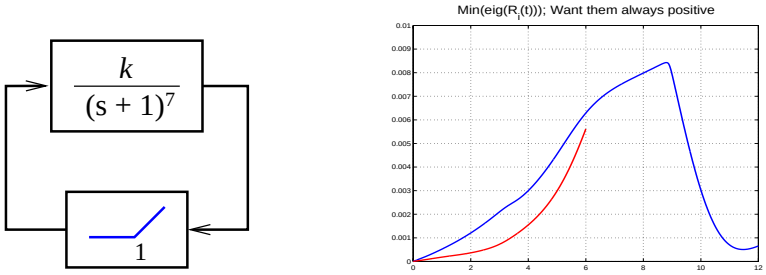

Figure 6-7: System with relative degree 7 (left); global stability analysis when $k = 2$ (right)

switching times. The results in section 6.7.3 guarantee the stability conditions are also satisfied for all $t_i > t_{imax}$. For details on how to find such bounds see section 6.7.3. ■

Example 6.3 Consider the OFS in figure 6-8 with $d = 1$. It is easy to see that the origin of this system is locally stable. A_1, however, is unstable.

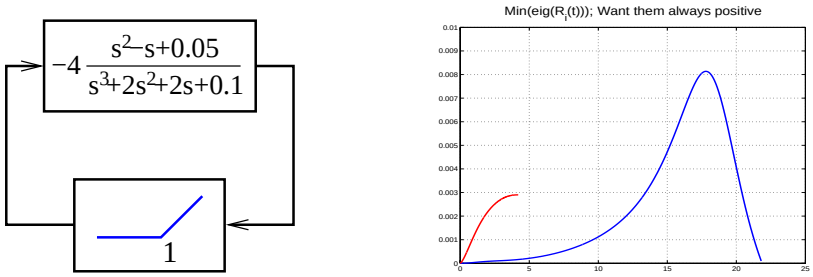

Figure 6-8: System with unstable A_1

Although A_1 is unstable, since this is a 3^{rd}-order system, it is easy to find bounds on the expected switching times for the subsystem $\dot{x} = A_1 x + B_1$. In this case, no point in S_+ has a switching time higher than 21.8. As for t_2, we use the same ideas as in the previous example, based on the results in section 6.7.3. Using conditions (6.6), we show that although A_1 is unstable, the origin is globally asymptotically stable. The right side of figure 6-8 shows how conditions (6.6) are satisfied in the intervals $(0, t_{imax})$, $i = 1, 2$ (the minimum eigenvalue of the second condition in (6.6) is scaled by 500 in figure 6-8, for purpose of visualization). ■

6.5 Improvement of stability conditions

Conditions (6.6) are sufficient conditions for the global stability of the origin. These conditions do not take into account that both Δ_0 and Δ_1 are restricted to $S_+ - x_0^*$ and $S_- \backslash S^* - x_1^*$, respectively. Using the same ideas in sections 4.3.1 and 5.5, conditions (6.6) can be improved.

For each point $x_0 \in S_+$, there is an associated switching time t_1. Define S_{t_1} as the set of initial conditions $x_0 \in S_+$ such that $y(t) \geq d$ on $[0, t_1]$, and $y(t_1) = d$. This set S_{t_1} forms a linear and convex set of dimension $n-2$. Analogously, define S_{t_2} as the set of initial conditions $x_1 \in S_- \backslash S^*$ such that $y(t) \leq d$ on $[0, t_2]$, and $y(t_2) = d$. Given this, conditions (6.6) can be improved to

$$\begin{cases} R_1(t_1) > 0 & \text{on } S_{t_1} - x_0^* \\ R_2(t_2) > 0 & \text{on } S_{t_2} - x_1^* \end{cases} \tag{6.9}$$

for some $P_1, P_2 > 0$, g_1, g_2, α, and for all expected switching times t_1, t_2.

The problem with conditions (6.9) is that, in general, the sets S_{t_i}, $i = 1, 2$, are not easily characterized. An alternative is to consider the sets $\tilde{S}_{t_i} \supset S_{t_i}$ obtained from equations (6.7), (6.8) given by

$$\tilde{S}_{t_1} = \{x_0^* + \Delta_0 \in S_+ : \ w_{1t}\Delta_0 = 1\}$$

and

$$\tilde{S}_{t_2} = \{x_1^* + \Delta_1 \in S_- \backslash S^* : \ w_{2t}\Delta_1 = 1\}$$

Since $\tilde{S}_{t_i} \supset S_{t_i}$, conditions (6.9) hold if there exist $P_1, P_2 > 0$, g_1, g_2, α such that

$$\begin{cases} R_1(t_1) > 0 & \text{on } \tilde{S}_{t_1} - x_0^* \\ R_2(t_2) > 0 & \text{on } \tilde{S}_{t_2} - x_1^* \end{cases} \tag{6.10}$$

for all expected switching times t_1, t_2. The same way as in section 4.3.1, $\Delta_i \in S_{t_i}$ satisfies a conic relation

$$\Delta_i' \beta_{t_i} \Delta_i > 0$$

for some matrices β_{t_i} (to see details of the construction of these matrices please refer to section 4.5. Using the S-procedure, conditions (6.10) are equivalent to

$$\begin{cases} R_1(t_1) - \tau_{t_1}\beta_{t_1} > 0 & \text{on } S - x_0^* \\ R_2(t_2) - \tau_{t_2}\beta_{t_2} > 0 & \text{on } S - x_1^* \end{cases} \tag{6.11}$$

for some $P_i > 0$, g_i, α, some scalar functions $\tau_{t_i} > 0$, and for all expected switching times t_i. For each t_1, t_2 these conditions are LMI which again can be solved using efficient available software.

It is still possible to improve conditions (6.11) further more. They do not take advantage that a trajectory starting at $x_0 \in \tilde{S}_{t_1}$ ($x_1 \in \tilde{S}_{t_2}$) must satisfy $y(t) \geq d$ ($y(t) \leq d$) on $[0, t_1]$ ($[0, t_2]$). This is captured by conditions (6.9) but not by conditions (6.11) since $\tilde{S}_{t_i} \supset S_{t_i}$. See sections 4.3.1 and 5.5 for more details.

6.6 Special case: $d = 0$

When $d = 0$ we can write stability conditions that are, in general, much less conservative than conditions (6.11). First, since the origin belongs to both systems $\dot{x} = Ax$

and $\dot{x} = (A + BC)x$, it is only required that both systems do not have real unstable poles. $d = 0$ also means $x_0^* = x_1^* = g_1 = g_2 = 0$ and $\alpha = 0$. All we need to find is $P_1, P_2 > 0$.

In this case, $\Delta_1 = e^{A_1 t_1}\Delta_0$ and $\Delta_2 = e^{At_2}\Delta_1$. Thus, the stability conditions come down to

$$\begin{aligned} & \Delta_1' P_2 \Delta_1 < \Delta_0' P_1 \Delta_0 \\ \Leftrightarrow \quad & \Delta_0' \left(P_1 - e^{A_1' t_1} P_2 e^{A_1 t_1} \right) \Delta_0 > 0 \end{aligned}$$

and

$$\begin{aligned} & \Delta_2' P_1 \Delta_2 < \Delta_1' P_2 \Delta_1 \\ \Leftrightarrow \quad & \Delta_1' \left(P_2 - e^{A' t_2} P_1 e^{A t_2} \right) \Delta_1 > 0 \end{aligned}$$

for some $P_1, P_2 > 0$, all expected switching times t_1, t_2, and all $\Delta_0 \in S_+$, $\Delta_1 \in S_- \backslash S^*$.

Notice that $C\Delta_0 = 0$, $C\Delta_1 = 0$, and $C\Delta_2 = 0$. Therefore $Ce^{A_1 t_1}\Delta_0 = 0$ and $Ce^{At_2}\Delta_1 = 0$. That is, for fixed values of t_1 and t_2, Δ_1 and Δ_2 are restricted to a subspace of dimension $n-2$. Let $\Pi \in C^\perp$, where $C^\perp$ are the *orthogonal complements* to C, i.e., matrices with a maximal number of column vectors forming an orthonormal set such that $CC^\perp = 0$. Let also $l_{t_1} \in (Ce^{A_1 t_1}\Pi)^\perp$ and $l_{t_2} \in (Ce^{At_2}\Pi)^\perp$. We have the following result.

Theorem 6.2 *The origin of the OFS with $d = 0$ is globally asymptotically stable if there exist $P_1, P_2 > 0$ such that*

$$\begin{cases} l_{t_1}' \Pi' \left(P_1 - e^{A_1' t_1} P_2 e^{A_1 t_1} \right) \Pi l_{t_1} > 0 \\ l_{t_2}' \Pi' \left(P_2 - e^{A' t_2} P_1 e^{A t_2} \right) \Pi l_{t_2} > 0 \end{cases} \tag{6.12}$$

for all expected switching times.

6.7 Technical Details

6.7.1 Choice of x_0^* and x_1^*

We now explain how we chose x_0^* and x_1^* such that both $Cx_0^*(t) < d$ and $Cx_1^*(t) < d$ for all $t > 0$. We start with x_1^*.

x_1^* is found as explained in section 6.2 (see figure 6-3). In this case, x_1^* is given by

$$x_1^* = \frac{P_d^{-1} C'}{C P_d^{-1} C'} d$$

where $P_d > 0$ satisfies $P_d A + A' P_d = -I$.

The choice of x_0^* is more tricky since A_1 may be unstable. If A_1 is stable then we can use the same ideas as we did for x_1^*. First, let $P_u > 0$ satisfy $P_u A_1 + A_1' P_u = -I$.

Then

$$x_0^* = (d + cA_1^{-1}B_1)\frac{P_u^{-1}C'}{CP_u^{-1}C'} - A_1^{-1}B_1$$

If A_1 is not stable (but it has at least one stable eigenvalue) then we need to find a point in S such that it belongs to a stable mode of A_1. If A_1 has real poles then these must be stable. Let λ be a real eigenvalue of A_1 with associated eigenvector v (assume $Cv \neq 0$). Then, if we find a point in S that only excites this mode, the trajectory $x(t)$ will converge to $-A_1^{-1}B_1$ and $Cx(t) < d$ for all $t > 0$. such a point in S is given by

$$x_0^* = -A_1^{-1}B_1 + \frac{d + CA_1^{-1}B_1}{Cv}v$$

In case A_1 only has complex poles, pick a stable complex conjugate pair of eigenvalues $\lambda, \underline{\lambda}$ with associated eigenvectors $v, \underline{v}$, where $\underline{x}$ stands for the complex conjugate of x. Let, $v_a = v + \underline{v}$ and $v_b = i(v - \underline{v})$. Then, any initial condition starting in the hyperplane defined by $-A_1^{-1}B_1 + \alpha_a v_a + \alpha_b v_b$, $\alpha_a, \alpha_b \in \mathbb{R}$ will converge to $-A_1^{-1}B_1$ as time goes to infinity since it only excites this stable complex conjugate mode. An orthogonal basis in this plane can be defined by letting $v_c = -(v_a' v_b)v_a + v_b$. The basis is then given by

$$V = \left[\frac{v_a}{\|v_a\|} \quad \frac{v_c}{\|v_c\|}\right]$$

The trajectory in this basis satisfies $\dot{\alpha} = V'A_1V\alpha = A_v\alpha$. We need to find an α_0 such that $C\left(-A_1^{-1}B_1 + V\alpha_0\right) = d$ and $C\left(-A_1^{-1}B_1 + V\alpha(t)\right) < d$ for all $t > 0$. This is a similar problem to the one we dealt above when finding x_1^*. In this case, α_0 is given by

$$\alpha_0 = \frac{d + CA_1^{-1}B_1}{CVP_v^{-1}V'C'}P_v^{-1}V'C'$$

where $P_v > 0$ satisfies $P_vA_v + A_v'P_v = -I$. Finally,

$$x_0^* = -A_1^{-1}B_1 + V\alpha_0$$

If A_1 only has complex unstable eigenvalues, then for any choice of x_0^*, $Cx(t) = d$ will have an infinity number of solutions for $t > 0$. In this case, x_0^* must be chosen such that the smallest solution $t > 0$ of $Cx(t) = d$ is higher than the maximum possible switching time t_1.

6.7.2 Constraints Imposed When $t_i = 0$

As seen in section 6.4, when $t_i = 0$, $V_1(\Delta_0) = V_2(\Delta_1)$, for all Δ_0, Δ_1 such that $CA(x_0^* + \Delta_0) = CA(x_1^* + \Delta_1) = 0$ and $C\Delta_0 = C\Delta_1 = 0$. This is equivalent to have $R_0 = R_1(0) = R_2(0) = 0$. Since analyzing $R_1(t)$ or $R_2(t)$ near zero will lead to the same results, we analyze $R_1(t)$ at $t = 0$. From section 6.3, $R_0 = R_1(0)$ is given by

$$R_0 = P_1 - P_2 - (g_1 + P_2v_0 - g_2)\,w - w'\,(g_1 + P_2v_0 - g_2)' + w'w\,(\alpha + 2v_0'g_2 - v_0'P_2v_0)$$

where $v_0 = x_0^* - x_1^*$ and

$$w\Delta_0 = \lim_{t\to 0} w_1(t)\Delta_0 = -\frac{CA}{CAx_0^*}\Delta_0$$

Let $l = w^\perp$, $z = w'/(ww')$, and $P = P_1 - P_2$. Since $R_0 = 0$, then $l'R_0l = l'Pl = 0$. This means that in the basis (l, z), the matrix P looks like

$$P_F = \begin{pmatrix} 0 & \Gamma_1 \\ \Gamma_1' & \Gamma_2 \end{pmatrix}$$

for some $\Gamma_1 \in \mathbb{R}^{n-1}$ and $\Gamma_2 \in \mathbb{R}$. In other words, $P = FP_FF'$, where $F = [l\ z]$. Therefore, once $P_2 > 0$ is fixed $P_1 > 0$ must satisfy

$$P_1 = FP_FF' + P_2$$

The same way $l'R_0z = 0$, or $l'\left(Pz - g_1 - P_2v_0 + g_2\right) = 0$. Hence, $Pz - g_1 - P_2v_0 + g_2 = kz$ for some $k \in \mathbb{R}$. For a given g_2, g_1 is then given by

$$g_1 = (P_1 - P_2)z - P_2v_0 + g_2 - kz$$

Finally, it must be true that $z'R_0z = 0$ leading to

$$\alpha = -z'\left(P_1 - P_2\right)z + 2z'\left(g_1 + P_2v_0 - g_2\right) + v_0'P_2v_0 - 2v_0'g_2$$

6.7.3 Checking Stability Conditions for $t_i > t_{imax}$

For simplicity, we are going to present the case when $d = 0$. The other cases follow analogously. Assume conditions (6.12) are satisfied for all $t_i \le t_{imax}$. We would like to easily check if they will also be satisfied for all $t_i > t_{imax}$. Let's concentrate on condition

$$l_{t_2}'\Pi'e^{A't_2}P_1e^{At_2}\Pi l_{t_2} < l_{t_2}'\Pi'P_2\Pi l_{t_2}$$

It is sufficient to show that

$$\Pi'e^{A't_2}\Pi Q_1\Pi'e^{At_2}\Pi < Q_2$$

for all $t > t_{2max}$, and where $Q_i = \Pi'P_i\Pi$. Next, we find an upper bound on the left side of the last inequality. Let $A_z = \Pi'A\Pi$. If A is a stable matrix, it is possible to find a Q and a $\lambda > 0$ such that

$$QA_z + A_z'Q < -\lambda Q$$

This in turn implies that

$$z'(t)Qz(t) < e^{-\lambda t}z_0'Qz_0$$

where $z(t)$ is the solution of $\dot{z} = A_z z$. Using the fact that $e^{A_z t} = \Pi' e^{At} \Pi$, we have

$$z_0' \Pi' e^{A' t_2} \Pi Q \Pi' e^{A t_2} \Pi z_0 < e^{-\lambda t} z_0' Q z_0$$

or simply

$$\Pi' e^{A' t_2} \Pi Q \Pi' e^{A t_2} \Pi < e^{-\lambda t} Q$$

Therefore, for some k

$$\begin{aligned} \Pi' e^{A' t_2} \Pi Q_1 \Pi' e^{A t_2} \Pi &< \Pi' e^{A' t_2} \Pi k Q \Pi' e^{A t_2} \Pi \\ &< k e^{-\lambda t} Q \\ &< k e^{-\lambda t_{2max}} Q \end{aligned}$$

Finally, all we need is to guarantee

$$k e^{-\lambda t_{2max}} Q < Q_2$$

Note that we want to chose the largest λ and the smallest k.

If A_1 (and also A if $d = 0$) has unstable complex poles, then this approach will not work since either e^{At} or $e^{A_1 t}$ is unbounded when $t \to \infty$. In these cases, it is fundamental to get upper bounds for t_{1max} or t_{2max} (depending if it is A_1 or A that has unstable eigenvalues). How to find such bounds is currently under investigation.

Chapter 7

Saturation Systems

This chapter considers impact maps and quadratic surface Lyapunov functions in the study of global asymptotic stability of the origin of *saturation systems* (SAT). Both impact maps and quadratic surface Lyapunov functions, introduced in chapter 4, were first successfully used to globally analyze stability of limit cycles of relay feedback systems (chapter 5). Later, we showed that equilibrium points of piecewise linear systems (PLS) could also be globally analyzed by applying quadratic surface Lyapunov functions to on/off systems (chapter 6). In the state space, on/off systems are composed of a single switching surface. In this chapter, we show that global analysis using quadratic surface Lyapunov functions can still be applied when a PLS has more than one switching surface. For that, we consider saturation systems (SAT). A SAT is characterized by an LTI system in feedback with a saturation controller. Again, we present conditions in the form of LMIs that, when satisfied, guarantee *global* asymptotic stability of equilibrium points. A large number of examples was successfully proven globally stable, including systems with unstable nonlinearity sectors, for which classical methods like small gain theorem, Popov criterion, Zames-Falb criterion, IQCs, fail to analyze. In fact, it is still an open problem whether there exists an example of a SAT with a globally stable equilibrium point that cannot be successfully analyzed with this new methodology. The results in this chapter confirm that quadratic surface Lyapunov functions are a viable and powerful approach to efficiently globally analyze PLS.

7.1 Introduction

The ideas introduced in chapter 4 and applied in chapters 5 and 6 were very successful in proving global asymptotic stability of limit cycles and equilibrium points of certain classes of PLS. On the switching surfaces, we efficiently constructed quadratic Lyapunov functions that were used to show that impact maps associated with the PLS were contracting in some sense. These results opened the door to the possibility that limit cycles and equilibrium points of more general PLS can be systematically globally analyzed using quadratic surface Lyapunov functions.

The results in chapter 6 represented the first step in analyzing equilibrium points of

PLS using quadratic surface Lyapunov functions. In the state space, on/off systems are divided in two partitions by a switching surface. Therefore, the analysis was focused on studying a single switching surface. In the present chapter, we want to show that quadratic surface Lyapunov functions can also be used to globally analyze PLS with more than two partitions and more than one switching surface.

To demonstrate these ideas, we chose a class of PLS known as saturation systems (SAT). The class of SAT we consider consists of an LTI system in feedback with a saturation. Every time the absolute value of the output of the LTI system exceeds a certain value, a switch occurs and the closed loop system dynamics change. The study of such systems is motivated by the possibility of actuator saturation or constraints on the actuators, reflected sometimes in bounds on available power supply or rate limits. These cannot be naturally dealt within the context of standard (algebraic) linear control theory, but are ubiquitous in control applications. The fact that linear feedback laws when saturated can lead to instability has motived a large amount of research. The well known result which states that a controllable linear system is globally state feedback stabilizable, holds as long as the control does not saturate. In many applications, more often than not, the control is restricted to take values within certain bounds which may be met under closed-loop operation. Because feedback is cut, control saturation induces a nonlinear behavior on the closed-loop system. The problem of stabilizing linear systems with bounded controls has been studied extensively. See, for example, [59, 55, 62] and references therein.

In this chapter, we focus on global stability analysis of saturation systems. We are interested in those SAT where the origin is locally stable and is the only equilibrium point. Then, the question is if the origin is also globally asymptotically stable. Rigorous stability analysis for SAT is rarely done. The Zames-Falb criterion [68] can be used when the nonlinearity's slope is restricted, like in this case, but the method is difficult to implement. The Popov criterion can be used as a simplified approach to the analysis, but it is expected to be very conservative for systems of order greater than three. IQC-based analysis [35, 16, 42, 44] gives conditions in the form of LMIs that, when satisfied, guarantee stability of SAT. However, none of these analysis tools can be used when a SAT has an unstable nonlinearity sector.

Here, we propose to construct quadratic Lyapunov functions on the switching surfaces of SAT to show that impact maps associated with the system are contracting in some sense. This, in turn, proves the origin of a SAT is globally asymptotically stable. The search for these quadratic surface Lyapunov functions is done by solving a set of linear matrix inequalities, which can be efficiently done using available computational tools.

As in the case of on/off systems, a large number of examples was successfully proven globally stable. These include high-order systems, systems of relative degree larger than one, and systems with unstable nonlinearity sectors for which all classical methods fail to analyze. In fact, existence of an example with a globally stable equilibrium point that could not be successfully analyzed with this new methodology is still an open problem.

This chapter is organized as follows. Section 7.2 starts by formulating the problem. Section 7.3 presents the main results of this chapter followed by some illustrative

examples in section 7.4.

7.2 Problem Formulation

The main purpose of this section is to introduce the problem we intend to solve in this chapter. We start by defining a saturation system (SAT) followed by some necessary conditions for global stability of a unique locally stable equilibrium point. We then talk about some of the properties of this class of PLS.

Consider a SISO LTI system satisfying the following linear dynamic equations

$$\begin{cases} \dot{x} &= Ax + Bu \\ y &= Cx \end{cases} \tag{7.1}$$

where $x \in \mathbb{R}^n$, in feedback with a saturation controller (see figure 7-1) defined as

$$u(t) = \begin{cases} -d & \text{if } y(t) < -d \\ y(t) & \text{if } |y(t)| \leq d \\ d & \text{if } y(t) > d \end{cases} \tag{7.2}$$

where $d > 0$ (if $d = 0$ then the system is simply linear). By a solution of (7.1)-(7.2) we mean functions (x, y, u) satisfying (7.1)-(7.2). Since u is continuous and globally Lipschitz, $Ax + Bu$ is also globally Lipschitz. Thus, the SAT has a unique solution for any initial state.

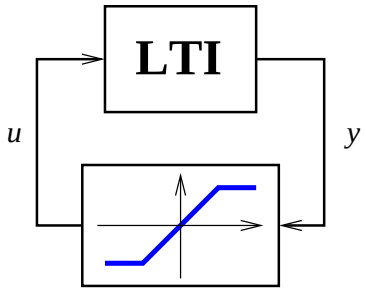

Figure 7-1: Saturation system

In the state space, the saturation controller introduces two switching surfaces composed of hyperplanes of dimension $n - 1$

$$S = \{x \in \mathbb{R}^n : \ Cx = d\}$$

and

$$\underline{S} = \{x \in \mathbb{R}^n : \ Cx = -d\}$$

On one side of the switching surface S $(Cx > d)$, the system is governed by $\dot{x} = Ax + Bd$. In between the two switching surfaces $(|Cx| \leq d)$, the system is given by $\dot{x} = Ax + BCx = A_1 x$, where $A_1 = A + BC$. Finally, on the other side of $\underline{S}$ $(Cx < -d)$

the system is governed by $\dot{x} = Ax - Bd$. Note that the vector field (7.1)-(7.2) is continuous along the switching surfaces since, for any $x \in S$, $A_1 x = (A + BC)x = Ax + Bd$, and for any $x \in \underline{S}$, $A_1 x = Ax - Bd$.

SAT can exhibit extremely complex behaviors. Some SAT may be chaotic, others may have one, three, or a continuum of equilibrium points, or limit cycles, or even some combination of all these behaviors. We are interested in those SAT with a unique locally stable equilibrium point. Only here can a SAT have a globally stable equilibrium point. Several necessary conditions must then be imposed on the system. For instance, it is necessary that A has no eigenvalues with positive real part, or otherwise there are initial conditions for which the system will grow unbounded (see for example [58]). A cannot have eigenvalues at zero since that would lead a continuum of equilibrium points. It is also necessary that $A+BC$ is Hurwitz in order to guarantee the origin is locally stable, and $-CA^{-1}B < 1$, so that the origin is the only equilibrium point.

Consider a subset S_+ of S given by

$$S_+ = \{x \in S : \ CA_1 x \geq 0\}$$

This set is important since it tells us which points in S correspond to the first switch of trajectories starting at any x_0 such that $Cx_0 < d$ (see figure 7-2). In other words, S_+ is the set of points in S that can be reached by trajectories of (7.1)-(7.2) when governed by the subsystem $\dot{x} = A_1 x$. In a similar way, define $S_- \subset S$ as

$$S_- = \{x \in S : \ CA_1 x \leq 0\}$$

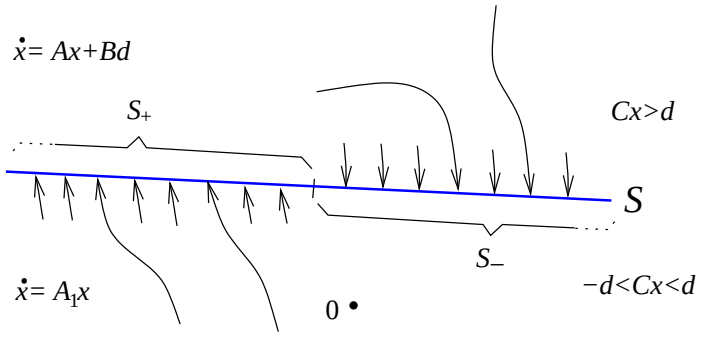

Figure 7-2: Both sets S_+ and S_- in S

Note that $S = S_+ \bigcup S_-$ and $S_+ \bigcap S_- = \{x \in S : \ CAx = 0\}$. Define also $\underline{S}_+ = -S_+$ and $\underline{S}_- = -S_-$.

As in on/off systems, since A_1 must be Hurwitz, there is a set of points in S_- such that any trajectory starting in that set will not switch again and will converge asymptotically to the origin. In other words, let $S^* \subset S_-$ be the set of points x_0 such that the following equations

$$Ce^{A_1 t} x_0 = \pm d$$

do not have a solution for any $t > 0$. Note that this set S^* is not empty. To see this, let $P > 0$ satisfy $PA_1 + A_1'P = -I$. Then, an obvious point in S^* is the point x_1^* obtained from the intersection of S with the level set $x'Px = k$, where $k \geq 0$ is chosen such that the ellipse $x'Px = k$ is tangent to both S and $\underline{S}$ (see figure 7-3).

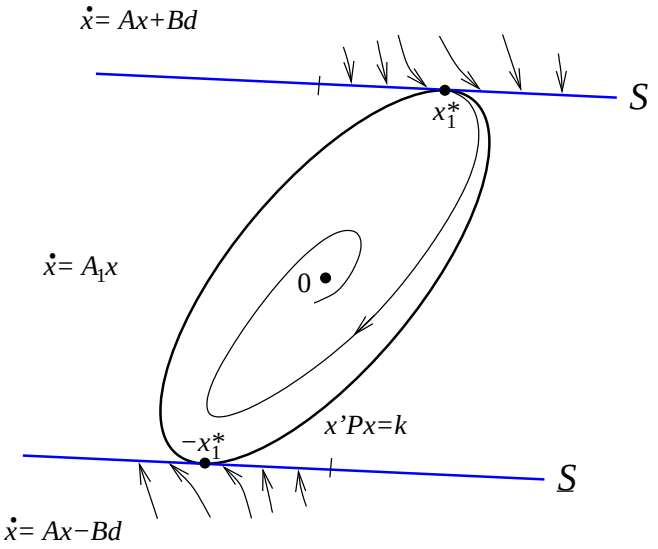

Figure 7-3: How to obtain x_1^*

The problem we propose to solve is to give sufficient conditions that, when satisfied, prove the origin of a SAT is globally asymptotically stable. The strategy of the proof is a follows. Consider a trajectory starting at some point $x_0 \in S_+$ (see figure 7-4). Since by assumption $-CA^{-1}B < 1$, the trajectory $x(t)$ will eventually switch at some time $t_1 > 0$, i.e., $Cx(t_1) = d$ and $Cx(t) \geq d$ for $t \in [0, t_1]$. Let $x_1 = x(t_1) \in S_-$. If $x_1 \in S^*$ then the trajectory will not switch again and converges asymptotically to the origin. Since we already know S^* is a stable set, we need to concentrate on those points in $S_- \backslash S^*$ since those are the ones that may lead to potentially unstable trajectories. Here, two scenarios can occur: either the trajectory switches at some point in S or it switches at some point in $\underline{S}$. Let $S_d \subset (S_- \backslash S^*)$ ($S_{-d} \subset (S_- \backslash S^*)$) be the set of points that will eventually switch in S ($\underline{S}$). If $x_1 \in S_d$ ($x_1 \in S_{-d}$) the trajectory switches at some finite time $t_{2a} > t_1$ ($t_{2b} > t_1$) at $x_{2a} = x(t_{2a}) \in S_+$ ($x_{2b} = x(t_{2b}) \in \underline{S}_+$). Again, it would switch at $x_{3a} = x(t_{3a})$ ($x_{3b} = x(t_{3b})$) and so on.

Just like RFS, an interesting property of SAT is their symmetry around the origin. In other words, if $x(t)$ is a trajectory of (7.1)-(7.2) with initial condition x_0, then $-x(t)$ is a trajectory of (7.1)-(7.2) with initial condition $-x_0$. This means that it is equivalent to analyze the trajectory starting at x_0 or the trajectory starting at $-x_0$. This property is due to the fact that the vector field is symmetric around the origin. If $Cx(t) > d$ then $\dot{x} = Ax + Bd$. Therefore, $-\dot{x} = A(-x) - Bd$ and $C(-x(t)) = -Cx(t) < -d$. If $|Cx(t)| \leq d$ then $\dot{x} = A_1 x$. Hence, $-\dot{x} = A_1(-x)$. Due to this symmetry, whenever a trajectory intersects $\underline{S}$ (like, for example, at x_{2b} in figure 7-4), for purposes of analysis, it is equivalent to consider the trajectory continuing from the symmetric point around the origin in S ($-x_{2b}$ in figure 7-4).

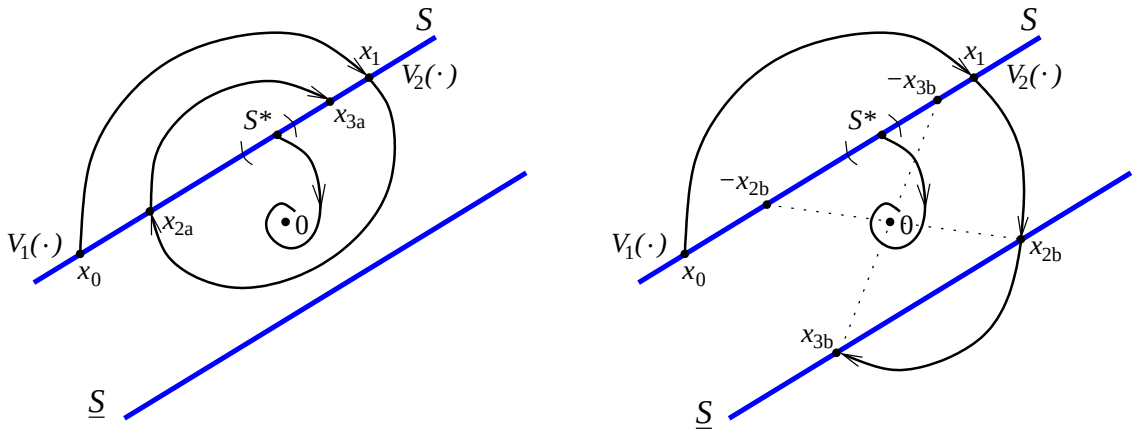

Figure 7-4: Possible state-space trajectories for a SAT

As in [21], the idea is to check if x_{3a} or $-x_{3b}$ are closer in some sense to S^* than x_1. If so, this would mean that eventually $x(t_N) \in S^*$, for some N, and prove that the origin is globally asymptotically stable. This is the idea behind the results in the next section.

Before presenting the main results, it is convenient to notice that $x_0, x_1, x_{2a} \in S$ and $x_{2b} \in \underline{S}$ can be parametrized. Let $x_0 = x_0^* + \Delta_0$, $x_1 = x_1^* + \Delta_1$, $x_{2a} = x_0^* + \Delta_{2a}$ and $x_{2b} = -x_0^* + \Delta_{2b}$, where $x_0^*, x_1^* \in S$ and $C\Delta_0 = C\Delta_1 = C\Delta_{2a} = C\Delta_{2b} = 0$. Also, define $x_0^*(t)$ $(x_1^*(t))$ as the trajectory of $\dot{x} = Ax + Bd$ $(\dot{x} = A_1 x)$, starting at x_0^* (x_1^*), for all $t > 0$. Since x_i^* are any points in S, we chose them to be such that $Cx_i^*(t) < d$ for all $t > 0$. The reason for this particular choice of x_0^* and x_1^* is so that $Cx_i^*(t) - d \neq 0$ for all $t > 0$. This will be necessary in proposition 7.1.

This choice of x_0^* and x_1^* is always possible. x_1^* is found as explained above (see figure 7-3). In this case, x_1^* is given by

$$x_1^* = \frac{P_d^{-1}C'}{CP_d^{-1}C'}d$$

where $P_d > 0$ satisfies $P_d A_1 + A_1' P_d = -I$. In a similar way, x_0^* is given by

$$x_0^* = (d + cA^{-1}Bd)\frac{P_u^{-1}C'}{CP_u^{-1}C'} - A^{-1}Bd$$

where $P_u > 0$ satisfies $P_u A + A' P_u = -I$.

7.3 Global Asymptotic Stability of Saturation Systems

There are three impact maps of interest associated with a SAT. The fist impact map (impact map 1) takes points from S_+ and maps them in S_-. The second impact map (impact map $2a$) takes points from $S_d \subset S_-$ and maps them back to S_+. Finally, the

third impact map (impact map $2b$) takes points from from $S_{-d} \subset S_-$ and maps them in $\underline{S}_+$. As in RFS and OFS, the impact maps associated with SAT are, in general, multivalued. Define the sets of expected switching times $\mathcal{T}_1$, $\mathcal{T}_{2a}$, and $\mathcal{T}_{2b}$ as the sets of all possible switching times associated with the respective impact map. See chapter 4 for a rigorous definition on expected switching times. In section 7.5, we show how to get bounds on these sets.

Before presenting the main result of this chapter, we show that each impact map associated with a SAT can be represented as a linear transformation analytically parametrized by the correspondent switching time.

Proposition 7.1 *Define*

$$w_1(t) = \frac{Ce^{At}}{d - Cx_0^*(t)}$$

$$w_{2a}(t) = \frac{Ce^{A_1 t}}{d - Cx_1^*(t)}$$

and

$$w_{2b}(t) = \frac{Ce^{A_1 t}}{-d - Cx_1^*(t)}$$

Let $H_1(t) = e^{At} + (x_0^*(t) - x_1^*)w_1(t)$, $H_{2a}(t) = e^{A_1 t} + (x_1^*(t) - x_0^*)w_{2a}(t)$, *and* $H_{2b}(t) = e^{A_1 t} + (x_1^*(t) + x_0^*)w_{2b}(t)$. *Then, for any* $\Delta_0 \in S_+ - x_0^*$ *there exists a* $t_1 \in \mathcal{T}_1$ *such that*

$$\Delta_1 = H_1(t_1)\Delta_0$$

Such t_1 *is the switching time associated with* Δ_1. *Similarly, for any* $\Delta_1 \in S_d - x_1^*$ *there exists a* $t_{2a} \in \mathcal{T}_{2a}$ *such that*

$$\Delta_{2a} = H_{2a}(t_{2a})\Delta_1$$

Such t_{2a} *is the switching time associated with* Δ_{2a}. *Finally, for any* $\Delta_1 \in S_{-d} - x_1^*$ *there exists a* $t_{2b} \in \mathcal{T}_{2b}$ *such that*

$$\Delta_{2b} = H_{2b}(t_{2b})\Delta_1$$

Such t_{2b} *is the switching time associated with* Δ_{2b}.

We need to show that these three impact maps are contracting in some sense. For that, define two quadratic Lyapunov functions on the switching surface S. Let V_1 and V_2 be given by

$$V_i(x) = x'P_i x - 2x'g_i + \alpha_i \tag{7.3}$$

where $P_i > 0$, for $i = 1, 2$. Global asymptotically stability of the origin follows if there exist $P_i > 0$, g_i, α_i such that

$$\begin{aligned} V_2(\Delta_1) &< V_1(\Delta_0) \quad \text{for all } \Delta_0 \in S_+ - x_0^* \\ V_1(\Delta_{2a}) &< V_2(\Delta_1) \quad \text{for all } \Delta_1 \in S_d - x_1^* \\ V_1(-\Delta_{2b}) &< V_2(\Delta_1) \quad \text{for all } \Delta_1 \in S_{-d} - x_1^* \end{aligned} \tag{7.4}$$

Note that in (7.4) we have mapped the point $\Delta_{2b} \in \underline{S}_+ + x_0^*$ into $S_+ - x_0^*$, taking advantage of the symmetry of the system. Let $P > 0$ on S stand for $x'Px > 0$ for all $x \in S$. As a short hand, in the following result we use $H_{it} = H_i(t)$ and $w_{it} = w_i(t)$.

Theorem 7.1 *Define*

$$\begin{aligned} R_1(t) &= P_1 - H_{1t}' P_2 H_{1t} - 2\left(g_1 - H_{1t}' g_2\right) w_{1t} + w_{1t}' \alpha w_{1t} \\ R_{2a}(t) &= P_2 - H_{2at}' P_1 H_{2at} - 2\left(g_2 - H_{2at}' g_1\right) w_{2at} - w_{2at}' \alpha w_{2at} \\ R_{2b}(t) &= P_2 - H_{2bt}' P_1 H_{2bt} - 2\left(g_2 + H_{2bt}' g_1\right) w_{2bt} - w_{2bt}' \alpha w_{2bt} \end{aligned}$$

where $\alpha = \alpha_1 - \alpha_2$. The origin of the SAT is globally asymptotically stable if there exist $P_1, P_2 > 0$ and g_1, g_2, α such that

$$\begin{cases} R_1(t_1) > 0 & \text{on } S_+ - x_0^* \\ R_{2a}(t_{2a}) > 0 & \text{on } S_d - x_1^* \\ R_{2b}(t_{2b}) > 0 & \text{on } S_{-d} - x_1^* \end{cases}$$

for all expected switching times $t_1 \in \mathcal{T}_1$, $t_{2a} \in \mathcal{T}_{2a}$, and $t_{2b} \in \mathcal{T}_{2b}$.

A relaxation of the constraints on Δ_0 and Δ_1 in the previous theorem results in computationally efficient conditions.

Corollary 7.1 *The origin of the SAT is globally asymptotically stable if there exist $P_1, P_2 > 0$ and g_1, g_2, α such that*

$$\begin{cases} R_1(t_1) > 0 & \text{on } S - x_0^* \\ R_{2a}(t_{2a}) > 0 & \text{on } S - x_1^* \\ R_{2b}(t_{2b}) > 0 & \text{on } S - x_1^* \end{cases} \tag{7.5}$$

for all expected switching times $t_1 \in \mathcal{T}_1$, $t_{2a} \in \mathcal{T}_{2a}$, and $t_{2b} \in \mathcal{T}_{2b}$.

For each t_1, t_{2a}, t_{2b}, these conditions are LMIs which can be solved for $P_1, P_2 > 0$ and g_1, g_2, α using efficient available software. As we will see in the next section, although these conditions are more conservative than the ones in theorem 6.1, they are already enough to prove global asymptotic stability of many important SAT.

As explained in chapter 6, each condition in (7.5) depends only on a single scalar parameter. Computationally, if we need m_1 samples of $\mathcal{T}_1$, m_{2a} samples of $\mathcal{T}_{2a}$, and m_{2b} samples of $\mathcal{T}_{2b}$, we end up with a total of $m_1 + m_{2a} + m_{2b}$ LMIs.

The proofs of these results are similar to the ones in sections 5.3 and 6.3, and are therefore omitted here.

Conditions (7.5) are sufficient conditions for the global stability of the origin. These conditions do not take into account that Δ_0, Δ_{1a}, and Δ_{1b} are restricted to S_+, S_d, and S_{-d}, respectively. Using the same ideas from sections 5.5 and 6.5, conditions (7.5) can be improved. For each point $x_0 \in S_+$, there is an associated switching time t_1. Define S_{t_1} as the set of initial conditions $x_0 \in S_+$ such that $y(t) \geq d$ on $[0, t_1]$, and $y(t_1) = d$. This set $S_{t_1} \subset S$ is a convex subset of a linear manifold of dimension $n-2$. Analogously, define $S_{t_{2a}}$ ($S_{t_{2b}}$) as the set of initial conditions $x_{1a} \in S_d$

($x_{1b} \in S_{-d}$) such that $-d \leq y(t) \leq d$ on $[0, t_{2a}]$, and $y(t_{2a}) = d$ ($y(t) \leq -d$ on $[0, t_{2b}]$, and $y(t_{2b}) = -d$). Given this, conditions (7.5) can be improved to

$$\begin{cases} R_1(t_1) > 0 & \text{on } S_{t_1} - x_0^* \\ R_{2a}(t_{2a}) > 0 & \text{on } S_{t_{2a}} - x_1^* \\ R_{2b}(t_{2b}) > 0 & \text{on } S_{t_{2b}} - x_1^* \end{cases} \tag{7.6}$$

for some $P_1, P_2 > 0$, g_1, g_2, α, and for all expected switching times $t_1 \in \mathcal{T}_1, t_{2a} \in \mathcal{T}_{2a}, t_{2b} \in \mathcal{T}_{2b}$. Approximation to a set of LMIs can be obtained just as in sections 4.3.1, 5.5, and 6.5.

Note that in many cases, conditions (7.5) and (7.6) do not need to be satisfied for all expected switching times. Section 7.5 shows that bounds on the expected switching times can be obtained. Basically, since $|u| \leq d$ is a bounded input, and when A is Hurwitz, there exists a bounded set such that any trajectory will eventually enter and stay there. This will lead to bounds on the difference between any two consecutive switching times. Let t_{i-} and t_{i+}, $i = 1, 2a, 2b$, be bounds on the minimum and maximum switching times of the associated impact maps. The expected switching times $\mathcal{T}_i$ can, in general, be reduced to a smaller set $[t_{-i}, t_{i+}]$. Conditions (7.5) and (7.6) can then be relaxed to be satisfied only on $[t_{i-}, t_{i+}]$ instead on all $t_i \in \mathcal{T}_i$. See section 7.5 for details.

7.4 Examples

The following examples were processed in `matlab` code. The latest version of this software is either available at [27] or upon request. Before we present the examples, we briefly explain the `matlab` function that we developed. The input to this function is a transfer function of an LTI system together with a parameter $d > 0$. If the SAT is proven globally stable, the `matlab` function returns the parameters of the two quadratic surface Lyapunov functions (7.3). We then confirm conditions (7.5) are satisfied by plotting the minimum eigenvalues of each $R_i(t)$ on $[t_{i-}, t_{i+}]$, and showing that these are indeed positive in those intervals.

Before moving into the examples, it is important to explain how the bounds $[t_{i-}, t_{i+}]$ on the expected switching times are found. First, notice that $t_{1-} = t_{2a-} = 0$. Zero switching time for the first impact map $\Delta_0 \to \Delta_1$ and the second impact map $\Delta_1 \to \Delta_{2a}$ correspond to points in S such that $CA_1x = 0$. At those points, the Lyapunov functions (7.3) must be continuous since this is the only way

$$\begin{cases} V_2(\Delta_1) \leq V_1(\Delta_0) \\ V_1(\Delta_{2a}) \leq V_2(\Delta_1) \end{cases}$$

can be satisfied simultaneously, for all $\Delta_0, \Delta_1, \Delta_{2a} = \Delta_0$ such that $x_0^* + \Delta_0 = x_1^* + \Delta_1 = x$ and $CAx = 0$. Therefore, for those points we need $V_1(\Delta_0) = V_2(\Delta_1)$. This imposes certain restrictions on $P_1, P_2 > 0$, g_1, g_2, and α. The analysis of zero switching time for these two impact maps is similar to the case of OFS. See section 6.7.2 for details.

As for the map $\Delta_1 \to \Delta_{2b}$, zero switching never occurs since there is a "gap"

between S and $\underline{S}$, resulting in a nonzero switching time for every trajectory starting in S_{-d}. For certain large values of $\|\Delta_1\|$, however, the switching times can be made arbitrarily small. But, when A is Hurwitz, we know all system trajectories eventually enter an invariant bounded set, just like in relay feedback systems. This can be seen from the fact that the open loop system is stable and $|u| \leq d$ is bounded. In this invariant bounded set, switching times for the impact map $\Delta_1 \to \Delta_{2b}$ cannot be made arbitrarily small, and a lower bound can be found. Using the same ideas, upper bounds on expected switching times for all impact maps can be found. All the details are in section 7.5. The case when A has imaginary eigenvalues is currently under investigation.

Example 7.1 Consider the SAT on the left of figure 7-5 with $d = 1$. It is easy to see the origin of this system is locally stable. The question is if the the origin is also globally asymptotically stable.

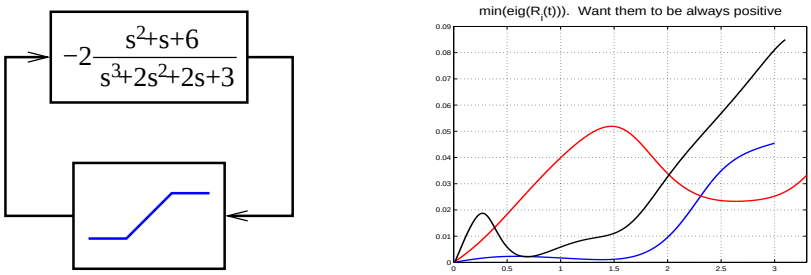

Figure 7-5: 3^{rd}-order system with unstable nonlinearity sector

Using conditions (7.5), we show that the origin is in fact asymptotically globally stable. The right side of figure 7-5 illustrates this fact: the minimum eigenvalue of each condition (7.5) is positive on its respective set of expected switching times. The expected switching times in this example are approximately $\mathcal{T}_1 = (0, 3)$, $\mathcal{T}_{2a} = (0, 3.3)$, and $\mathcal{T}_{2b} = (0, 3.1)$. For instance, if $t_1 \geq 3$, there is no point in S_+ with switching time equal to t_1.

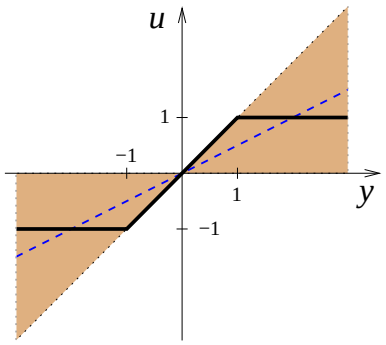

Figure 7-6: Saturation controller versus constant gain of 1/2 (dashed)

Note that this system has an unstable nonlinearity sector. If the saturation is replaced by a linear constant gain of $1/2$, the system becomes unstable (see figure 7-6). This is very interesting since it tells us that classical analysis tools like small gain theorem, Popov criterion, Zames-Falb criterion, and integral quadratic constraints, fail to analyze SAT of this nature. ■

Example 7.2 Consider the SAT in figure 7-7 with $d = 1$ and $k > 0$. The origin of the SAT is locally stable for any $k > 0$.

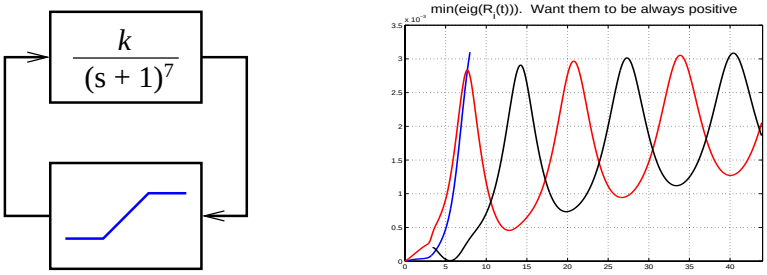

Figure 7-7: System with relative degree 7 (left); global stability analysis when $k = 2$ (right)

As seen in example 6.2, $\|Ce^{At}B\|_{\mathcal{L}_1} = k$, and the small gain theorem can only be applied when $k < 1$.

Let $k = 2$. The right side of figure 7-7 shows how conditions (7.5) are satisfied in some intervals (t_{i-}, t_{i+}), $i = 1, 2a, 2b$. The intervals (t_{i-}, t_{i+}) are bounds on the expected switching times. Such bounds are such that if conditions (7.5) are satisfied on (t_{i-}, t_{i+}), then the system is globally asymptotically stable. For details on how to find these bounds see section 7.5. ■

7.5 Technical Details: Bounds on Switching Times

In this section, we will talk about computational aspects related to finding $P_i > 0$, g_i, and α in (7.5) or (7.6). For many SAT, the sets of expected switching times are equal to the set $[0, \infty)$. Thus, in general, it is impossible to check directly if the stability conditions (7.5) or (7.6) are satisfied for all expected switching times. An alternative is to find some intervals (t_{i-}, t_{i+}) such that if (7.5) or (7.6) are satisfied in those intervals, then stability follows.

In chapter 5, and in particular, in section 5.6, we showed that in the case of RFS, there is a bounded invariant set where every trajectory will eventually enter. Hence, bounds on the expected switching times could be found by computing bounds on switching times of trajectories inside that bounded invariant set. This same idea can be used here whenever A is Hurwitz. In fact, since $u = \pm d$ is a bounded input, a bounded and invariant set such that any trajectory will eventually enter can be found. This will lead to bounds on the difference between any two consecutive switching

times. This way, the search for $P_i > 0$, g_i, and α in (7.5) and (7.6) becomes restricted to $0 \leq t_{i-} < t < t_{i+} < \infty$, $i = 1, 2a, 2b$.

As explained before, $t_{1-} = t_{2a-} = 0$ since the associated impact maps are defined on the same switching surface, and are allowed to have zero switching time. We then focus on upper bounds for all impact maps and on the lower bound t_{2b-} of impact map $2b$. Notice there are many ways to finds such bounds and the method we propose next is not unique, and can surely be improved.

Before we find such bounds, we need to show there is a particular bounded invariant set such that any trajectory will eventually enter and stay there. This proposition is similar to proposition 5.5. Thus, the proof is omitted here.

Proposition 7.2 *Consider the system $\dot{x} = Ax + Bu$, $y = Fx$, where A is Hurwitz, $u(t) = \pm d$, and F is a row vector. Then*

$$\limsup_{t\to\infty} |Fx(t)| \leq d\|Fe^{At}B\|_{\mathcal{L}_1}$$

Remember that, by definition, $\|Fe^{At}B\|_{\mathcal{L}_1}$ is given by

$$\|Fe^{At}B\|_{\mathcal{L}_1} = \int_0^\infty \left|Fe^{At}B\right| dt$$

As a remark, if $F = C$ and $\|Fe^{At}B\|_{\mathcal{L}_1} < 1$, it follows the origin is globally asymptotically stable. When $\limsup_{t\to\infty} |Cx(t)| < d$, eventually all trajectories enter the set $\{x|\ |Cx| < d\}$, where the system is linear and stable. Note that this remark also follows from the well known small-gain theorem.

We first focus our attention on upper bounds of the switching times t_{i+}, starting with t_{1+}. A trajectory $x(t)$ starting at $x_0 \in S_+$ is given by $x(t) = e^{At}(x_0 + A^{-1}Bd) - A^{-1}Bd$. Thus, the output $y(t) = Cx(t)$ is given by

$$y(t) = Ce^{At}(x_0 + A^{-1}Bd) - CA^{-1}Bd$$

Since we are assuming $-CA^{-1}Bd < d$, and A Hurwitz, it is easy to see that $y(t)$ cannot remain larger than d for all $t > 0$. For any initial condition $x_0 \in S_+$, $Ce^{At}(x_0 + A^{-1}Bd) \to 0$ as $t \to \infty$, which means $y(t) = d$ for some t. Thus, a switch must occur in finite time. Since for a sufficiently large enough time t, $x(t)$ enters a bounded invariant set (from the above proposition), an upper bound on this switching time t_{1+} can be obtained. The following proposition is similar to proposition 5.6.

Proposition 7.3 *Let $t_{1+} > 0$ be the smallest solution of*

$$\int_{t_{1+}}^\infty \left|Ce^{At}B\right| dt + |Ce^{At_{1+}}A^{-1}B| \leq (CA^{-1}B + 1)$$

If t_a and t_b are sufficiently large consecutive switching times of the first impact map then $|t_a - t_b| \leq t_{1+}$.

Next, we find upper bounds on the expected switching times of impact maps $2a$ and $2b$. The idea here is to find the minimum $t_2 \geq 0$ such that

$$|y(t)| = \left|Ce^{A_1 t}x_0\right| \leq d$$

for all $t \geq t_2$ and all x_0 in the bounded invariant set. In this derivation, $t_{2a+} = t_{2b+} = t_2$.

Proposition 7.4 *Let $t_2 > 0$ be the smallest solution of*

$$\int_0^\infty \left|Ce^{A_1 t_2}e^{At}B\right| dt \leq 1 \tag{7.7}$$

If t_a and t_b are sufficiently large consecutive switching times of impact maps $2a$ or $2b$, then $|t_a - t_b| \leq t_2$, and $t_{2a+} = t_{2b+} = t_2$.

We now focus on the lower bound on the expected switching times of impact map $2b$, i.e, t_{2b-}. Remember that if $x_0 \in S_+$, then $y(0) = d$. Since $d > 0$, it must be true that $y(t) > -d$ at least in some interval $(0, \epsilon)$. Basically, the time it takes to go from S to $\underline{S}$ must be always nonzero. The next result shows that when a trajectory enters the bounded invariant set characterized above, ϵ cannot be made arbitrarily small. Thus, a lower bound on the time it takes between two consecutive switches from S to $\underline{S}$ can be obtained.

Proposition 7.5 *Let $k_{dd} = \|CA_1^2e^{At}B\|_{\mathcal{L}_1}$, and $k_{dl} = \|CA_1e^{At}B\|_{\mathcal{L}_1}$ and define*

$$t_{21} = \frac{2}{\sqrt{k_{dd}}}, \quad t_{22} = \frac{2}{k_{dl}}$$

Let $t_{2b-} = \max\{t_{21}, t_{22}\}$. If t_a and t_b are sufficiently large consecutive switching times of impact map $2b$, then $|t_a - t_b| \geq t_{2b-}$.

The proof is similar to the proof of proposition 5.7.

Chapter 8

Robustness and Performance of PLS

The previous chapters were dedicated to study global stability analysis of PLS. The notions of impact maps and quadratic surface Lyapunov functions, introduced in chapter 4, were successfully applied to prove global asymptotic stability of limit cycles and equilibrium points of PLS. Two important assumptions behind these results were (1) the model of a PLS accurately represented the physical system of interest and (2) the system was autonomous, i.e., it did not depended on any external input. In this chapter, we want to show that similar ideas to those in chapter 4 can be used to guarantee *finite gain $\mathcal{L}_2$ stability*, i.e., "well-behaved" inputs generate "well-behaved" outputs, of many PLS. For that, we use on/off systems (OFS). This is the simplest class of PLS with globally stable equilibrium points. The formulation and solution of the problem for this class of systems serves as an example and demonstration that robustness and performance of many and more complex classes of PLS can done using impact maps and quadratic surface Lyapunov functions.

Global stability analysis of OFS was studied in chapter 6. Here, we show that many OFS are not only globally asymptotically stable, but also $\mathcal{L}_2$ to $\mathcal{L}_2$ bounded. By solving a set of LMIs, a quadratic Lyapunov function on the switching surface of an OFS can be constructed to prove performance of the system. As in chapter 6, examples analyzed include systems with unstable nonlinearity sectors, for which classical methods fail to analyze.

This chapter is organized as follows. Next section gives some background on $\mathcal{L}_2$ gain stability. Section 8.2 reviews some results on H_2 optimization, followed by the main results of the chapter in section 8.3. Using OFS, we find conditions in the form of LMIs that can be used to show the system is $\mathcal{L}_2$ to $\mathcal{L}_2$ bounded. This section includes several illustrative examples, including OFS with unstable nonlinearity sectors. Finally, section 8.4 summarizes the results obtained in this chapter and discusses topics of further research in robustness and performance of PLS.

8.1 Preliminaries

Consider a system whose input-output relation is represented by

$$y = Gu$$

where G is some mapping or operator that specifies y in terms of u (see figure 8-1). The input u belongs to a space of signals, which in our case is the normed linear space $\mathcal{L}_2$ of functions $u : [0, \infty) \to \mathbb{R}$ that are square-integrable, i.e., satisfy

$$\|u\|_{\mathcal{L}_2}^2 = \int_0^\infty u^2(t)dt < \infty$$

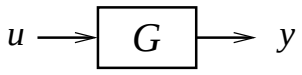

Figure 8-1: Input-output relation

In order to allow dealing with unstable systems as well as stable ones, G is usually defined as a mapping from an extended space $\mathcal{L}_{2e}$ to an extended space $\mathcal{L}_{2e}$, where $\mathcal{L}_{2e}$ is defined as

$$\mathcal{L}_{2e} = \{u |\ u_t \in \mathcal{L}_2,\ \forall t \geq 0\}$$

and u_t is a truncation of u, given by

$$u_t(\tau) = \begin{cases} u(\tau), & 0 \leq \tau \leq t \\ 0, & \tau > t \end{cases}$$

The extended space $\mathcal{L}_{2e}$ is a linear space that contains the unextended space $\mathcal{L}_2$ as a subset.

If we think of $u \in \mathcal{L}_{2e}$ as a "well-behaved" input, the question to ask is whether the output y will be "well-behaved" in the sense that $y \in \mathcal{L}_{2e}$. A system that has the property that any "well-behaved" input will generate a "well-behaved" output will be defined as a stable system. More precisely, we say a mapping $G :\ \mathcal{L}_{2e} \to \mathcal{L}_{2e}$ is *finite-gain* $\mathcal{L}_2$ *stable* if there exists a nonnegative constant γ such that

$$\|(Gu)_t\|_{\mathcal{L}_2}^2 \leq \gamma \|u_t^2\|_{\mathcal{L}_2} \tag{8.1}$$

for all $u \in \mathcal{L}_2$ and $t \in [0, \infty)$. Note that (8.1) can be written as

$$\int_0^t y^2(\tau)d\tau \leq \gamma \int_0^t u^2(\tau)d\tau$$

for all $u \in \mathcal{L}_2$ and $t \in [0, \infty)$ which, in turn, is equivalent to

$$\min_{u \in \mathcal{L}_2} \int_0^t \left(\gamma u^2(\tau) - y^2(\tau)\right) d\tau \geq 0$$

for all $t \geq 0$.

A similar definition can given if the system is in its state-space model

$$\left\{ \begin{array}{rcl} \dot{x} & = & f(x) + g(x)u \\ y & = & h(x) \end{array} \right. \tag{8.2}$$

where $x(t) \in \mathbb{R}^n$, $u(t), y(t) \in \mathbb{R}$, $f(x)$ and $g(x)$ are smooth vector fields, and $h(x)$ is a smooth function. Assume also $f(0) = 0$ and $h(0) = 0$.

Definition 8.1 The system (8.2) is *finite-gain $\mathcal{L}_2$ stable* if the response $x(t)$ of (8.2) with initial state $x(0) = 0$ exists for all $t \geq 0$ and satisfies

$$\min_{u \in \mathcal{L}_2} \int_0^t \left(\gamma u^2(\tau) - h^2(x(\tau)) \right) d\tau \geq 0 \tag{8.3}$$

for some $\gamma \geq 0$ and for all $t > 0$.

A function $V(x)$ is *positive definite* if $V(0) = 0$ and $V(x) > 0$ for all $x \neq 0$. A sufficient condition for system (8.2) to be finite-gain $\mathcal{L}_2$ stable is the following.

Proposition 8.1 *The system (8.2) is finite-gain $\mathcal{L}_2$ stable if there exists a positive definite function $V(x)$ such that the response $x(t)$ of (8.2) from the initial state $x(0) = 0$ exists for all $t \geq 0$ and satisfies*

$$\min_{u \in \mathcal{L}_2} \int_0^t \left(\gamma u^2(\tau) - h^2(x(\tau)) \right) d\tau \geq V(x(t))$$

for some $\gamma \geq 0$ and for all $t > 0$.

The proof follows since, by definition, $V(x(t)) \geq 0$.

A result that is of particular interest to us is the following.

Proposition 8.2 *Consider a sequence of times $\{t_k\}$, $k = 1, 2, ...$, where $t_1 > t_0 = 0$, $t_{k+1} > t_k$, and $t_k \to \infty$ as $k \to \infty$. The system (8.2) is finite-gain $\mathcal{L}_2$ stable if there exists a positive definite function $V(x)$ such that the response $x(t)$ of (8.2) from the initial state $x(0) = 0$ exists for all $t \geq 0$ and satisfies*

$$\min_{u \in \mathcal{L}_2} \int_{t_{k-1}}^{t_k} \left(\gamma u^2(\tau) - h^2(x(\tau)) \right) d\tau \geq V(x(t_k)) - V(x(t_{k-1})) \tag{8.4}$$

for some $\gamma \geq 0$ and for all $k = 1, 2, ...$

To prove the result, take any $T > 0$. Let N be such that $t_N > T$. Summing each side of (8.4) for all $k = 1, 2, ..., N$, we get

$$\min_{u \in \mathcal{L}_2} \int_0^{t_N} \left(\gamma u^2(\tau) - h^2(x(\tau)) \right) d\tau \geq V(x(t_N))$$

Proposition 8.1 can now be applied and the result follows.

For a more detailed introduction to $\mathcal{L}_2$ stability the reader is referred to any of the numerous references in the field like, for example, [15, 36, 32].

8.2 H_2 Optimization

In this chapter, we are interested in minimizing over $u \in \mathcal{L}_2$ the functional

$$J(u(\cdot)) = \int_0^T \left(\gamma u^2(t) - y^2(t)\right) dt \tag{8.5}$$

subject to

$$\begin{aligned} \dot{x} &= Ax + Bu \\ y &= Cx, \quad x(0) = x_0, \quad x(T) = x_T \end{aligned}$$

and $T > 0$ (for $T = 0$, $J(u(\cdot)) = 0$). This is a typical linear quadratic optimal control problem which can be solved using the well known Pontryagin's maximum principle. For completeness, we include here the derivation of the solution. Let

$$L(u, x, \psi) = \int_0^T \left(\gamma u^2 - x'C'Cx + 2\psi'(\dot{x} - Ax - Bu)\right) dt$$

where ψ is the adjoint vector. It is a well known result that if u^* is the solution to (8.5) then u^* minimizes L. Thus,

$$\begin{aligned} \frac{\partial L}{\partial x} &= -2\dot{\psi} - 2C'Cx - 2A'\psi = 0 \\ \frac{\partial L}{\partial u} &= 2\gamma u - 2B'\psi = 0 \end{aligned}$$

From the last equality,

$$u^*(t) = \frac{1}{\gamma} B'\psi(t)$$

yielding the linear time-invariant system known as the Hamiltonian system

$$\begin{pmatrix} \dot{x} \\ \dot{\psi} \end{pmatrix} = H \begin{pmatrix} x \\ \psi \end{pmatrix}$$

where

$$H = \begin{pmatrix} A & \frac{1}{\gamma}BB' \\ -C'C & -A' \end{pmatrix}$$

and $x_0 = x(0)$, $x_T = x(T)$ are given. Then, the optimal cost $J(u^*) = J^*(x_0, x_T, T)$ is

$$J^*(x_0, x_T, T) = \psi_T' x_T - \psi_0' x_0$$

where $\psi_T = \psi(T)$ and $\psi_0 = \psi(0)$.

The solution to the Hamiltonian system is simply the solution of a linear time-invariant autonomous system

$$\begin{bmatrix} x(t) \\ \psi(t) \end{bmatrix} = e^{Ht} \begin{bmatrix} x_0 \\ \psi_0 \end{bmatrix}$$

In order to find $J(u^*)$ we still need to write ψ_0 and ψ_T as functions of T, x_0, and x_T. At $t = T$, the solution to the Hamiltonian system is

$$\begin{pmatrix} x_T \\ \psi_T \end{pmatrix} = e^{HT} \begin{pmatrix} x_0 \\ \psi_0 \end{pmatrix}$$

Define

$$e^{HT} = \begin{pmatrix} e_{11} & e_{12} \\ e_{21} & e_{22} \end{pmatrix}$$

Note that for simplification of notation we write e_{ij}, although these are actually functions of T, i.e., $e_{ij} = e_{ij}(T)$. Then,

$$\psi_0 = e_{12}^{-1} \left(x_T - e_{11} x_0 \right)$$

and

$$\psi_T = \left(e_{21} - e_{12}^{-1} e_{11} \right) x_0 + e_{12}^{-1} x_T$$

Finally, the optimal cost $J(u^*) = J^*(x_0, x_T, T)$ can be written as

$$J^*(x_0, x_T, T) = \begin{pmatrix} x_T \\ x_0 \end{pmatrix}' W_T \begin{pmatrix} x_T \\ x_0 \end{pmatrix} \tag{8.6}$$

where W_T is the symmetric matrix

$$W_T = \begin{bmatrix} e_{22} e_{12}^{-1} & \left(e_{21} - e_{22} e_{12}^{-1} e_{11} - (e_{12}^{-1})' \right) /2 \\ \left(e_{21} - e_{22} e_{12}^{-1} e_{11} - (e_{12}^{-1})' \right)' /2 & e_{12}^{-1} e_{11} \end{bmatrix} \tag{8.7}$$

Optimal control references are numerous. For more detailed and general solutions see, for example, [7, 43].

8.3 Performance of On/Off Systems

As mentioned earlier, the purpose of this chapter is to show that impact maps and quadratic surface Lyapunov functions can be used in the analysis of performance of PLS. For that, we choose to first analyze on/off systems (OFS) for their simplicity. We will start with OFS with $d = 0$, i.e., with the origin belonging to the switching surface. This is simplest class of PLS with globally stable equilibrium points. Figure 8-2 shows the system we will be analyzing for the remaining of the chapter.

After showing the origin of a certain OFS is global asymptotically stable, the question is if there exists a nonnegative γ satisfying (8.1).

In figure 8-2, the input to the LTI system is given by

$$e = u + \max(0, Cx)$$

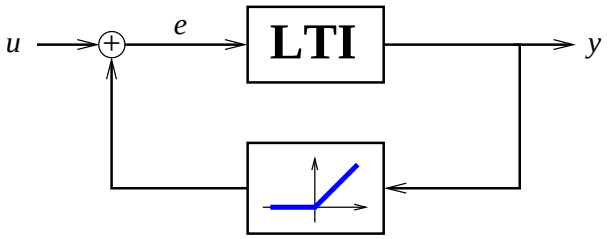

Figure 8-2: On/off system with output disturbance u

Thus, the closed loop dynamics are

$$\dot{x} = Ax + Bu + B\max(0, Cx) \tag{8.8}$$

In the state space, the on/off controller introduces a switching surface that does not depend on the input u. This switching surface

$$S = \{x \in \mathbb{R}^n : \ Cx = 0\}$$

divides the state space in two equal parts. On one side ($Cx > 0$), the system is given by $\dot{x} = Ax + BCx + Bu = A_1 x + Bu$, where $A_1 = A + BC$. On the other side ($Cx < 0$) the system dynamics are given by $\dot{x} = Ax + Bu$. For purposes of analysis, we assume the origin of the OFS is globally asymptotically stable when $u = 0$. This can be checked using the results from chapter 6.

Define the *Catersian product* $X \times Y$ of two sets X and Y as

$$X \times Y = \left\{ \begin{pmatrix} x \\ y \end{pmatrix} \mid x \in X, y \in Y \right\}$$

Let $\gamma \geq 0$. Define

$$H_1 = \begin{pmatrix} A_1 & \frac{1}{\gamma} BB' \\ -C'C & -A_1' \end{pmatrix}$$

and

$$e^{H_1 T} = \begin{pmatrix} e_{11} & e_{12} \\ e_{21} & e_{22} \end{pmatrix}$$

where $T > 0$. Define also W_{T1} as in (8.7). Let

$$H_2 = \begin{pmatrix} A & \frac{1}{\gamma} BB' \\ -C'C & -A' \end{pmatrix}$$

and W_{T2} be given in a similar way as W_{T1}. In the following result, $Q > 0$ on X stands for $x'Qx > 0$ for all $x \in X$.

Theorem 8.1 *The OFS (8.8) is finite-gain $\mathcal{L}_2$ stable if there exists a $\gamma \geq 0$ and a*

matrix $P > 0$ such that

$$\begin{cases} W_{T1} - \begin{pmatrix} P & 0 \\ 0 & -P \end{pmatrix} > 0 & \text{on } S \times S \\ W_{T2} - \begin{pmatrix} P & 0 \\ 0 & -P \end{pmatrix} > 0 & \text{on } S \times S \end{cases} \tag{8.9}$$

for all $T > 0$.

There are several ways to improve the computationally aspects of conditions (8.9). Conditions (8.9) involve the computation of the inverse of e_{12}. This matrix is composed of both stable and unstable modes of H. As T goes to zero and as it grows large, this matrix approximates non-singular matrices. Computationally, it is very hard to find the inverse of e_{12} for extreme values of T, and numerical errors occur. In order to reduce numerical errors and have high confidence on the results, it is necessary to find equivalent conditions to (8.9) that do not involve the computation of an inverse of a matrix. Also, as we will see, this will help in the analysis when $T \to 0$.

From section 8.2, we know the optimal cost (8.5) is given by

$$J^*(x_0, x_T, T) = \psi_T' x_T - \psi_0' x_0$$

The outline of proof of theorem 8.1 is as follows. For each condition in (8.9), we use the Hamiltonian system to solve for ψ_T and ψ_0 as functions of x_0, x_T, and T, and then replacing them in the optimal cost, resulting in (8.6). Thus, the optimal cost (8.5) is a quadratic function of x_0 and x_T. The solution of ψ_T and ψ_0 as functions of x_0 and x_T, however, involves inverting e_{12}.

Another way to look at the problem is that since e_{12} is invertible for all $T > 0$, it makes no difference in writing the optimal cost as a function of x_0 and x_T or as a function of x_0 and ψ_0. Given x_0 and x_T, ψ_0 is uniquely defined, and vice versa.

Define

$$S_{T1} = \left\{ x \in S \times \mathbb{R}^n \mid \begin{pmatrix} C & 0 \end{pmatrix} e^{H_1 T} x = 0 \right\}$$

and

$$S_{T2} = \left\{ x \in S \times \mathbb{R}^n \mid \begin{pmatrix} C & 0 \end{pmatrix} e^{HT} x = 0 \right\}$$

The results in the following theorem are equivalent to the results in theorem 8.1.

Theorem 8.2 *The OFS (8.8) is finite-gain $\mathcal{L}_2$ stable if there exists a $\gamma \geq 0$ and a matrix $P > 0$ such that*

$$\begin{cases} e^{H_1' T} \begin{pmatrix} -P & I/2 \\ I/2 & 0 \end{pmatrix} e^{H_1 T} - \begin{pmatrix} -P & I/2 \\ I/2 & 0 \end{pmatrix} > 0 & \text{on } S_{T1} \\ e^{H_2' T} \begin{pmatrix} -P & I/2 \\ I/2 & 0 \end{pmatrix} e^{H_2 T} - \begin{pmatrix} -P & I/2 \\ I/2 & 0 \end{pmatrix} > 0 & \text{on } S_{T2} \end{cases} \tag{8.10}$$

for all $T > 0$.

For each $T > 0$, these conditions are LMIs which can efficiently be solved for $P > 0$ using available software.

8.3.1 Examples

The following examples were processed in `matlab` code. The latest version of this software is either available at [27] or upon request. Both stability conditions (8.9) and (8.10) need to be satisfied for all $T > 0$. Computationally, the idea is to show they are satisfied in some interval $[t_{min}, t_{max}]$ and then guarantee they are also satisfied for all $0 < T < t_{min}$ and $T > t_{max}$.

The analysis near $T = 0$ is done in several steps. First, we notice that if $T = 0$ then the cost function is zero. Thus, both conditions are zero for $T = 0$. The next step is to check if the derivatives at zero are positive semidefinite. This can be done using conditions (8.10). Details can be found in the technical details section (section 8.3.3). Then, for a small enough t_{min}, it can be shown that conditions (8.10) are satisfied for all $0 < T < t_{min}$. The idea is to find bounds on the second derivative of the stability conditions over $(0, t_{min})$, and to use them to show nothing can go wrong in that interval.

The analysis when T is large is done by first guaranteeing the stability conditions are satisfied at $T = \infty$. This can be done using conditions (8.9). Details can also be found in section 8.3.3. Then, for a large enough t_{max}, it can be shown that conditions (8.9) are satisfied for all $T > t_{max}$. The idea is to take a function $r(t)$ that maps $(0, \infty)$ to $(0, 1)$, and then find a r_{max} close enough to 1 such that the bounds on the derivative of the stability conditions on $(r_{max}, 1)$ are small enough to show nothing can go wrong on that interval.

Example 8.1 Consider the OFS in figure 8-2 where the LTI system is given by

$$G(s) = 2\frac{s-4}{(s+1)(s+2)(s+3)}$$

First, we need to check if the origin is globally asymptotically stable. Using the results from chapter 6, the origin is found globally asymptotically stable (see figure 8-3).

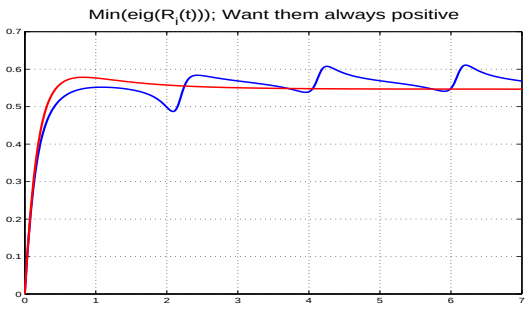

Figure 8-3: Origin is globally asymptotically stable

The question is if this system is also finite-gain $\mathcal{L}_2$ stable. Using the software described above, we were able to to find a $P > 0$ satisfying both (8.9) and (8.10), for all $T > 0$. Figure 8-4 shows the minimum eigenvalues of conditions (8.9) (on the left) and conditions (8.10) (on the right) on some intervals $(0, t_{max})$.

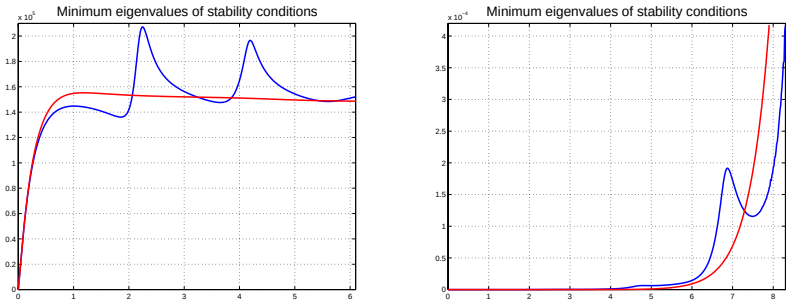

Figure 8-4: Minimum eigenvalue of stability conditions

Therefore, we conclude the system is not only globally asymptotically stable, but also finite-gain $\mathcal{L}_2$ stable. ■

Example 8.2 Consider the OFS in figure 8-2 where the LTI system is given by

$$G(s) = -2\frac{s^2 + s + 6}{s^3 + 2s^2 + 2s + 3}$$

Note that this system has an unstable nonlinearity sector (see figure 8-5). This means that all classical methods fail to analyze the system.

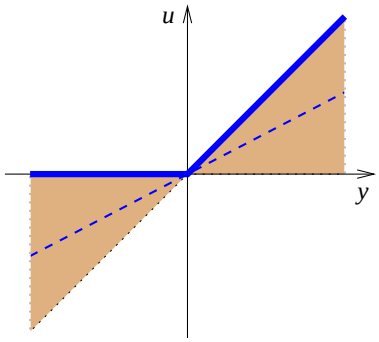

Figure 8-5: Unstable nonlinearity sector with constant gain of 1/2 (dashed)

Nevertheless, the system is global asymptotically stable, as we see in figure 8-6. In this figure, we see the stability conditions (6.12) satisfied in some bounds of the expected switching times.

In terms of performance, using again the software described above, we were able to to find a $P > 0$ satisfying both (8.9) and (8.10), for all $T > 0$. Figure 8-7 shows the minimum eigenvalues of conditions (8.9) (on the left) and conditions (8.10) (on the

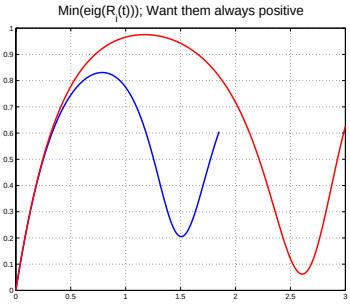

Figure 8-6: Origin is globally asymptotically stable

right) on some intervals $(0, t_{max})$. For purpose of visualization, the second conditions in (8.9) and (8.10) in figure 8-7 are scaled.

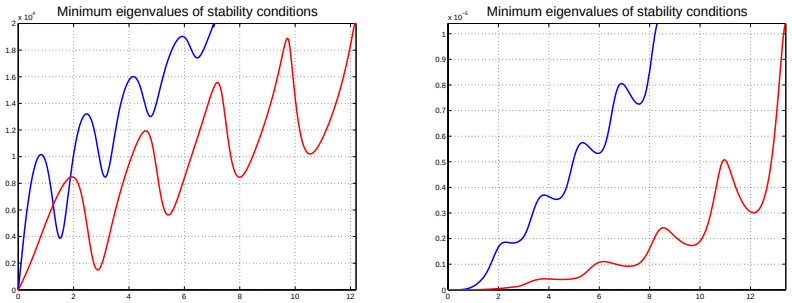

Figure 8-7: Minimum eigenvalue of stability conditions

Therefore, we conclude the system is not only globally asymptotically stable, but also finite-gain $\mathcal{L}_2$ stable. ■

8.3.2 Proof of Results

Proof of theorem 8.1: According to proposition 8.2, all it is left to show is the "worst" input $u \in \mathcal{L}_2$ from one switch to the next switch satisfies (8.4). Over a single switch, this can be written as

$$J(u^*(\cdot)) = \min_{u \in \mathcal{L}_{2e}} \int_0^T \left(\gamma u^2(\tau) - y^2(\tau)\right) d\tau \tag{8.11}$$

where $T \geq 0$ is the switching time associated with a single impact map. We are interested in finding the control action u^* that takes a point $x_0 \in S$ and maps it to $x_1 \in S$ such that the cost function $J(u(\cdot))$ is minimized. This is a typical optimal control problem, whose solution can be found in section 8.2.

Note that in order to guarantee the assumptions of proposition 8.2, we need to guarantee (8.11) is satisfied for both impact maps: one when the system is governed by $\dot{x} = A_1 x + Bu$ $(Cx \geq 0)$, and the other when the system is governed by $\dot{x} = Ax + Bu$

($Cx \leq 0$). Each impact map will lead to a different stability condition. We will show how the first condition in (8.9) is obtained. The second condition follows similarly.

Let the switching time $T > 0$. Consider a trajectory of $\dot{x} = A_1 x + Bu$ with $x(0) = x_0 \in S$, $x(T) = x_T \in S$, and the minimization problem (8.11). Solving the optimal control problem as explained in section 8.2, yields the following optimal cost $J_1(u^*) = J_1^*(x_0, x_T, T)$

$$J_1^*(x_0, x_T, T) = \begin{pmatrix} x_T \\ x_0 \end{pmatrix}' W_{T1} \begin{pmatrix} x_T \\ x_0 \end{pmatrix}$$

We need

$$J_1^* > V_1(x_T) - V_0(x_0) = \begin{pmatrix} x_T \\ x_0 \end{pmatrix}' \begin{pmatrix} P_1 & 0 \\ 0 & -P_0 \end{pmatrix} \begin{pmatrix} x_T \\ x_0 \end{pmatrix}$$

where $V_i(x)$ are quadratic forms defined on the switching surface S, i.e., $V_i(x) = x' P_i x$, $x \in S$, $P_i > 0$. Conditions on the second map can be found similarly

$$J_2^* > V_0(x_T) - V_1(x_0)$$

for all $T > 0$, and $x_0, x_T \in S$.

Note that when the switching time is equal to zero, $J_1^* = J_2^* = 0$. Thus,

$$\begin{aligned} 0 &\geq V_1(x_0) - V_0(x_0) \\ 0 &\geq V_0(x_0) - V_1(x_0) \end{aligned}$$

which implies that

$$V_0(x) = V_1(x), \quad \forall x \in S$$

Therefore, $P_0 = P_1 = P > 0$, and the result follows. ■

Note that conditions (8.9) are conservative in the sense that they do not take in account the trajectory starting on the switching surface, stays on one side of S until it switches again at S, at the specified switching time. Finding the optimal control under such assumption is not an easy task. Moreover, the optimal cost would most likely not be given in a quadratic form in terms of the initial and final conditions, as it is in theorem 8.1. A less conservative condition based on these considerations is part of future research.

Proof of theorem 8.2: Again, we show how the first condition in (8.10) is obtained. The second, follows similarly. The cost function over one switch is given by

$$J^*(x_0, x_T, T) = \psi_T' x_T - \psi_0' x_0 \tag{8.12}$$

and we know the relation between these variables is given by the solution of the Hamiltonian system

$$\begin{pmatrix} x_T \\ \psi_T \end{pmatrix} = e^{H_1 T} \begin{pmatrix} x_0 \\ \psi_0 \end{pmatrix}$$

Thus, the cost function can be rewritten as

$$\begin{aligned} J^* &= \frac{1}{2}\begin{pmatrix} x_T \\ \psi_T \end{pmatrix}' \begin{pmatrix} 0 & I \\ I & 0 \end{pmatrix} \begin{pmatrix} x_T \\ \psi_T \end{pmatrix} - \frac{1}{2}\begin{pmatrix} x_0 \\ \psi_0 \end{pmatrix}' \begin{pmatrix} 0 & I \\ I & 0 \end{pmatrix} \begin{pmatrix} x_0 \\ \psi_0 \end{pmatrix} \\ &= \frac{1}{2}\begin{pmatrix} x_0 \\ \psi_0 \end{pmatrix}' e^{H_1' T} \begin{pmatrix} 0 & I \\ I & 0 \end{pmatrix} e^{H_1 T} \begin{pmatrix} x_0 \\ \psi_0 \end{pmatrix} - \frac{1}{2}\begin{pmatrix} x_0 \\ \psi_0 \end{pmatrix}' \begin{pmatrix} 0 & I \\ I & 0 \end{pmatrix} \begin{pmatrix} x_0 \\ \psi_0 \end{pmatrix} \\ &= \frac{1}{2}\begin{pmatrix} x_0 \\ \psi_0 \end{pmatrix}' \left[e^{H_1' T} \begin{pmatrix} 0 & I \\ I & 0 \end{pmatrix} e^{H_1 T} - \begin{pmatrix} 0 & I \\ I & 0 \end{pmatrix} \right] \begin{pmatrix} x_0 \\ \psi_0 \end{pmatrix} \end{aligned}$$

On the other hand

$$\begin{aligned} V_1(x_T) - V_0(x_0) &= \begin{pmatrix} x_T \\ \psi_T \end{pmatrix}' \begin{pmatrix} P & 0 \\ 0 & 0 \end{pmatrix} \begin{pmatrix} x_T \\ \psi_T \end{pmatrix} - \begin{pmatrix} x_0 \\ \psi_0 \end{pmatrix}' \begin{pmatrix} P & 0 \\ 0 & 0 \end{pmatrix} \begin{pmatrix} x_0 \\ \psi_0 \end{pmatrix} \\ &= \begin{pmatrix} x_0 \\ \psi_0 \end{pmatrix}' \left[e^{H_1' T} \begin{pmatrix} P & 0 \\ 0 & 0 \end{pmatrix} e^{H_1 T} - \begin{pmatrix} P & 0 \\ 0 & 0 \end{pmatrix} \right] \begin{pmatrix} x_0 \\ \psi_0 \end{pmatrix} \end{aligned}$$

From the fact that we need

$$J^* > V_1(x_T) - V_0(x_0)$$

we get

$$\begin{pmatrix} x_0 \\ \psi_0 \end{pmatrix}' R_1(T) \begin{pmatrix} x_0 \\ \psi_0 \end{pmatrix} > 0 \tag{8.13}$$

where

$$R_1(T) = e^{H_1' T} \begin{pmatrix} -P & I/2 \\ I/2 & 0 \end{pmatrix} e^{H_1 T} - \begin{pmatrix} -P & I/2 \\ I/2 & 0 \end{pmatrix}$$

The last part of the proof is to find out for what values of x_0 and ψ_0 must condition (8.13) be satisfied on. We already know that $x_0 \in S$. Also, $x_T \in S$, i.e., $Cx_T = 0$, or

$$\begin{pmatrix} C & 0 \end{pmatrix} \begin{pmatrix} x_T \\ \psi_T \end{pmatrix} = 0$$

Hence,

$$\begin{pmatrix} C & 0 \end{pmatrix} e^{H_1 T} \begin{pmatrix} x_0 \\ \psi_0 \end{pmatrix} = 0$$

Therefore,

$$\begin{pmatrix} x_0 \\ \psi_0 \end{pmatrix} \in S_{T1}$$

which proves the result. ■

8.3.3 Technical Details: Analysis at $T = 0$ and $T = \infty$

Analysis at $T = 0$

Computationally, conditions (8.9) and (8.10) can both be easily checked in some intervals $[t_{min}, t_{max}]$ using efficient available software. Although we can check the stability conditions for arbitrarily small and large values of T, it still remains to show

that they are satisfied for $0 < T < t_{min}$ and $T > t_{max}$. The analysis for large values of T is currently under investigation. Here, we focus on the analysis for small values of T.

Since both conditions are equivalent, we concentrate on conditions (8.10). To recall, these conditions are

$$R_i(T) > 0 \quad \text{on } S_{Ti}$$

for $i = 1, 2$, where $R_2(T)$ is defined similarly as $R_1(T)$ was defined in the proof of theorem 8.2.

When $T = 0$, $x_T = x_0$ and $\psi_T = \psi_0$. Thus, the optimal cost (8.12) is $J^* = 0$. This means we need to guarantee the derivative of the stability conditions at $T = 0$ are positive semidefinite.

We focus on the first condition in (8.10). The second follows similarly. Let $S_0 = \lim_{T\to 0} S_{T1}$, i.e.,

$$S_0 = \{x \in S \times \mathbb{R}^n | \ (\, C \quad 0\,) H_1 x = 0\}$$

Note that $\lim_{T\to 0} S_{T1} = \lim_{T\to 0} S_{T2}$ since

$$\begin{aligned}
(\, C \quad 0\,) H_1 \begin{pmatrix} x_0 \\ \psi_0 \end{pmatrix} &= (\, CA_1 \quad \tfrac{1}{\gamma} CBB'\,) \begin{pmatrix} x_0 \\ \psi_0 \end{pmatrix} \\
&= C(A + BC)x_0 + \frac{1}{\gamma} CBB'\psi_0 \\
&= CAx_0 + \frac{1}{\gamma} CBB'\psi_0 \\
&= (\, C \quad 0\,) H \begin{pmatrix} x_0 \\ \psi_0 \end{pmatrix}
\end{aligned}$$

where we use the fact $Cx_0 = 0$.

Finding the derivative of $R_1(T)$ is straightforward

$$\frac{dR_1(T)}{dt} = \dot{R}_1(T) = e^{H_1' T} H_1' \begin{pmatrix} -P & I/2 \\ I/2 & 0 \end{pmatrix} e^{H_1 T} + e^{H_1' T} \begin{pmatrix} -P & I/2 \\ I/2 & 0 \end{pmatrix} H_1 e^{H_1 T}$$

which means

$$\dot{R}_1(0) = H_1' \begin{pmatrix} -P & I/2 \\ I/2 & 0 \end{pmatrix} + \begin{pmatrix} -P & I/2 \\ I/2 & 0 \end{pmatrix} H_1$$

Therefore, it is necessary that

$$\dot{R}_1(0) \geq 0 \quad \text{on } S_0$$

This derivative also helps to choose a small enough value of $t_{min} > 0$ such that the stability conditions are guaranteed to be satisfied for all $T \in (0, t_{min})$.

Analysis at $T = \infty$

In this subsection, we present a result that gives us LMIs at $T = \infty$. These are based in finding the limits of W_{T1} and W_{T2} in (8.9) as $T \to \infty$. We will show how to find

the LMI for the first condition in (8.9). The other follows similarly.

Remember that the eigenvalues of an Hamiltonian matrix are symmetric around the jw axis. This means we can always find a representation for H_1 of the form $H_1 = V\Sigma U$, where the matrices V and Σ, are real, $U = V^{-1}$, and

$$\Sigma = \begin{pmatrix} D & 0 \\ 0 & -D \end{pmatrix}$$

where the eigenvalues of D are all the stable eigenvalues of H_1. Consider the following block partition of V and U

$$V = \begin{pmatrix} V_{11} & V_{12} \\ V_{21} & V_{22} \end{pmatrix} \qquad U = \begin{pmatrix} U_{11} & U_{12} \\ U_{21} & U_{22} \end{pmatrix}$$

We have the following result for the first condition in (8.9). A similar results can be obtained for the second condition.

Proposition 8.3 *If $P > 0$ satisfies conditions (8.9) and (8.10) then it also satisfies*

$$\begin{cases} V_{22}V_{12}^{-1} - P \geq 0 & \text{on } S \\ U_{22}^{-1}U_{21} + P \geq 0 & \text{on } S \end{cases}$$

Proof: We need to find the limit when $T \to \infty$ of the first condition in (8.9). Hence, we need the

$$\lim_{T\to\infty} W_{T1}$$

First notice that $e^{H_1 T}$ can be written as

$$e^{H_1 T} = \begin{bmatrix} V_{11}e^{DT}U_{11} + V_{12}e^{-DT}U_{21} & V_{11}e^{DT}U_{12} + V_{12}e^{-DT}U_{22} \\ V_{21}e^{DT}U_{11} + V_{22}e^{-DT}U_{21} & V_{21}e^{DT}U_{12} + V_{22}e^{-DT}U_{22} \end{bmatrix}$$

Since $e^{DT} \to 0$ as $T \to \infty$,

$$e^{H_1 T} \to \begin{bmatrix} V_{12}e^{-DT}U_{21} & V_{12}e^{-DT}U_{22} \\ V_{22}e^{-DT}U_{21} & V_{22}e^{-DT}U_{22} \end{bmatrix}$$

as $T \to \infty$. Each block of the matrix W_{T1} (in the form of (8.7)) when $T \to \infty$, starting with block $(1,1)$, is given by

$$\begin{aligned} e_{22}e_{12}^{-1} &\to V_{22}e^{-DT}U_{22}U_{22}^{-1}e^{DT}V_{12}^{-1} \\ &= V_{22}V_{12}^{-1} \end{aligned}$$

Noticing that

$$\begin{aligned} e_{22}e_{12}^{-1}e_{11} &\to V_{22}e^{-DT}U_{22}U_{22}^{-1}e^{DT}V_{12}^{-1}V_{12}e^{-DT}U_{21} \\ &= V_{22}e^{-DT}U_{21} \\ &= e_{21} \end{aligned}$$

block $(1,2)$ given by

$$\begin{aligned} e_{21} - e_{22}e_{12}^{-1}e_{11} - (e_{12}^{-1})' &\rightarrow e_{21} - e_{21} - (U_{22}^{-1}e^{DT}V_{12}^{-1})' \\ &\rightarrow 0 \end{aligned}$$

Block $(2,1)$ is just the transpose of block $(1,2)$. Finally, block $(2,2)$ is given by

$$\begin{aligned} e_{12}^{-1}e_{11} &\rightarrow U_{22}^{-1}e^{DT}V_{12}^{-1}V_{12}e^{-DT}U_{21} \\ &= U_{22}^{-1}U_{12} \end{aligned}$$

This proves the result. ■

8.4 Discussion

In this chapter we showed that performance analysis of PLS can be done using impact maps and quadratic surface Lyapunov functions. Although the results are still preliminary, they were enough to convince that the ideas developed for stability analysis are also powerful in performance and robustness analysis of PLS.

The class of PLS we analyzed was on/off systems, with $d = 0$. This class had already been studied in chapter 6. There, the focus was stability analysis of equilibrium points of OFS. Since this is the simplest class of PLS with global asymptotic equilibrium points, it was the best place to develop new concepts and results. The goal was to show the system was finite-gain $\mathcal{L}_2$ stable. As in stability analysis, the approach was to analyze the system at the switching surface. Using several well known results from H_2 optimization, we were able to find conditions in the form of LMIs that, when satisfied, guarantee finite-gain $\mathcal{L}_2$ stability of OFS. Through the use of several illustrative examples, we showed the methodology can be efficiently and successfully applied to a wide range of OFS, including those with unstable nonlinearity sectors, for which all classical methods fail to analyze.

Several topics in this area are still open and in need of further research, and will most certainly be the topic of future publications. One is the technical detail related to guaranteeing the stability conditions are satisfied for all $T > t_{max}$, knowing they are satisfied for all $[0, t_{max}]$, where t_{max} is some large positive number. Although this is a very important detail that needs to be solved, numerically, by increasing t_{max}, we can get a high level of confidence that the stability conditions are in fact satisfied for all $T \geq 0$. This is exactly what we have done in the previous section.

The next logical step is to analyze performance of OFS for which the switching surface does not include the origin. As in stability analysis in chapter 6, there should not be much difference from what we have done here. In fact, here, the difference is even smaller since we do not take advantage of the sets S_{t_i}, i.e., the sets of points is the switching surface that have same switching time.

Then, we believe saturation systems can also be analyzed using similar ideas. In time, the goal is to develop a general framework where large classes of PLS can systematically be globally analyzed, not only in terms of stability analysis, but also

in terms of robustness and performance analysis.

Chapter 9

Conclusion

Motivated by the need of better, more general, and more efficient global analysis tools for certain classes of hybrid systems, this thesis developed a new constructive analysis methodology using *impact maps* and *quadratic surface Lyapunov functions*. The main idea came from the discovery that impact maps induced by an LTI flow between two switching surfaces can be expressed as linear transformations analytically parametrized by a scalar function of the state. Furthermore, level sets of this function are convex subsets of linear manifolds. As a result, the problem of finding quadratic Lyapunov functions on switching surfaces was reduced to solving a set of LMIs, which can be efficiently done using available computational tools.

The success and power of this new methodology were well demonstrated in globally analyzing equilibrium points and limit cycles of several classes of piecewise linear systems (PLS): relay feedback systems (RFS), on/off systems (OFS), and saturation systems (SAT).

The first class of systems we analyzed was RFS. It is well known that for a large class of RFS there will be limit cycle oscillations. Although RFS is a very simple class of PLS, there were almost no results available to globally analyze such limit cycles. However, with these new results, a large number of examples with a locally stable symmetric unimodal limit cycle were proven globally asymptotically stable. Systems analyzed include minimum-phase systems, systems of relative degree larger than one, and of high dimension. In fact, it is still an open problem whether there exists an example with a globally stable symmetric unimodal limit cycle that could not be successfully analyzed with this new methodology. Such positive results led us to believe that globally stable limit cycles of RFS frequently have quadratic surface Lyapunov functions.

After demonstrating the success of this methodology in globally analyzing limit cycles of PLS, we showed that the same ideas can be used to check global asymptotic stability of equilibrium points of PLS. For that, we used OFS, the simplest class of PLS with globally stable equilibrium points. This simplicity comes from the fact that, in the state space, OFS are characterized by a single switching surface. Equilibrium points of OFS analyzed included those that did not belong to the switching surface. Although the analysis in this case was different from RFS, we were able to prove global asymptotic stability for a large number of examples analyzed. These included

systems with an unstable affine linear subsystem, systems of relative degree larger than one and of high dimension, and systems with unstable nonlinearity sectors, for which no results existed so far. In fact, existence of an example with a globally stable equilibrium point that could not be successfully analyzed with this new methodology is still an open problem.

The next natural step was to show the same ideas hold even when a PLS has more than one switching surface. We considered a class of PLS known as SAT. In the state space, these systems are characterized by two switching surfaces, separating three different affine linear subsystems. As before, we were able to express stability conditions as sets of LMIs, which can be solved efficiently. Moreover, a large number of examples of SAT analyzed was successfully proven to have a globally stable equilibrium point. Systems analyzed included high-order systems, systems of relative degree larger than one, and systems with unstable nonlinearity sectors for which all classical methods failed to analyze. In fact, it is still an open problem whether there exists an example with a globally stable equilibrium point that could not be successfully analyzed with this new methodology. With SAT, we confirmed the idea that global asymptotic stability of equilibrium points of PLS can be checked using impact maps and quadratic surface Lyapunov functions. In particular, we showed that this new methodology successfully globally analyzes PLS with more than one switching surface.

The last part of this thesis was dedicated to show that impact maps and quadratic surface Lyapunov functions can be efficiently and successfully used to not only check stability, but also performance and robustness properties of PLS. We found conditions in form of LMIs that, when satisfied, guarantee finite-gain $\mathcal{L}_2$ stability of OFS. These conditions were use to show that many globally asymptotically stable OFS are also finite-gain $\mathcal{L}_2$ stable. Systems analyzed include OFS with unstable nonlinearity sectors, for which all classical methods fail to analyze.

This work has open a door to a new area of research and, as a consequence, has left numerous open problems. Some of these are currently under investigation. Topics of *future work* are include:

- The main goal of this research was to build a framework where piecewise linear systems can be systematically analyze in terms of stability, robustness, and performance. We have already seen this is possible for certain classes of PLS. The questions now are: given a PLS, how to set up the analysis problem? How to address it? And, how to solve it? Ideally, one would like to have a software package that, through a user friendly interface, allows a user to supply a PLS. In terms of stability, the first result of this software would be a characterization of all equilibrium points and limit cycles. Then, the user could decide which one of these trajectories to analyze. If there are several of these trajectories, then maybe we are interested in a reasonably large region of stability of the specified trajectory. If there is only one, the software would check if the specified trajectory is globally stable.

  In terms of robustness and performance, the applications are endless. As a nonlinear system is approximated by a linear system, an hybrid system could be

approximated by a PLS together with external perturbations and a set of uncertainties, modeling not only the nonlinearities inherent to the hybrid system, but also unmodeled dynamics. Once characterized, structured and unstructured uncertainties, and external perturbations, could be supplied to the software, and have this return robustness and performance properties of the PLS.

The *ultimate goal* is to have a theory for PLS somehow similar to the existent theory for linear systems. Although such general framework is still faraway, we believe that with the present work we have taken the first steps in that direction.

- There are several physical systems that can be modeled and analyzed as a PLS. Among these are several classes of walking robots. As a cases study, we intend to apply quadratic surface Lyapunov functions to analyze walking robots.

- When studying RFS, we mention that certain classes of RFS exhibit sliding modes. Although sliding modes were not considered then, the analysis of such systems is not that different from what we have done so far. With the definition of a relay in chapter 5, there may exist points in the switching surface for which no solution exists. This can happen when the vector field on both sides of the switching surface points towards the switching surface. Changing slightly this definition to allow trajectories to evolve in the switching surface, leads to the so-called sliding modes. Thus, whenever a trajectory enters the set of points leading to sliding modes, we consider a new affine linear system of dimension lower than the one of the original system, defined on the switching surface. This system evolves until it reaches a certain linear manifold on the switching surface. Then, the trajectory is again free to evolve in the state space. Hence, the analysis is similar to other cases considered in this thesis.

  To be more general, quadratic surface Lyapunov functions can be used to analyze PLS that switch between affine linear systems of different dimension.

- An important topic of research following this thesis is to find conditions that do not depend on the parameters of the Lyapunov functions but guarantees their existence. Such conditions should depend on the plant or on certain properties of a class of systems, and should, obviously, be easier to check than the ones presented here.

- Many PLS have more than one equilibrium point and/or limit cycle that is locally stable. The question here is: what is the region of attraction for each of these locally stable trajectories? Before studying global analysis, we dealt with this exact problem for RFS. The work reported in [23] characterizes reasonably large regions of stability around limit cycles. After the discovery that impact maps could be represented as linear transformations parametrized by the associated switching time, this line of research became secondary, and the focus was then on globally analysis. Using these new tools, it would be very interesting to go back and see how they could be used to guarantee regions of stability around locally stable trajectories. The ideas reported in this thesis would undoubtfully improve the results in [23].

Bibliography

[1] A. A. Andronov, S. E. Khaikin, and A. A. Vitt. *Theory of Oscillators*. Pergamon Press, Oxford, 1966.

[2] S. H Ardalan and J. J. Paulos. An analysis of nonlinear behavior in delta-sigma modulators. *IEEE Trans. Circuits and Sys.*, 6:33–43, 1987.

[3] Karl J. Åström. Oscillations in systems with relay feedback. *The IMA Volumes in Mathematics and its Applications: Adaptive Control, Filtering, and Signal Processing*, 74:1–25, 1995.

[4] Karl J. Åström and K. Furuta. Swinging up a pendulum by energy control. *IFAC 13th World Congress, San Francisco, California*, 1996.

[5] Karl J. Åström and T. Hagglund. Automatic tuning of simple regulators. *In Preprints 9th IFAC World Congress, Budapest, Hungary*, pages 267–272, 1984.

[6] Karl J. Åström and T. Hagglund. Automatic tuning of simple regulators with specifications on phase and amplitude margins. *Automatica*, 20:645–651, 1984.

[7] Michael Athans and Peter L. Falb. *Optimal Control; an Introduction to the Theory and its Applications*. McGraw-Hill, 1966.

[8] D. P. Atherton. *Nonlinear Control Engineering*. Van Nostrand, 1975.

[9] Hendrik W. Bode. *Network Analysis and Feedback Amplifier Design*. Princeton, N.J.: Van Nostrand, 1945.

[10] N. N. Bogoliubov and Y. A. Mitropolsky. *Asymptotic Methods in the Theory of Nonlinear Oscillations*. Hindustan, India, 1961.

[11] S. Boyd, L. El Ghaoui, Eric Feron, and V. Balakrishnan. *Linear Matrix Inequalities in System and Control Theory*. SIAM, Philadelphia, 1994.

[12] M. S. Branicky. *Studies in Hybrid Systems: Modeling, Analysis, and Control*. PhD. thesis, Massachusetts Institute of Technology, 1995.

[13] Paul B. Brugarolas, Vincent Fromion, and Michael G. Safonov. Robust switching missile autopilot. *ACC, Philadelphia, PA*, June 1998.

[14] Kermal Ciliz and Kumpati S. Narendra. Multiple model based adaptive control of robotic manipulators. *IEEE Conference on Decision and Control, Lake Buena Vista, FL*, pages 1305–1310, December 1994.

[15] Munther A. Dahleh and Ignacio J. Diaz-Bobillo. *Control of Uncertain Systems: A Linear Programming Approach*. Prentice Hall, N.J., 1995.

[16] Fernando D'Amato, Alexandre Megretski, Ulf Jönsson, and M. Rotea. Integral quadratic constraints for monotonic and slope-restricted diagonal operators. In *ACC*, pages 2375–2379, San Diego, CA, USA, June 1999.

[17] C. Desoer and M. Vidyasagar. *Feedback Systems: Input-Output Properties*. Academic Press, N.Y., 1975.

[18] Peter Dorato and Rama K. Yedavalli. *Recent Advances in Robust Control*. Ieee Press, New York, N. Y., 1990.

[19] John C. Doyle, Bruce A. Francis, and Allen R. Tannenbaum. *Feedback Control Theory*. Macmillan, N.Y., 1992.

[20] Randy A. Freeman and Petar V. Kokotović. *Robust Nonlinear Control Design: State-Space and Lyapunov Techniques*. Birkhäuser, Boston, 1996.

[21] Jorge M. Gonçalves. Global stability analysis of on/off systems. In *CDC, Sydney, Australia*, December 2000.

[22] Jorge M. Gonçalves. Surface Lyapunov functions in global stability analysis of saturation systems. *Technical report LIDS-P-2477, MIT*, August 2000.

[23] Jorge M. Gonçalves, Alexandre Megretski, and Munther A. Dahleh. Semi-global analysis of relay feedback systems. *Proc. CDC, Tampa, Florida*, Dec 1998.

[24] Jorge M. Gonçalves, Alexandre Megretski, and Munther A. Dahleh. Global stability analysis of relay feedback systems. *Technical report LIDS-P-2458, MIT*, August 1999.

[25] Jorge M. Gonçalves, Alexandre Megretski, and Munther A. Dahleh. Global stability of relay feedback systems. In *ACC, Chicago, IL*, June 2000.

[26] Jorge M. Gonçalves, Alexandre Megretski, and Munther A. Dahleh. Global stability of relay feedback systems. Accepted for publication in *IEEE Transactions on Automatic Control*, 2000.

[27] Jorge M. Gonçalves' web page. `http://web.mit.edu/jmg/www/`.

[28] John Guckenheimer and Philip Holmes. *Nonlinear Oscillations, Dynamical Systems, and Bifurcations of Vector Fields*. Springer-Verlag, N.Y., 1983.

[29] Wolfgang Hahn. *Stability of Motion*. Springer-Verlag, N.Y., 1967.

[30] Arash Hassibi and Stephen Boyd. Quadratic stabilization and control of piecewise linear systems. In *ACC, Philadelphia, Pennsylvania*, June 1998.

[31] Chihiro Hayashi. *Nonlinear Oscillations in Physical Systems.* McGraw-Hill, N.Y., 1964.

[32] Alberto Isidori. *Nonlinear Control Systems.* Springer, N. Y., 1995.

[33] Karl H. Johansson, Anders Rantzer, and Karl J. Åström. Fast switches in relay feedback systems. *Automatica*, 35(4), April 1999.

[34] Mikael Johansson and Anders Rantzer. Computation of piecewise quadratic Lyapunov functions for hybrid systems. *IEEE Transactions on Automatic Control*, 43(4):555–559, April 1998.

[35] Ulf Jönsson and Alexandre Megretski. The Zames Falb IQC for systems with integrators. *IEEE Transactions on Automatic Control*, 45(3):560–565, March 2000.

[36] Hassan K. Khalil. *Nonlinear Systems.* Prentice Hall, N.J., 2nd edition, 1996.

[37] Miroslav Krstić, Ioannin Kanellakopoulos, and Petar V. Kokotović. *Nonlinear and Adaptive Control Design.* Wiley, N.Y., 1995.

[38] David G. Luenberger. *Introduction to Dynamic Systems : Theory, Models, and Applications.* Wiley, N.Y., 1992.

[39] Marc W. McConley, B. Appleby, Munther A. Dahleh, and Eric Feron. A computationally efficient Lyapunov-based scheduling procedure for control of nonlinear systems with stability guarantees. *IEEE Transactions on Automatic Control*, 45(1):33–49, Jan 2000.

[40] Marc W. McConley, Munther A. Dahleh, and Eric Feron. Polytopic control Lyapunov functions for robust stabilization of a class of nonlinear systems. *Systems & Control Letters*, 34(1–2):77–83, 1998.

[41] Alexandre Megretski. Global stability of oscillations induced by a relay feedback. *In Preprints 9th IFAC World Congress, San Francisco, California*, E:49–54, 1996.

[42] Alexandre Megretski. New IQC for quasi-concave nonlinearities. In *ACC, San Diego, California*, June 1999.

[43] Alexandre Megretski, 2000. Lecture notes on Multivariable Control Systems, MIT, Cambridge, MA.

[44] Alexandre Megretski and Anders Rantzer. System analysis via integral quadratic constrains. *IEEE Transactions on Automatic Control*, 42(6):819–830, June 1997.

[45] Nicholas Minorsky. *Nonlinear Oscillations*. Robert E. Krieger, Malabar, Fl, 1974.

[46] Ali Hasan Nayfeh and Dean T. Mook. *Nonlinear Oscillations*. Wiley, N.Y., 1979.

[47] H. Nyquist. Regeneration theory. *Bell. Syst. Tech. J.*, 11:126–147, 1932.

[48] Katsuhiko Ogata. *Modern Control Engineering*. Prentice Hall, N.J., 3rd edition, 1970.

[49] Henrick Olsson, Karl J. Åström, C. Canudas de Wit, Magnus Gäfvert, and P. Lischinsky. Friction models and friction compensation. *To appear in: European Journal of Control*, 1998.

[50] Stefan Pettersson and Bengt Lennartson. An LMI approach for stability analysis of nonlinear systems. In *EEC, Brussels, Belgium*, July 1997.

[51] Stefan Pettersson and Bengt Lennartson. Lmi for stability and robustness of hybrid systems. *ACC, Albuquerque, NM*, pages 1714–1718, June 1997.

[52] N. B. Pettit. The analysis of piecewise linear dynamical systems. *Control Using Logic-Based Switching*, pages 49–58, 1997.

[53] Robert P. Ringrose. *Self-Stabilizing Running*. PhD Thesis at the Massachusetts Institute of Technology, Cambridge, MA, February 1997.

[54] Walter Rudin. *Principles of Mathematical Analysis*. McGraw-Hill, 1976.

[55] Ali Saberi, Zongli Lin, and Andrew Teel. Control of linear systems with saturating actuators. *IEEE Transactions on Automatic Control*, 41(3):368–378, March 1996.

[56] Jeff S. Shamma. *Analysis and Design of Gain Scheduled Control Systems*. PhD thesis, Massachusetts Institute of Technology, Cambridge, MA, May 1988.

[57] Jean-Jacques E. Slotine and Weiping Li. *Applied Nonlinear Control*. Prentice Hall, N.J., 1991.

[58] Rodolfo Suárez, José Alvarez, and Jesús Alvarez. Linear systems with single saturated input: stability analysis. In *30th CDC, Brighton, England*, December 1991.

[59] Héctor J. Sussman, Eduardo D. Sontag, and Yudi Yang. A general result on the stabilization of linear systems using bounded controls. *IEEE Transactions on Automatic Control*, 39(12):2411–2425, December 1994.

[60] Yasundo Takahashi, Michael J. Rabins, and David M. Auslander. *Control and Dynamic Systems*. Addison-Wesley, Reading, Massachusetts, 1970.

[61] Gang Tao and Petar V. Kokotović. *Adaptive Control of Systems with Actuator and Sensor Nonlinearities*. Wiley, N.Y., 1996.

[62] Andrew R. Teel. A nonlinear small gain theorem for the analysis of control systems with saturation. *IEEE Transactions on Automatic Control*, 41(9):1256–1270, September 1996.

[63] Claire Tomlin, John Lygeros, and Shankar Sastry. Aerodynamic envelope protection using hybrid control. *ACC, Philadelphia, PA*, June 1998.

[64] Ya. Z. Tsypkin. *Relay control systems*. Cambridge University Press, Cambridge, UK, 1984.

[65] Vadim I. Utkin. *Sliding Modes in Control Optimization*. Springer-Verlag, N. Y., 1995.

[66] Subbarao Varigonda and Tryphon Georgiou. Dynamics of relay relaxation oscillators. Accepted for publication in *IEEE Transactions on Automatic Control*, 2000.

[67] M. Vidyasagar. *Nonlinear Systems Analysis*. Prentice Hall, N.J., 1993.

[68] G. Zames and P. L. Falb. Stability conditions for systems with monotone and slope-restricted nonlinearities. *SIAM Journal of Control*, 6(1):89–108, 1968.

[69] George Zames. On the input-output stability of nonlinear time-varying feedback systems, parts i and ii. *IEEE Transactions on Automatic Control*, AC-11:228 and 465, 1966.

[70] Kemin Zhou, John C. Doyle, and Keith Glover. *Robust and Optimal Control*. Prentice Hall, N. J., 1996.